NASA CONTRACTOR REPORT

NASA CR-690

SIMULATION OF GASEOUS CORE NUCLEAR ROCKET MIXING CHARACTERISTICS USING COLD AND ARC HEATED FLOWS

by Peter M. Williams and Jerry Grey

Prepared by
PRINCETON UNIVERSITY
Princeton, N. J.
for Lewis Research Center
and NASA/AEC Space Nuclear Propulsion Office

NATIONAL AERONAUTICS AND SPACE ADMINISTRATION • WASHINGTON, D. C. • JUNE 1967

NASA CR-690

SIMULATION OF GASEOUS CORE NUCLEAR ROCKET MIXING CHARACTERISTICS USING COLD AND ARC HEATED FLOWS

By Peter M. Williams and Jerry Grey

Prepared under Contract No. NASr-216 by
PRINCETON UNIVERSITY
Princeton, N.J.

for Lewis Research Center
and NASA/AEC Space Nuclear Propulsion Office

NATIONAL AERONAUTICS AND SPACE ADMINISTRATION

For sale by the Clearinghouse for Federal Scientific and Technical Information
Springfield, Virginia 22151 – CFSTI price $3.00

FOREWORD

The research described herein, which was conducted at the Guggenheim Laboratories for the Aerospace Propulsion Sciences, Department of Aerospace and Mechanical Sciences, Princeton University, was performed under NASA Contract NASr-216/31-001-028. Captain William A. Yingling, NASA Headquarters, and Robert G. Ragsdale, Nuclear Systems Division, NASA Lewis Research Center, were the Technical Managers. The work made use of computer facilities supported in part by NSF Grant N8EGP579.

ABSTRACT

Mixing phenomena of cold and arc heated jets of one and two centimeters in diameter exhausting into coaxial flows of either helium or nitrogen were investigated over ranges of jet temperatures between room and 9000°R, of jet Reynolds numbers between 10 and 10^4 and of coaxial to jet velocity ratios from 0 to 780. Velocity, temperature, and composition profiles were obtained at the jet exit plane and downstream locations of 1/2, 1 and 2 jet diameters at a total of 47 different flow conditions including three variations of the coaxial flow injection scheme.

This work was undertaken to investigate the mixing processes related to the coaxial flow nuclear rocket concept in which a central flow of nuclear fuel in the gaseous state is surrounded by a flow of hydrogen at much greater velocity. The appropriate experimental data have been correlated in terms of the separation ratio for the two streams and show a consistent agreement in the effects of velocities, temperatures, Reynolds numbers, molecular weights, and an exit plane mixing factor. Under conditions of interest to the coaxial flow rocket the mixing processes were strongly dominated by an apparent wake phenomena at the exit plane and thus could not be described by even an empirical application of the arcjet mixing theory developed in earlier work. Immediate application of these studies to the question of the feasibility of the coaxial flow rocket is premature since the effect of scale on the exit plane mixing factor is unknown.

TABLE OF CONTENTS

I. INTRODUCTION

The key to feasibility of any gaseous core nuclear rocket concept is the ability of the rocket to retain a suitably high fraction of the fissioning gaseous fuel while propellant is expelled at comparatively attractive temperatures and flow rates. A 1957 analytical study by Kerrebrock and Meghreblian[1] considered vortex motion as a scheme to effect the required separation and since this time other possible variations and concepts of the gaseous core rocket have received attention[2,3].

The concept proposed in 1960 by Weinstein and Ragsdale[4] has formed the stimulus for the experiments reported here and is diagrammed in Figure 1. A central jet flow of fissioning material is surrounded by a coaxial flow of propellant at substantially greater velocity. The concept eliminates many of the characteristic problems of vortex containment, but since particle contact must be minimized to prevent sweeping the fuel along with the propellant, heat transmission from the core to the coaxial flow is necessarily by radiation. It, therefore, appears necessary to "seed" the relatively transparent coaxial hydrogen flow with small particles of high-emissivity material.

Through use of the arcjet it is possible to simulate some of the fluid mechanics and heat transfer features of the coaxial concept. In this work the fluid mechanics has been investigated using both cold and arc heated flows.

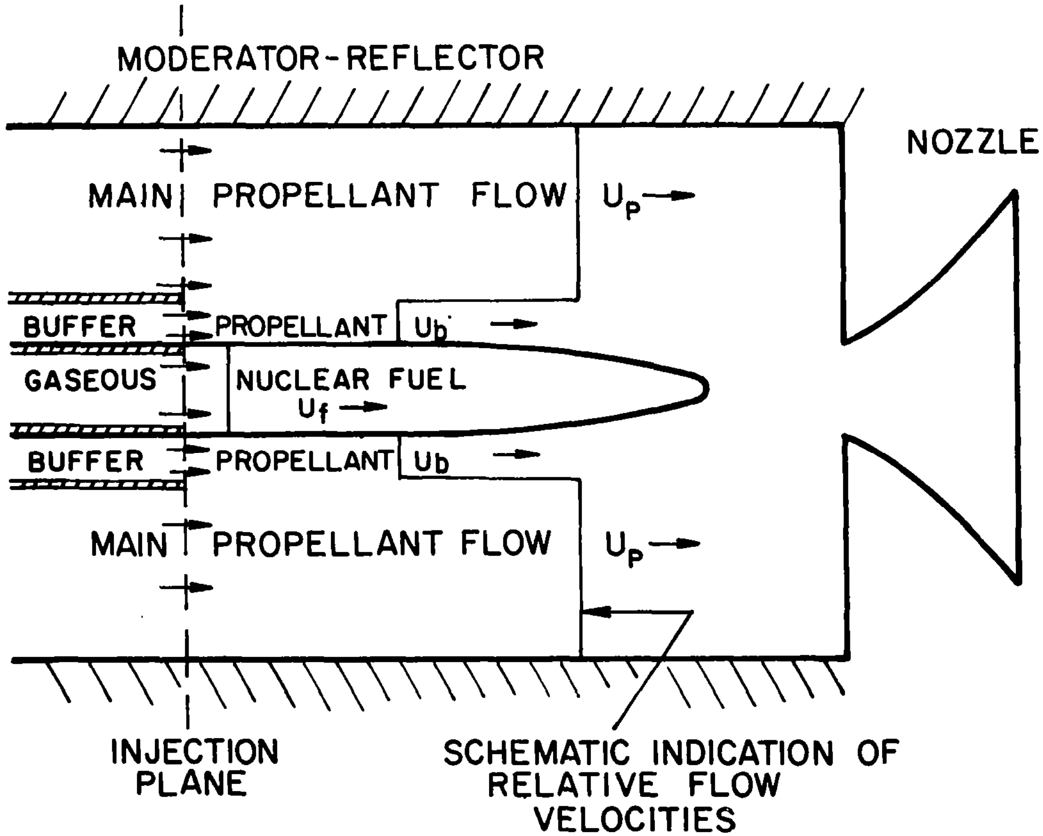

THE COAXIAL FLOW GASEOUS CORE NUCLEAR ROCKET

FIGURE 1

Weinstein and Ragsdale showed analytically that in the reactor cavity, if the flow remains laminar, there would be little mixing of the fuel and propellant, and that the degree of fuel retention in the cavity would be sufficient for economic feasibility. This concept has received substantial analytical and experimental attention in recent years. The nuclear criticality requirements were investigated by Ragsdale and Hyland,[5] a turbulent flow jet mixing experiment was performed by Ragsdale, Weinstein and Lanzo,[6] and recently an analytical study by Ragsdale[7] illustrated the advantages of both turbulent and laminar mixing of a buffer flow between the main stream of coaxial propellant flow and the fuel flow.

The arcjet simulation experiments have been underway at Princeton since early 1963, making use of previously developed diagnostic techniques[8,9,10] and an analytical formulation developed for laminar arcjet mixing.[11,14] Early Princeton experiments were addressed to mixing characteristics of a laminar jet, since it was the laminar case which showed such high promise in the initial conceptual studies. The results of this research, reported in References 12, 13, and 14 showed that with coaxial flows, even well below the jet velocity, laminar jet flow could not be maintained. Otherwise, mechanisms favorable to the concept were apparent, and it was thus decided to extend the investigation to the case of turbulent flows.

The practical operating conditions of the arcjet differ considerably, of course, from the design characteristics of the gaseous-core nuclear rocket. The electric arc does, however, provide a very high temperature jet which offers an approach to investigate large differences in temperature, molecular weight and velocity between central and coaxial flows. It is, therefore, possible to examine mixing characteristics of some pertinence to the coaxial gaseous-core scheme over a wide range of variables, with the aim of bringing to light the fluid mechanical properties of most apparent significance to the coaxial concept. The basic technique was to radially probe the mixing region for velocity, composition and enthalpy at axial stations beginning at the exit plane and down to two initial central-jet diameters. The mixing profiles are presented in detail in this report.

A detailed search of the literature has revealed no data of hot jet mixing of coaxial-to-core velocity ratios greater than unity, and no profiles of cold mixing within a few diameters of the nozzle exit plane. Alpinieri[15] offers cold mixing profiles in the range greater than two jet diameters downstream for the jets of carbon dioxide or hydrogen mixing with air, and Ragsdale, et. al.,[6] have presented average composition data for a cold bromine jet mixing with coaxial flowing air. Neither of those experiments give data directly comparable with those reported here.

In addition to presentation of the data in a manner suitable for general fluid mechanics interest, certain of the data have been correlated in terms of the separation ratio S , the parameter which relates directly to the feasibility of any gaseous core nuclear rocket concept. The separation ratio is defined as the ratio of the life of propellant particles to the life of fuel particles in the reactor cavity, and for the coaxial flow concept, this results in the simple expression

$$S = \frac{V_c}{V_e} ,$$

where V_c and V_e are the average velocities of the core (or jet) flow and the exterior (or coaxial) flow respectively. It has been argued by Bussard and DeLauer[16] that for economic feasibility S must be less than 10^{-3}. Weinstein and Ragsdale[4] suggested a range of 10^{-2} to 10^{-3}, while Rom[22] gives 10^{-2}.

II. TECHNIQUES AND EQUIPMENT

A. General

The technique and equipment used in the simulation experiments are direct outgrowths of earlier work, and for this reason only equipment which was developed specifically for the current research is described in detail. Figure 2 is an overall diagram of the equipment, showing the plasma generator which delivers an argon jet into a test chamber containing a movable calorimetric probe. Measured quantities are indicated on the diagram. The main difference from the apparatus used earlier[8,12,14, etc.] is provision for injection of high speed coaxial flow through a two-inch-long injection section surrounding the jet nozzle. This arrangement is illustrated by Figure 3, which shows one of the several configurations used. All arcjets were generated by a Thermal Dynamics Corporation F-80 Plasma Flame Torch modified both to accomodate the special nozzle arrangements and to operate with a two-inch-long arc. Detailed experiments performed as part of an Air-Force-sponsored program[17] show improved plasma generator performance with the longer arc, since for a given arc power the current is roughly inversely proportional to arc length. With lower currents a more uniform arcjet is obtained. Figure 4 shows that portion of the plasma generator in which separately cooled constrictor segments have been added to form a longer arc passage.

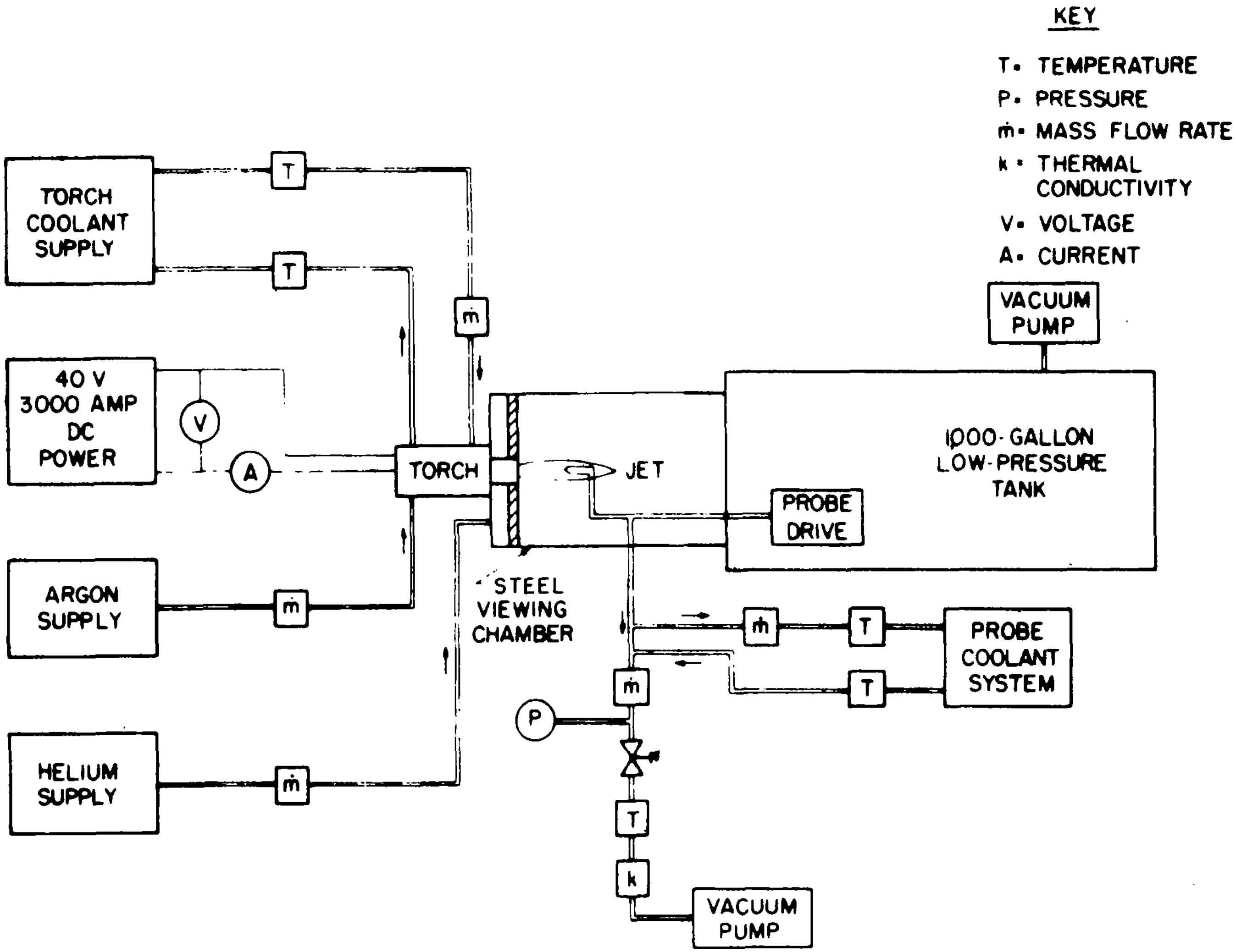

DIAGRAM OF APPARATUS

FIGURE 2

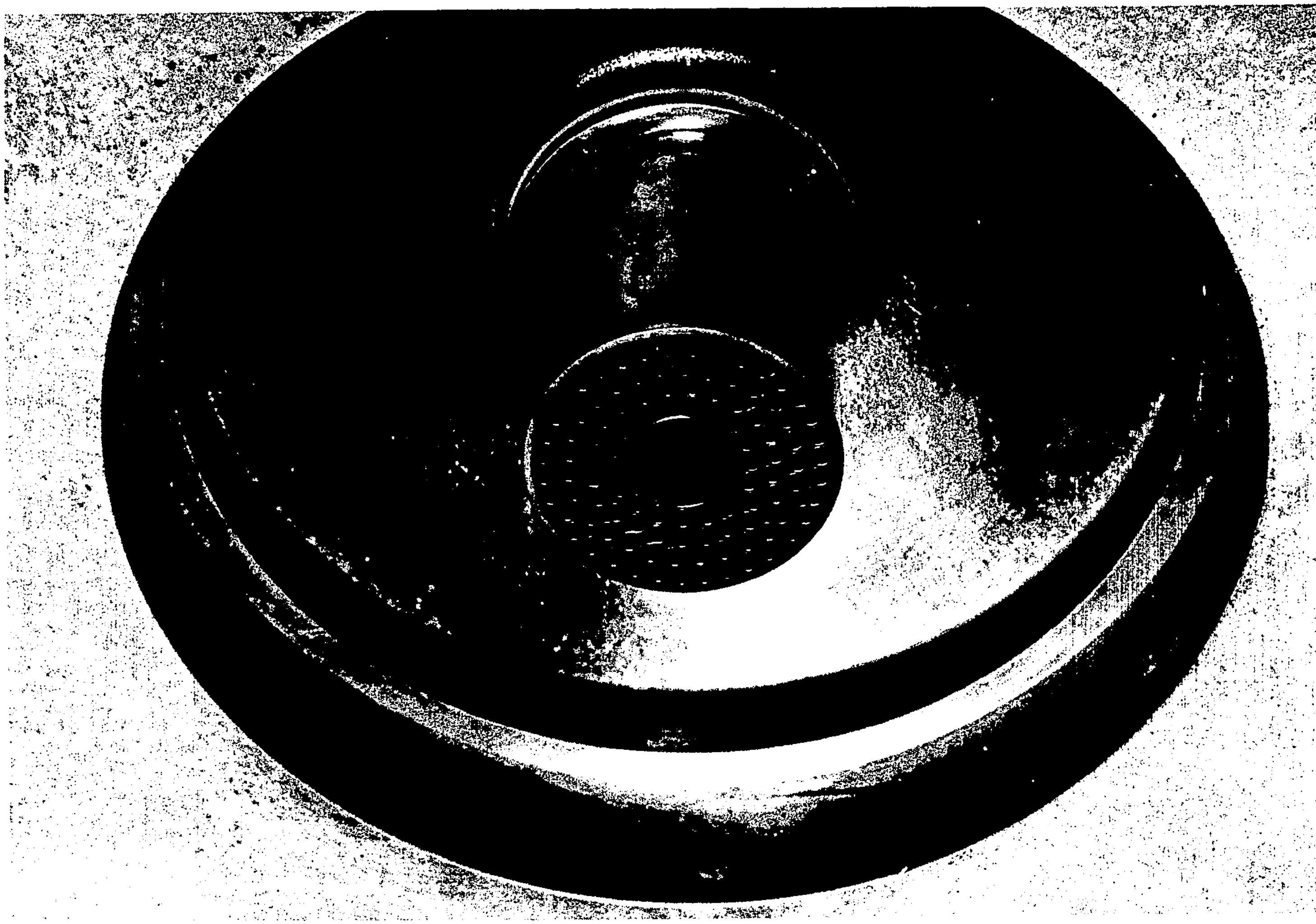

INJECTION PLATE & NOZZLE FOR MODIFIED F-80 ARCJET TORCH
FOR USE WITH HIGH COAXIAL FLOWS

FIGURE 3

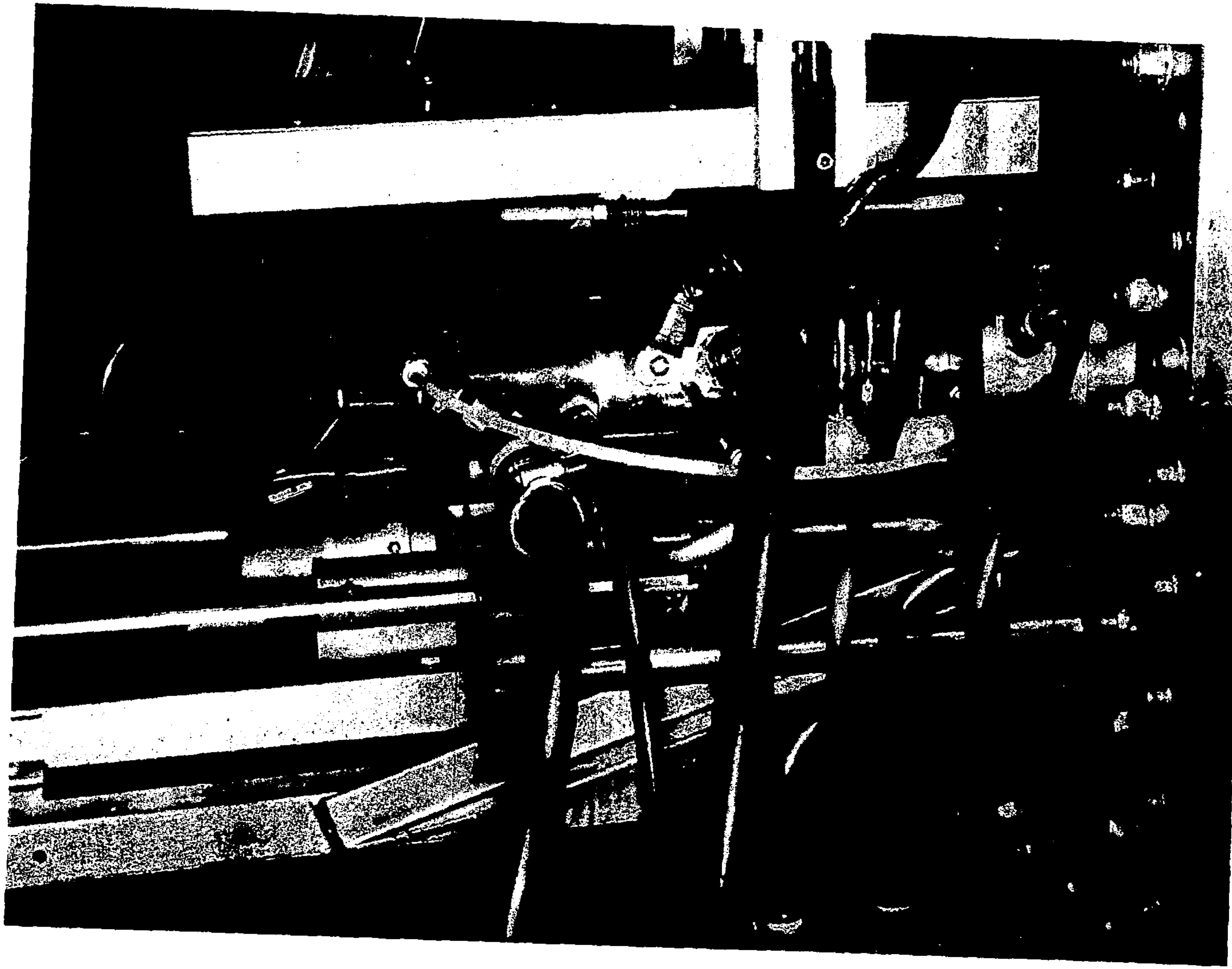

FIGURE 4

MODIFIED F-80 PLASMA GENERATOR

B. Calorimetric Sampling Probe

The calorimetric probe is an instrument which measures enthalpy, stagnation pressure, and composition of gases at temperatures up to 25,000°F. It has been used for some time in arcjet diagnosis, and since it has been described in detail elsewhere,[8-9] only its general nature is outlined here. A photograph of the probe is given in Figure 5.

The construction of the probe itself is of copper, with a brass base. Cooling water from a high-pressure source (up to 1,000 psi) enters through the mounting block, passes through the outer channel to the tip, and leaves via the inner channel. Sheathed, ungrounded thermocouple junctions are located where the probe cooling water flow enters and leaves the sampling tube. A steady flow of sample gas can be drawn by a vacuum pump from the probe tip, through the central tube past a thermocouple junction located in the tube, and then through the support shaft to valving and instrumentation.

The flow of the hot sample gas in the central tube causes the probe cooling water to rise in temperature a greater amount than when the gas sample flow is not permitted to flow through the tube. A flowmeter measures the probe coolant flow and a critical orifice measures the gas flow. These measurements are sufficient to compute the enthalpy of the gas sample at the point where it enters the probe.

The composition of the two-component gas sample is determined by measuring its thermal conductivity in a carefully calibrated commercial cell, and stagnation pressure is measured when the gas sample is not flowing by simply diverting, through appropriate valving, the gas sample line from the vacuum pump to a water manometer. Enthalpy can be converted to temperature, once the gas composition is known, from an equilibrium theory such as the Saha equation. The measured stagnation pressure is converted to velocity using the Bernoulli equation for lower Mach numbers while the compressible flow equation is used for Mach numbers greater than 0.3. The complete data reduction procedure is given in Appendix B.

The sensitivity and calibration of the probe under similar experimental conditions have been described elsewhere.[8-9] In previous work, energy and mass balances showed that the probe's accuracy (standard deviation from the mean) was about 3 per cent.[8]

C. Test Operations

The range of operating variables investigated is given in Table I together with the identification of conditions for the rocket.[18] In all experiments the heavy core flow was simulated by argon and the effect of molecular weight ratio was studied by using either helium or nitrogen as the coaxial flow material. Jet diameters of one and two centimeters were studied with the coaxial flow stream sufficiently wide so that its exterior boundary condition had no effect on the central mixing process for at least two central jet diameters. Jet

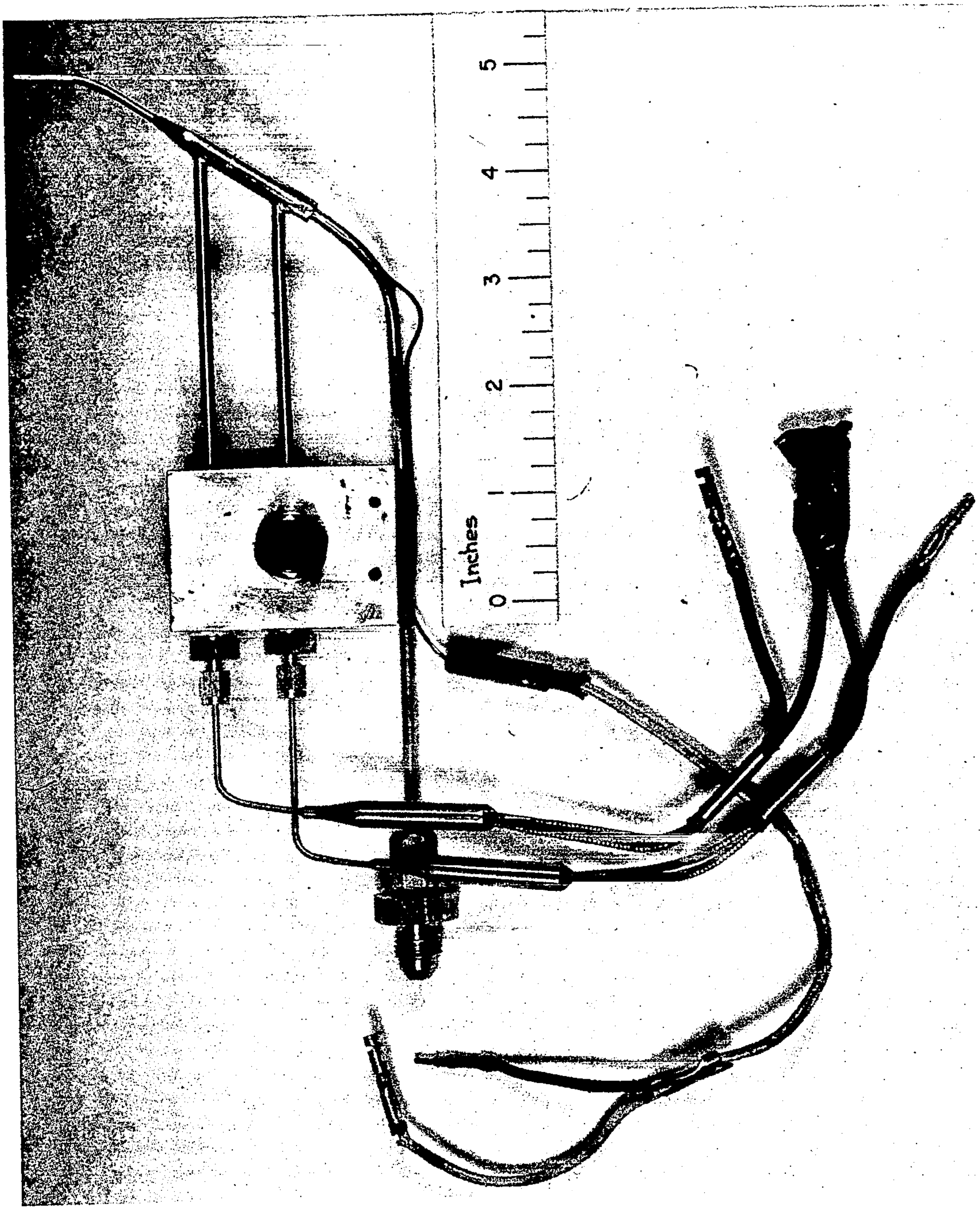

CALORIMETRIC PROBE

FIGURE 5

TABLE I

RANGE OF VARIABLES STUDIED

RUN	COAXIAL VELOCITY ft/sec	COAXIAL FLUID	INJECTOR TYPE	VELOCITY RATIO	JET Re	JET DIAMETER CM	JET INITIAL TEMP., °R
Rocket Concept	25 to 250	Hydrogen	-	35 co 300	10,000 to 40,000		100,000
A-1	100	N_2	1/16 tubes	71	238	1	550
A-2	100	N_2	1/16 "	1.6	7,577	1	550
A-3	100	N_2	1/16 "	0.66	18,748	1	550
A-4	308	N_2	1/8 "	54.97	953	1	550
A-5	305	N_2	1/8 "	12.89	2,939	1	550
A-6	308	N_2	1/8 "	2.85	13,391	1	550
A-7	573	N_2	1/8 "	9.29	10,490	1	550
A-8	563	N_2	1/8 "	9.73	7,185	1	550
A-9	560	N_2	1/8 "	5.19	13,391	1	550
B-1	10	Helium	1/8 "	7.13	238	1	550
B-2	10	Helium	1/8 "	0.17	7,022	1	550
B-3	49	Helium	1/8 "	34.98	238	1	550
B-4	48	Helium	1/8 "	2.31	2,612	1	550
C-1	10	Helium	1/16 "	7.13	238	1	550
C-2	49	Helium	1/16 "	2.07	2,939	1	550
D-1	565	N_2	1/16 "	9.76	7,185	1	550
E-2	780	N_2	1/16	32.96	2,939	1	550
E-3	780	N_2	1/16 "	7.41	13,064	1	550
F-1	0	Helium	1/16 "	0.00	3,919	1	550
F-2	0	Helium	1/16 "	0.00	7,838	1	550
F-3	29	Helium	1/16 "	0.46	7,838	1	550
F-4	1	Helium	1/16 "	0.71	238	1	550

TABLE I
(CONTINUED)

RUN	COAXIAL VELOCITY ft/sec	COAXIAL FLUID	INJECTOR TYPE	VELOCITY RATIO	JET Re	JET DIAMETER CM	JET INITIAL TEMP., °R
F-5	3	Helium	1/16 tubes	1.07	476	1	550
G-1	0	N_2	1/16 "	0.00	7,838	1	550
G-2	1	N_2	1/16 "	0.71	238	1	550
G-3	3	N_2	1/16 "	1.07	476	1	550
P-2	100	N_2	Porous	1.72	7,185	1	550
P-3	100	N_2	Porous	1.72	7,185	1	550
2CA	1	N_2	1/16 "	0.67	636	2	550
2CB	37	N_2	1/16 "	2.87	3,200	2	550
2CC	176	N_2	1/16 "	4.25	10,288	2	550
HA 3	200	N_2	1/16 "	1.19	1,295	1	3496
HA 4	135	N_2	1/16 "	0.96	1,416	1	2922
HA 5	67	N_2	1/16 "	0.46	1,392	1	3025
HA 6	130	N_2	1/16 "	2.22	2,191	1	1221
HA 7	67	Helium	1/16 "	0.42	1,331	1	3309
HA 8	170	N_2	1/16 "	1.21	1,416	1	2926
HA 9	355	N_2	1/16 "	1.22	5,116	1	2017
HA 10	530	N_2	1/16 "	1.11	3,998	1	3302
HA 12	300	N_2	1/16 "	3.63	1,319	1	2158
HA 13	780	N_2	1/16 "	15.21	1,673	1	1340
2HA 1	74	N_2	1/16 "	0.52	1,485	2	4495
2HB 1	45	N_2	1/16 "	0.42	1,007	2	4842
2HB 2	134	N_2	1/16 "	1.41	1,065	2	4329
2HB 3	450	N_2	1/16 "	8.74	1,445	2	2352
2HC 1	27	N_2	1/16 "	0.68	708	2	3157
HP 1	130	N_2	Porous	1.01	1,478	1	2684

temperatures from room temperature to a peak of 9000°R were studied, with jet Reynolds number varying between 10 and 10^4, and coaxial to core velocity ratios ranging from 0 to 780. Three different coaxial-flow injection configurations were also investigated. In total, 47 runs were performed in which composition, velocity and temperature profiles were obtained at the nozzle exit plane, and at downstream locations of 1/2, 1 and 2 nozzle diameters. Because of the great number of different test conditions studied, the number of data points per profile was substantially lower than that usually taken in flow experiments, particularly in the case of high velocity coaxial flows where cost considerations limited the run duration. The use of many different test conditions gives good statistical weight to the empirical correlation developed, although because of limited profile data good agreement between analytical predictions and any single mixing profile cannot always be expected.

Figures 6 and 7 show the nozzle and coaxial flow geometry for the two nozzle diameters studied, and include notation giving flow characteristics of the injection sections used. It can be seen that the nozzle wall has appreciable thickness relative to the nozzle diameter, and was, therefore, tapered at the exit plane. This thickness was necessary to accommodate water cooling passages, but, of course, leads to difficulty in establishing the exact conditions at the nozzle exit plane. However, Schlieren photography has established that

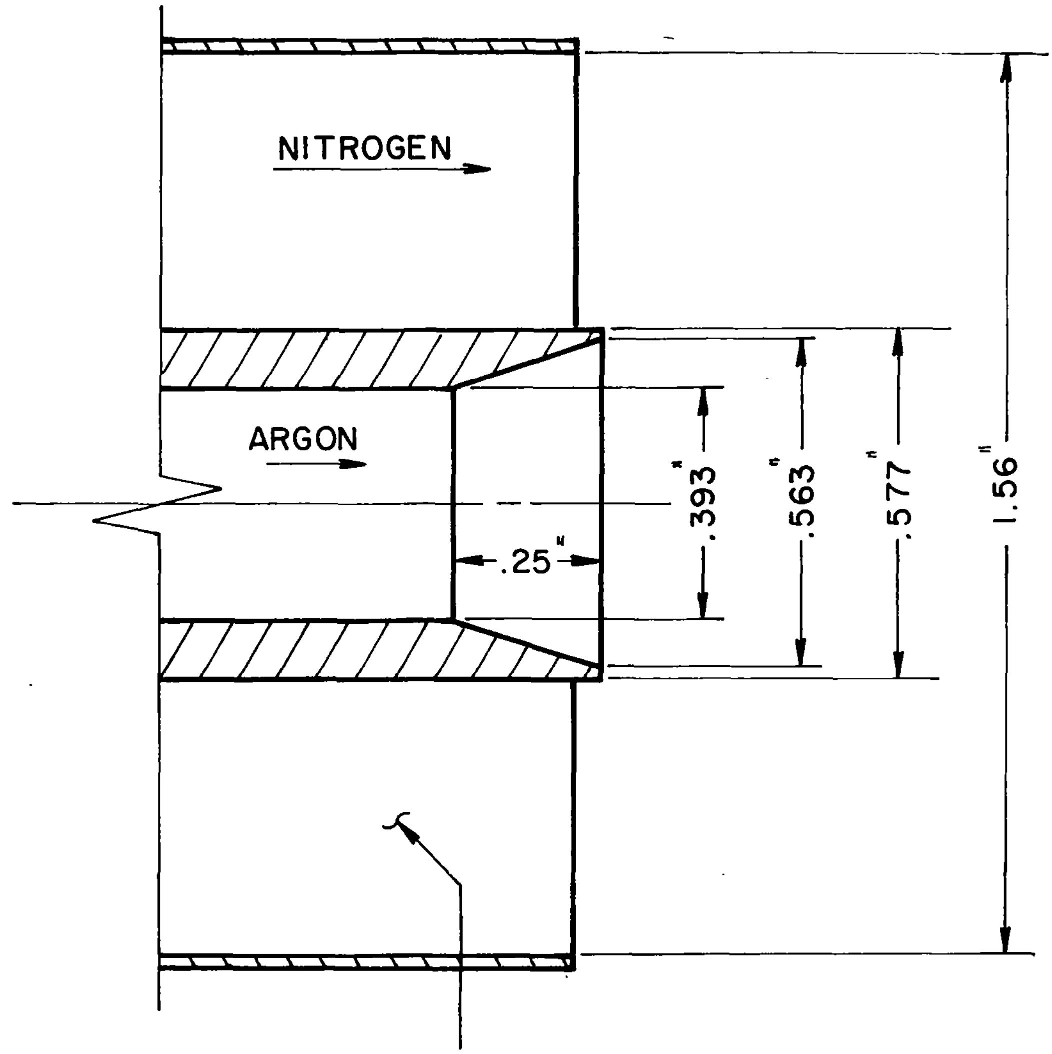

OPTIONAL INJECTOR SECTION

1. $\frac{1}{8}$ TUBE BUNDLE - 104 TUBES, 0.101" ID, 0.125 O.D., OPEN FLOW AREA = 1.47 SQ. IN.

2. $\frac{1}{16}$ TUBE BUNDLE - 447 TUBE, 0.045" I.D., 0.062 OO., OPEN FLOW AREA = 1.04 SQ. IN.

3. POROUS PLUG, $\frac{1}{2}$" THK., 10 MICRONS, AREA = 2.02 SQ. IN.

FLOW INJECTION GEOMETRY – 1CM JET

FIGURE 6

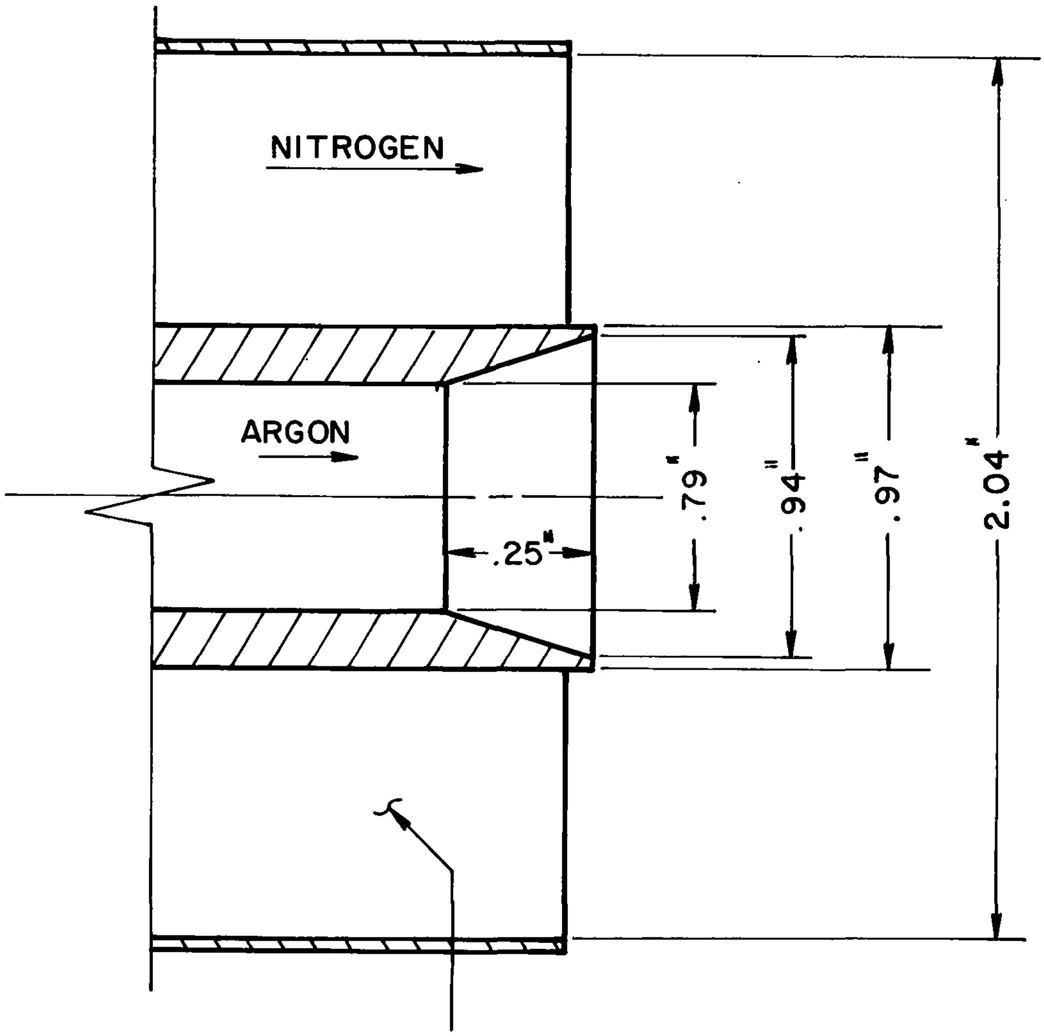

OPTIONAL INJECTOR SECTION

$\frac{1}{16}$ TUBE BUNDLE-618 TUBES, 0.045" ID, 0.062 O.D., OPEN FLOW AREA = 1.09 SQ. IN.

FLOW INJECTION GEOMETRY-2CM JET

FIGURE 7

at jet flow velocities of ten feet per second, no separation occurs and the jet is expanded to the full dimension of the nozzle taper. In those cases studied for which the flow velocity was greater than ten feet per second, the initial jet diameter needed to compute the average initial velocity, was taken as the internal diameter of the nozzle, i.e., it was assumed that the jet separated from the tapered portion of the nozzle.

The effect of the injection tubing on the character of the coaxial flow is illustrated by typical Schlieren photography in Figures 8A and 8B. In Figure 8A, where jet and coaxial velocities were nearly equal, it can be seen that the injection tubing inhibits large-scale turbulence to about one jet diameter downstream. Note that for this case there is visible radiation from the arcjet because mixing has been relatively slow. In Figure 8B, a high-velocity-ratio run, it can be seen that coaxial flow is stratified in individual jets for even a greater distance than the earlier case. Flow concentration caused by the injection tubing has the effect that individual coaxial velocity measurements near the exit plane exceed what would be the average value of the exterior velocity. The average exterior velocity is best represented by the nominal coaxial velocity listed in Table I. The nominal coaxial velocity, later identified as u_e^o was computed from the measured mass flow and the total coaxial flow cross sectional area, not taking account of the flow area occupied by the injection tubes. One or two jet diameters downstream, the

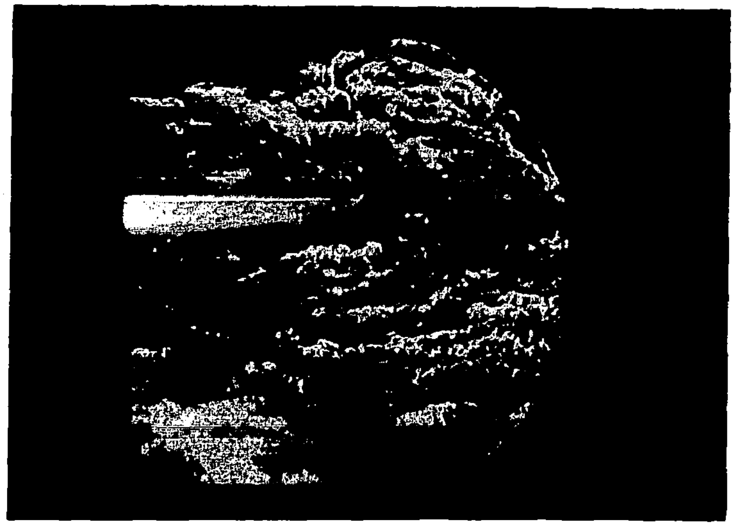

RUN HA-7 NOMINAL COAXIAL VELOCITY 67 FT/SEC VELOCITY RATIO 0.42
8A

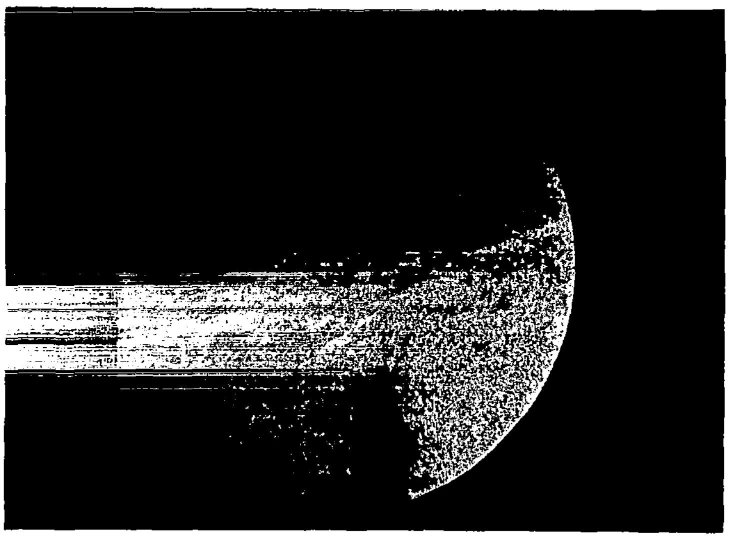

RUN E-2, NOMINAL COAXIAL VELOCITY 780 FT/SEC VELOCITY RATIO 33
8B

SCHLIEREN ILLUSTRATIONS OF MIXING REGION

FIGURE 8

injection flow characteristics vanish, as illustrated by the Schlieren photographs of Figure 8A and 8B and the nominal coaxial velocity, as can be seen from the profile data in Appendix C is the same as the measured value.

D. Electrostatic Probe

Experiments performed under an Air Force contract had shown that a water-cooled electrostatic probe would yield current-voltage characteristics which were influenced by the degree of the jet turbulence.[19] Figure 9 shows a typical current-voltage trace for both laminar and turbulence arcjets. Also under Air Force sponsorship a criterion was developed for predicting electron-heavy-particle non-equilibrium in a cooling arcjet.[20,21] Consequently, work was undertaken in the simulation studies to evaluate the potential of an electrostatic probe as an instrument for quantitatively measuring the degree of turbulence in a mixing arcjet. The electrostatic probe used was the same as the calorimetric probe, except the entire probe surface but for a small region at the tip was electrically insulated with a ceramic coating.

After initial tests it was concluded that the best procedure was not to use the full current-voltage trace as shown in Figure 9, but rather to obtain a signal proportional to the rms value of the probe current when the probe was connected directly to ground (zero applied voltage). In this way the probe current would be proportional to the random current of electrons (the ion random current was shown in Reference 19 to be negligible

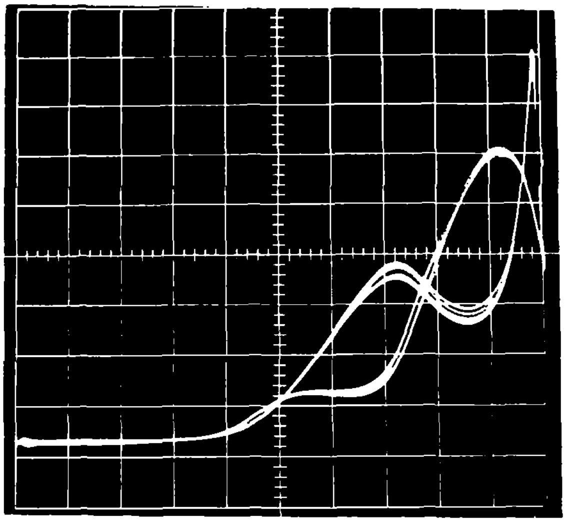

TURBULENT

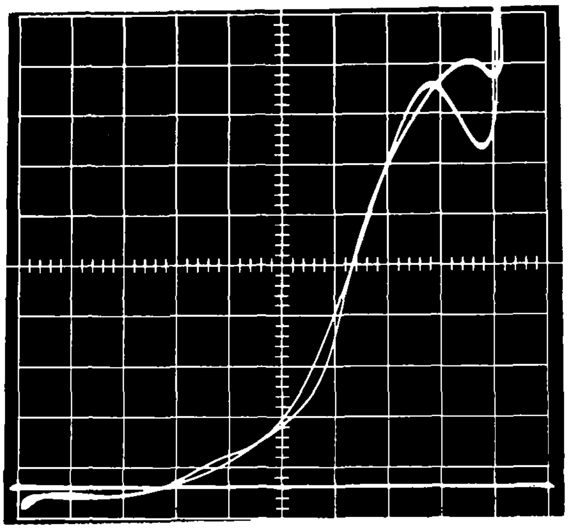

LAMINAR

VOLTAGE-CURRENT TRACES OF AN ELECTROSTATIC PROBE
IN TURBULENT AND LAMINAR ARCJETS

FIGURE 9

by comparison). Thus the measured current is directly proportional to the local number density of the electrons and the square root of their temperatures.

The probe current was observed on a Ballantine rms voltage meter connected across a 10-ohm resistor placed between the probe and ground. Oscillographs of the voltage fluctuation in a laminar and turbulent test case are shown in Figure 10. Similar oscillographs and corresponding rms measurements were obtained for a number of conditions, some corresponding to runs HA-3, HA-4, HA-5, HA-6, HA-8 and HA-12. The repeatable variations observed in the laminar signal were traced to the ripple in the selenium rectifiers supplying power to the arc, and are considered background noise in the measurement.

In spite of the very obvious ability of the electrostatic probe to respond to turbulence, it was not found possible within the scope of the present contract to relate the measurements directly to the relative scale of turbulence. The essence of the problem resides in the fact that at the extremely low temperatures of the mixed jet (usually below 2,000°F), it is not possible to identify the amount of contribution to the probe current from the electron density and the electron temperature. The reason for this is that the ionized fraction at these temperatures is in an extreme nonequilibrium condition.[18] For higher temperatures, if a relationship between temperature and density is known (e.g., the Saha equation), the scale of

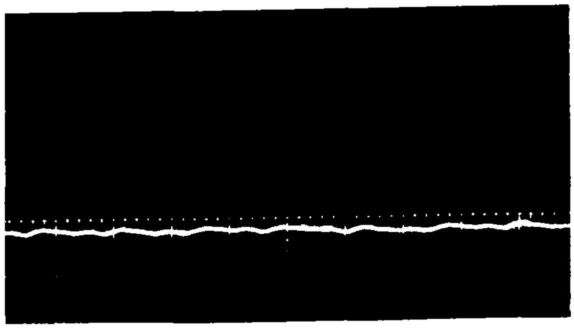

rms VOLTAGE=
23 mv

LAMINAR

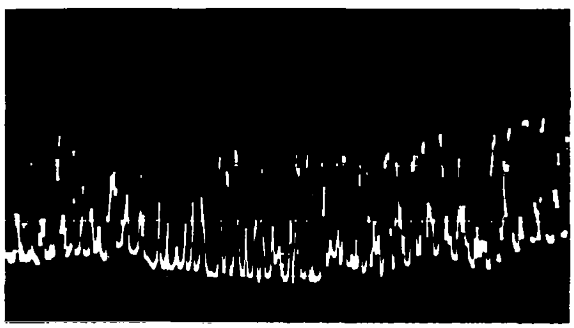

rms VOLTAGE=
360 mv

TURBULENT rms

VERTICAL SENSITIVITY—50 mu/cm
HORIZONTAL SWEEP - 2 msec/cm

RESPONSE OF GROUNDED ELECTROSTATIC PROBE TO LAMINAR AND TURBULENT ARCJETS

FIGURE 10

turbulence could be readily identified in terms of either electron density fluctuations or electron temperature fluctuations. Note that the electrostatic probe does not utilize the same velocity-sensitive-cooling relationship of the conventional hot-wire, and therefore, does not provide the usual velocity correlation measurements.

III. MIXING DATA

Profiles and centerline decay curves of velocity and composition for unheated jets and similar graphs of velocity, composition and temperature for arc-heated jets are presented in Appendix C. Test conditions are identified on the profiles, and details of each test are tabulated on separate pages together with certain other information of use in the empirical correlation to be discussed later.

Because of the necessary limitations on the amount of profile data obtained, the accuracy of individual profiles cannot in general be expected to be as good as the profiles presented in the earlier laminar mixing experiments.[12,13,14] This degradation in individual accuracy is probably more acute in the cases of the higher velocity profiles, since in some cases asymmetries were observed which necessitate adjustment of the location of the jet centerline. As will be seen later, it has been possible to correlate results obtainable from the higher velocity profiles into a single expression, however, so that the random individual errors have been statistically minimized in conclusions regarding the mixing processes involved.

Unlike the cited laminar mixing experiments[12,13,14] and earlier turbulent mixing experiments,[21] the data are not compared with an analytical treatment. Originally it was believed that use could have been made of the detailed machine computation program developed for laminar mixing by modifying the transport properties to include turbulence exchange coefficients. Experimentally it was found; however, that within a few diameter of the nozzle with the high coaxial velocity ratios of greatest interest, there was little resemblance to conventional jet mixing, and use of conventional jet mixing theory would be both fruitless and misleading.

The experimental discrepancy between the present data and what might normally be expected in turbulent jet mixing can be seen from profiles of the higher velocity-ratio experiments, where at the center of the jet exit plane the composition is not pure argon but was measured as a mixture of coaxial gas and jet gas. Also it should be noted that in many cases the measured velocity data have been omitted from the plots. In these cases stagnation pressure measurements in the jet close to the exit plane were highly unsteady, and often even below the static pressure. The physical explanation of such behavior, of course, is that a wake-like flow pattern extends all the way to the jet centerline as a result of complete domination by the high velocity coaxial flow. The presence of this wake phenomenon had not been previously observed or accounted for (e.g., in References 6 or 7), and is an important result of the present experiments. As will be discussed later, understanding of the factors causing and controlling this phenomenon is believed to be the most important remaining question in the fluid mechanics of the coaxial gaseous-core nuclear rocket.

A number of additional phenomena can be observed by inspection of the mixing profiles and are summarized in Table II. The validity of any comprehensive theory which might be established for high-velocity coaxial mixing should be checked against these tabulated observations. That is, any theory must consider that when the coaxial velocity exceeds the jet velocity, the coaxial flow spreads into the jet and the jet material is accelerated. When the jet is heated, this process is augmented because of the reduced density of the cooling jet and the increased diffusion rates of the heated coaxial gas. To this simplified description must be added the effects of the wake phenomena already discussed; e.g., is the wake purely a shear effect, dependent only on velocity ratio and independent of the dimensions of the flow field, or is it a base-drag phenomenon, whose characteristics are a direct function of the jet diameter? Also, we must consider the general effect of turbulence, which, as can be seen from the Schlieren photographs, is not consistent in scale over the mixing region.

IV. SEPARATION RATIO CORRELATION

As we have just seen, any theory using the usual jet mixing techniques is not adequate to predict the flow behavior at high ratios of coaxial to jet velocity with a few diameters of the nozzle. Development of a turbulent wake analysis

TABLE II

GENERAL OBSERVATIONS OF MIXING EXPERIMENTS

1. The dominant mixing process for both heated and unheated jet (core) flows is the acceleration of the core due to the inflow of the exterior gas and the inflow of momentum.

2. Containment of argon within a cylinder defined by nozzle diameter is essentially complete for cases of high velocity exterior (coaxial) flows.

3. Effects of core temperature on composition profiles are observable but not large.

4. Differences in centerline velocity and exterior velocity are well preserved even under widely differing initial flow conditions.

5. Cooling and composition decay are more rapid at higher velocity ratios.

6. Mixing at the same exterior flow velocity is more rapid when the exterior flow injector is a porous plug than when it is either the 1/16 or 1/8 tube bundle.

7. There was no significant effect on mixing caused by using a 1/16 tubing injector in place of a 1/8 inch tubing injector.

8. Decay characteristics are more rapid for 2 cm jets than 1 cm jets.

9. A lower degree of mixing occurs with higher velocity jets.

10. In some cases the "turbulent wake effect" at the exit plane apparently caused reversal of the usual mixing gradients.

of the exit plane region is clearly a portion of the indicated approach, but this work is far beyond the scope of the present program. In view of these theoretical difficulties, an empirical technique has been developed to correlate the data. The value of this approach is primarily to demonstrate the degree of consistency of the data, rather than to establish a model of immediate application to the coaxial flow rocket. The empirical correlation has nevertheless been cast in terms of the separation ratio, because in this way quantities plainly obvious to the feasibility of the coaxial flow rocket can be emphasized.

We have stated previously that the expression for the separation ratio S , for the coaxial rocket is

$$S = \frac{V_c}{V_e}$$

where V_c and V_e are the average velocities of the core (or jet) flow and the exterior (or coaxial) flow respectively. By the methods described in Appendix D, the profile data are used to compute average local values of the core (or jet) velocity u_c , at the exit plane and at the downstream locations of 1/2, 1 and 2 jet diameters and, as we have seen in Section II-C, the average local coaxial velocity u_e is most appropriately taken as the initial nominal coaxial velocity, u_e .

The expression for S_L becomes,

$$S_L = \frac{u_c}{u_e} = \frac{u_c}{u_e^o}$$

S_L is correlated with the various experimental conditions, including the ratio of the length of the core to its initial diameter, Z/D. Then the separation ratio can be found by averaging the local separation ratio over the length of interest:

$$S = \frac{\int_0^L S_L \, dz}{\int_0^L dz}$$

where L would be the chamber length of the gaseous-core rocket (Figure 1). In the simulation experiments, L is simply the final downstream position studied in initial jet diameters.

In order to arrive at correlations for S, all velocity data were first displayed as shown in Figure 11 to determine a region in which correlation is suitable. In this plot the ratio of the local jet velocity u_c to the nominal initial jet velocity u_c^o is plotted against the ratio of the coaxial velocity u_e^o to u_c^o. The plot is in essence the fractional change in core velocity versus the initial velocity ratio. The nominal initial jet velocity u_c^o is computed on the basis of the measured argon mass flow rate, the nozzle cross-sectional flow area and the average jet temperature at the exit plane.

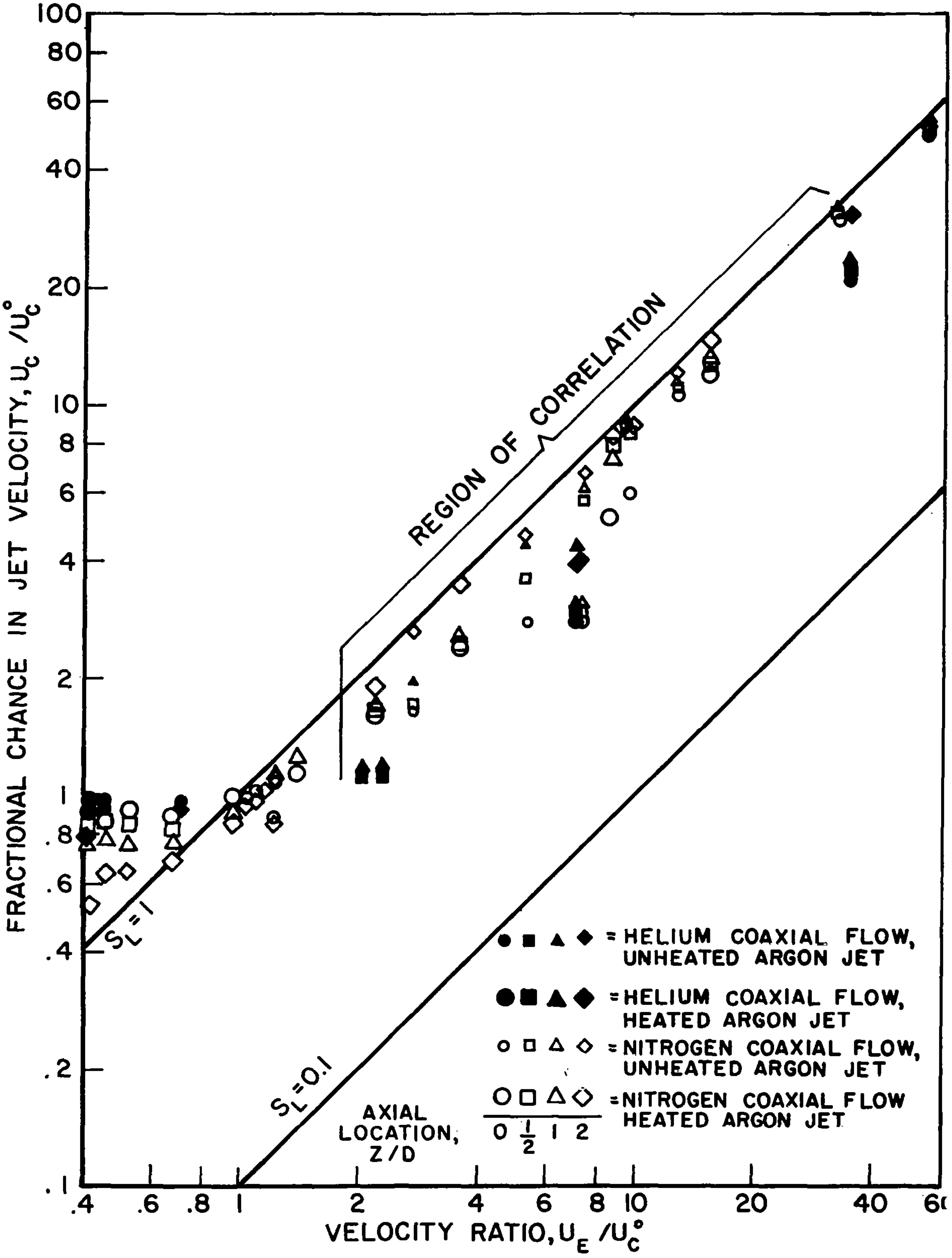

FRACTIONAL CHANGE IN JET VELOCITY vs VELOCITY RATIO

FIGURE 11

The 45° line drawn in this plot represents a separation ratio of unity; i.e., equal core velocity and exterior velocity. When the initial velocity ratio $\frac{u_c}{u_e^\circ}$ exceeds unity, the points fall below the line, i.e., the core must be accelerated to approach the exterior velocity, whereas when $\frac{u_c}{u_e^\circ}$ is less than unity the jet is being decelerated and the points fall above the line. The data with initial velocity ratios greater than two are suitable for correlation because evidently the wake phenomenon which dominates the mixing process has become well developed at this point. Points near a velocity ratio of unity and below are excluded from the correlation, because there is relatively little similarity between the fundamental flow phenomena in these cases and those of the high velocity ratio data. The data obtained in this lower region of velocity ratio were used to complete the picture of the mixing process as described in Table II.

The empirical correlation for values of separation ratio S is based on the following argument. First, if there were no influence by the exterior flow on the core flow, we could define an "uninfluenced" separation ratio, S°

$$S^\circ = \frac{u_c^\circ}{u_e^\circ} = \frac{1}{V_R}$$

where the nominal velocity ratio V_R is defined as the ratio of the nominal coaxial velocity u_e° divided by the nominal initial jet velocity u_c^o . The definition and computational procedure for both the core and exterior nominal initial velocities have been discussed previously.

We now define an "influence function" f such that the actual separation ratio is given by

$$S_L = S^o f$$

Within the scope of the present experiments, this influence function can be empirically expressed as

$$f = f\left(\alpha, V_R, R_c, T_c, \frac{z}{D}, \epsilon\right)$$

where $\alpha = \dfrac{\text{molecular weight of exterior gas}}{\text{molecular weight of core gas (argon)}} = \dfrac{M_e}{M_c}$

V_R = initial velocity ratio

R_c = initial nominal core (jet) Reynolds number

$T_c = \dfrac{\text{initial average core temperature}}{\text{initial temperature of the exterior flow}} = \dfrac{T_c}{T_e}$

z = downstream distance from exit plane

D = initial core diameter

ϵ = exit plane mixing factor

Using data from 14 of the 16 experiments in the region of interest identified in Figure 11, f is determined empirically by

$$f = \epsilon\, \alpha^{0.1} R_c^{0.1} T_c^{0.1} V_R^{1.1} \left(1 + \alpha \epsilon^2 \frac{z}{D}\right)$$

Numerically, the turbulent wake factor ϵ is 0.53 with a statistical probable error of 7%. Appendix E identifies the data used to compute ϵ and lists the computed values. Using this formulation for f , with appropriate numerical values,

$$S_L = [0.53 + \alpha 0.15 \frac{Z}{D}] \alpha^{0.1} \left(\frac{V_R R_c T_c}{1,000}\right)^{0.1}$$

The single most important feature of the resulting correlation is the apparent dominance of exit plane mixing represented by ϵ . This is intuitively apparent from Figure 11 since in spite of the wide range of variables studied all points are relatively close to the diagonal line representing $S_L = 1$. It should be noted that jet Reynolds number, temperature, and velocity ratio have little effect on the calculated value of S_L . Actually, velocity ratio is dominant in the expression for the coaxial flow influence function f , but since the initial velocity ratio itself is the inverse of the initial separation ratio, the velocity ratio appears as a weak term in the expression for S_L . The chief influence of the molecular weight ratio is evidently to diminish almost to insignificance the effects of geometry, as expressed by the ratio of axial position to initial jet diameter.

It is evident then, both from considering the nature of the above correlations and inspection of the profile data, that wake mixing phenomena at the exit plane are strongly dominant in the regime studied, and that normal jet spreading and mixing characteristics are only very weakly present. The factors controlling the influence of these wake phenomena are not obvious from analysis of the data. The delay of large scale turbulence to a point well beyond the exit plane by the injection tubing had little apparent effect on mixing at the exit plane.

Scale, rather than injection techniques, may be the factor determining the degree of the wake mixing effect on separation ratio. The maximum jet diameter studied was two centimeters, and no discernable difference between the one-centimeter jets can be found, although reference to Appendix E does show the values of ϵ at the exit plane for the two-centimeter jets were among the lowest recorded. If increasing scale could be shown to have a truly diminishing affect on ϵ, this knowledge would be of extreme importance to the coaxial flow concept. The present experiments must be regarded as inconclusive in this matter.

The almost negligible effect on the separation ratio of jet Reynolds number and temperature, which are included in the term $V_R R_c T_c$, further emphasizes the fact that at high velocity ratios it is the character of the external flow which dominates the mixing process. It is of some interest, nevertheless, to investigate the product $V_R R_c T_c$. Assuming roughly that the equation of state for a perfect gas is applicable, and that viscosity increases as the square root of temperature, it can be readily shown that

$$V_R R_c T_c = \frac{u_e D P M}{\mu \mathcal{R}\, T_c\, T_e} = \frac{u_e D \bar{\rho}}{\mu}$$

Here P is the pressure, $\mathcal{R}$ is the universal gas constant, and μ is the viscosity taken at a reference temperature T_e. The other terms have been defined previously. Note that the core velocity does not appear, and that the result can be written as a Reynolds number which contains a gas density based on the geometric mean temperature of the core gas and exterior gas. It is seen that even in this relatively weak expression exterior flow properties dominate, and, in particular, the core temperature has only a weak influence on the overall mixing process.

The expression for the overall separation ratio S is obtained as discussed previously:

$$S = \frac{\int_0^L S_L \, dz}{\int_0^L dz} = \left(\epsilon + \frac{\epsilon^3 \alpha L}{2D}\right) \alpha^{0.1} \left(\frac{V_R R_c T_c}{1.000}\right)^{0.1}$$

where L in all cases is the maximum length studied and is equal to 2 initial core diameters.

It is premature to use the above expression to predict the feasibility of the coaxial flow rocket. The present work has chiefly shown that exterior flow characteristics dominate the separation ratio, but has shed little light on the dependence of ϵ on system dimensions. An experiment mainly concerned with exit plane mixing phenomena is indicated at this point, before further arcjet simulation experiments are warranted.

REFERENCES

1. Kerrebrock, J. L. and Meghreblian, R. V., "An Analysis of Vortex Tubes for Combined Gas-Phase Fission Heating and Separation of the Fissionable Material," Oak Ridge National Laboratory Memorandum CF 57-11-3, November 1, 1957, revised April 1958, (See also J. Aerospace Sci., Vol. 28, No. 9, (September 1961), pp. 710-724).

2. Grey, Jerry "A Gaseous-Core Nuclear Rocket Utilizing Hydrodynamic Containment of Fissionable Materials," ARS Preprint 848-859, 1959.

3. Cooper, Ralph S., "Prospects for Advanced High-Thrust Nuclear Propulsion," Astronautics and Aeronautics, January 1966, pp. 54-58.

4. Weinstein, Herbert and Ragsdale, Robert G., "A Coaxial Flow Reactor - a Gaseous Nuclear-Rocket Concept," Presented at ARS 15th Annual Meeting, Washington, D. C., December 1960, ARS Preprint 1518-60.

5. Hyland, Robert E., Ragsdale, Robert G. and Gunn, Eugene, J., "Two-dimensional Criticality Calculations of Gaseous-Core Cylindrical Cavity Reactors," NASA TN D-1575, 1962.

6. Ragsdale, Robert G., Weinstein, Herbert and Lanzo, Chester D., "Correlation of a Turbulent Air-Bromine Coaxial-Flow Experiment," NASA TN D-2121, Lewis Research Center, Cleveland, Ohio, February 1964.

7. Ragsdale, Robert G., "Effects of a Momentum Buffer Region on the Coaxial Flow of Dissimilar Gases," NASA TN D-3138, Lewis Research Center, Cleveland, Ohio, December 1965.

8. Grey, Jerry, Jacobs, Paul F. and Sherman, Martin P., "Calorimetric Probe for the Measurement of Extremely High Temperature," Review of Scientific Instruments, Vol. 33, No. 7, July 1962, pp. 738-741.

9. Grey, Jerry "Sensitivity Analysis for the Calorimetric Probe," Review of Scientific Instruments, Vol. 34, No. 8, August 1963, pp. 857-859.

10. Grey, Jerry and Jacobs, Paul F., "The Cooled Electrostatic Probe," AIAA Paper 66-73, presented at the 3rd Aerospace Sciences Meeting, New York, New York, January 1966.

11. Sherman, Martin P., "Interactions Between a Partly-Ionized Laminar Subsonic Jet and a Cool Stagnant Gas," PhD Thesis, Princeton University, September 1964. Also Princeton University Aeronautical Engineering Laboratory Report No. 707, June 1965.

12. Grey, Jerry, Williams, Peter M. and Fradkin, David B., "Mixing and Heat Transfer of an Argon Arcjet with a Coaxial Flow of Cold Helium," NASA CR-54438, NASA Lewis Research Center, Cleveland, Ohio, October 1964. Also issued as Princeton University Aeronautical Engineering Laboratory Report No. 710, October 1964.

13. Fradkin, David B., "Mixing and Heat Transfer of a Partially Ionized Argon Jet with a Coaxial Flow of Cold Helium," MSE Thesis, Princeton University, June 1965. Also Princeton University Aeronautical Engineering Laboratory Report No. 729, June 1965.

14. Grey, Jerry, Sherman, Martin P., Williams, Peter M. and Fradkin, David B., "Laminar Arcjet Mixing and Heat Transfer: Theory and Experiments," AIAA Journal, Vol. 4, No. 6, June 1966, pp. 986-993.

15. Alpinieri, L. J., "Turbulent Mixing of Coaxial Jets," AIAA Journal, Vol. 2, No. 9, September 1964, pp. 1560-1567.

16. Bussard, R. W. and DeLauer, R. D., Fundamentals of Nuclear Flight, McGraw-Hill, New York, 1965, p. 14.

17. Williams, P. M., Mills, R. G. and Peoples, T. H., "Cathode Power Loss and Performance of a Short, Low Power, Constricted Arc Heater," Seventh Symposium on Engineering Aspects of Magnetohydrodynamics, Princeton, N. J., March 1966, pp. 15-16.

18. Ragsdale, Robert, Letter to Jerry Grey, April 13, 1965.

19. Jacobs, Paul F., "Electron-Heavy Particle Non-Equilibrium in a Dense Argon Plasma," PhD Thesis, Princeton University, Princeton, N. J., May 1966.

20. Jacobs, Paul F. and Grey, Jerry "Criterion for Electron-Heavy Particle Nonequilibrium in a Partly-Ionized Gas," AIAA Paper 66-192. Presented at the AIAA Plasmadynamics Conference, Monterey, California, March 1966.

21. Grey, J. and Jacobs, P. F., "Experiments on Turbulent Mixing in a Partially Ionized Gas," AIAA Journal, Vol. 2, March 1964, pp. 433-438.

22. Rom, Frank "Nuclear Rocket Propulsion", NASA SP-20, NASA Lewis Research Center, Cleveland, Ohio, December 1962, pp. 3-16.

APPENDIX A: List of Symbols

Symbols used in the main body of the report and in Appendix B are listed here. Special symbols used in Appendix D are defined in Figure Appendix D-1.

C_p	Specific heat (Btu/lb-°F)
$\bar{C}_p$	Effective specific heat (Btu/lb-°F)
C^*	Cold helium mole fraction
D	Nozzle diameter (appropriate units)
f	Influence function (dimensionless)
h	Total enthalpy (Btu/lb)
I	Ionization energy per ionization (erg)
k	Boltzmann constant (1.38 x 10^{-16} erg/°K)
L	Chamber length, also maximum downstream location
M	Molecular weight
m	Mass flow rate (gm/sec)
n	Number density
P	Static pressure (psi or dynes/cm^2)
$\mathcal{R}$	Universal gas constant
R	Reynolds number
S	Separation ratio
T	Temperature (°R or °K)
u	Local axial velocity
V	Average axial velocity
V_R	Initial velocity ratio
X_i	Mole fraction of species i

List of Symbols Contd.

$\bar{X}$	$X_{AR} + \frac{M_E}{M_{AR}} + X_E$
z	Axial coordinate

Greek Letters

α	Molecular weight ratio, exterior to core
μ	Viscosity
ρ	Density
ϵ	Exit plane mixing factor
χ	Argon mole fraction

Subscripts

a	Atmosphere
Ar	Argon atoms
AI	Argon atoms and ions
c	Core (jet)
E	Electrons
e	Exterior (coaxial)
L	Local value
1	Exit plane location
2	1/2 Nozzle diameter downstream
3	1 Nozzle diameter downstream
4	2 Nozzle diameters downstream

Superscript

o	Nominal initial conditions

APPENDIX B: Data Reduction

The necessary input data for the computerized data reduction program are the output from the thermal conductivity cell, probe water thermocouples, gas sample exit temperature thermocouple, radial position potentiometer, probe water flow, and critical orifice stagnation pressure. These data were obtained in the following manner:

The probe was aligned optically with the left and right edges of the nozzle to calibrate the radial potentiometer position indicator. The thermal conductivity cell readings for pure argon and pure helium (nitrogen for certain tests) were used to set zero and range on the recording potentiometer. The 1,000-gallon test tank was evacuated and filled with the desired atmosphere.

The probe was then placed at the desired axial position and moved radially through a series of positions, each of which constituted a data "point". After passing through the region of interest the probe was moved to another axial location and the procedure repeated. During the time the gas sample was flowing, recordings were taken of the thermal conductivity cell reading, the gas sample flow rate manometer levels, the probe water differential temperature, and the probe exit gas temperature. When the gas sample was shut off for the "tare" reading, the stagnation pressure manometer indication was also recorded. The torch readings, consisting of coolant flow rate and temperature rise, torch current and voltage, and argon flow rate, all of which remained constant during the taking of a "point", were recorded while waiting for the probe instrumentation to stabilize. The outputs from the thermal conductivity cell, probe water thermocouples, gas sample exit temperature thermocouple, and radial position potentiometer were recorded on Leeds and Northrop recording potentiometers in the Guggenheim Laboratories central recording room. All other data were noted visually from the control panel in the test cell.

The above mentioned data, along with the barometric pressure, were listed on a data sheet from which IBM punched cards were made. The information was then processed on an IBM 1620 computer. The computer output gave values of temperature, velocity, gas composition, degree of ionization, mass flow, and jet power at each data point.

The computer program contained all the necessary calibrations to convert the probe output into useful information. From this information the enthalpy at the probe tip was given by

$$h = \Delta^2 T_w \frac{\dot{m}_w}{\dot{m}_g} + \bar{C}_{go} T_{go}$$

where $\Delta^2 T_w$ was the change in temperature rise of the probe water for the gas "flow" and "no flow" conditions. In a plasma with any degree of ionization the enthalpy is a complex function of temperature and helium mole fraction (nitrogen will be discussed later). It is impossible to compute the temperature directly since the true helium mole fraction in the plasma is not the same as the value measured in the thermal conductivity cell. The two values are related by

$$C^* = (1 - X_E)C$$

The value of X_E is determined, assuming thermal equilibrium and low ionization fractions, by use of the Saha equation

$$K_n = \frac{n_E^2}{n_{AR}} = \frac{X_E^2}{X_{AR}} n = \text{const.}\, T^{3/2} e^{-E_{ION}/kT}$$

Define

$$K_x = \frac{X_E^2}{X_{AR}} = \frac{K_n}{n}$$

Assuming a perfect gas,

$$P = nkT$$

and

$$K_x = \frac{X_E^2}{X_{AR}} = \frac{K_n k T}{P}$$

Putting in the values for argon gives:

$$K_x = 2.309 \times 10^{-6}\, T^{2.551}\, e^{-1.8282 \times 10^5 / T}$$

From continuity

$$X_A + 2X_E = 1 - C^*$$

Thus $$X_E = -K_x + \sqrt{K_x^2 + K_\lambda(1 - C^*)}$$

By assuming initial values of T and C*, the composition and enthalpy are computed. The computed values of enthalpy and "cold" (cell reading) helium mole fraction are compared to the known experimental values. Using a Newton-Raphson technique, the actual temperature and composition are obtained by iterating until computed and experimental values agree. A flow diagram from the temperature determination loop is given at the end of this Appendix.

The procedure for determining the temperature when the secondary gas was nitrogen was essentially the same; however, several added problems arise. The secondary gas can now dissociate and ionize, and the specific heat is now a function of temperature. In order to simplify the calculations it was assumed that the nitrogen would not ionize, since only very small amounts of nitrogen would be found in the regions of the jet hot enough to cause any measurable degree of ionization. This assumption was verified experimentally.

The amount of dissociated nitrogen was determined from the relations:

$$\frac{[n_N]^2}{[n_{N_2}]} = \frac{K_s}{K_R} = K_n$$

$$K_x = \frac{K_n}{n} = \frac{kT}{p} K_n$$

Putting in the values for nitrogen gives:

$$K_x = \frac{[X_N]^2}{[X_{N_2}]} = 1.57 \times 10^3 \frac{T}{P_a} e^{-113,200/T}$$

From continuity

$$\frac{[X_N]^2}{K_x} + X_N = X^*_{N_2}$$

where

$X^*_{N_2}$ is the mole fraction of nitrogen as read by the thermal conductivity cell.

Thus:

$$X_N = -\frac{K_x}{2} + \frac{1}{2}\sqrt{K_x^2 + 4K_x X^*_{N_2}}$$

Since the enthalpy of the sample gas must be computed theoretically, the enthalpy of the nitrogen was calculated as follows:

$$C_V = C_V \text{ translation} + C_V \text{ rotation} + C_V \text{ vibration} + C_V \text{ excitation}$$

$$C_V \text{ translation} = \frac{3}{2} R$$

$$C_V \text{ rotation} = R$$

$$C_V \text{ vibration} = \sum_i \frac{R\left(\frac{\Theta_i}{T}\right)^2 e^{\Theta_i/T}}{\left(e^{\Theta_i/T} - 1\right)^2}$$

where for nitrogen $\Theta_i^i = 3400\,^\circ K$

$$C_p = C_V + R$$

Thus $$C_p = \frac{7}{2}R + \sum \frac{R(3400/T)^2 e^{3400/T}}{(e^{3400/T}-1)^2} + C_{V\,EXCITATION}$$

where C_V excitation was determined from tabulated data.

By definition:

$$H = C_p (T)\, dT$$

Defining an effective specific heat

$$\bar{C}_p = \int_0^T C_p (T')\, dT'/T$$

$$H = \bar{C}_p T$$

$\bar{C}_p$ was computed by numerical integration of the above definitions.

Knowing the temperature and composition, the density was computed using the perfect gas law. Velocity could then be computed using the Bernoulli equation or the equation for compressible flow, as appropriate.

Figure B-1

TEMPERATURE LOOP
FLOW DIAGRAM

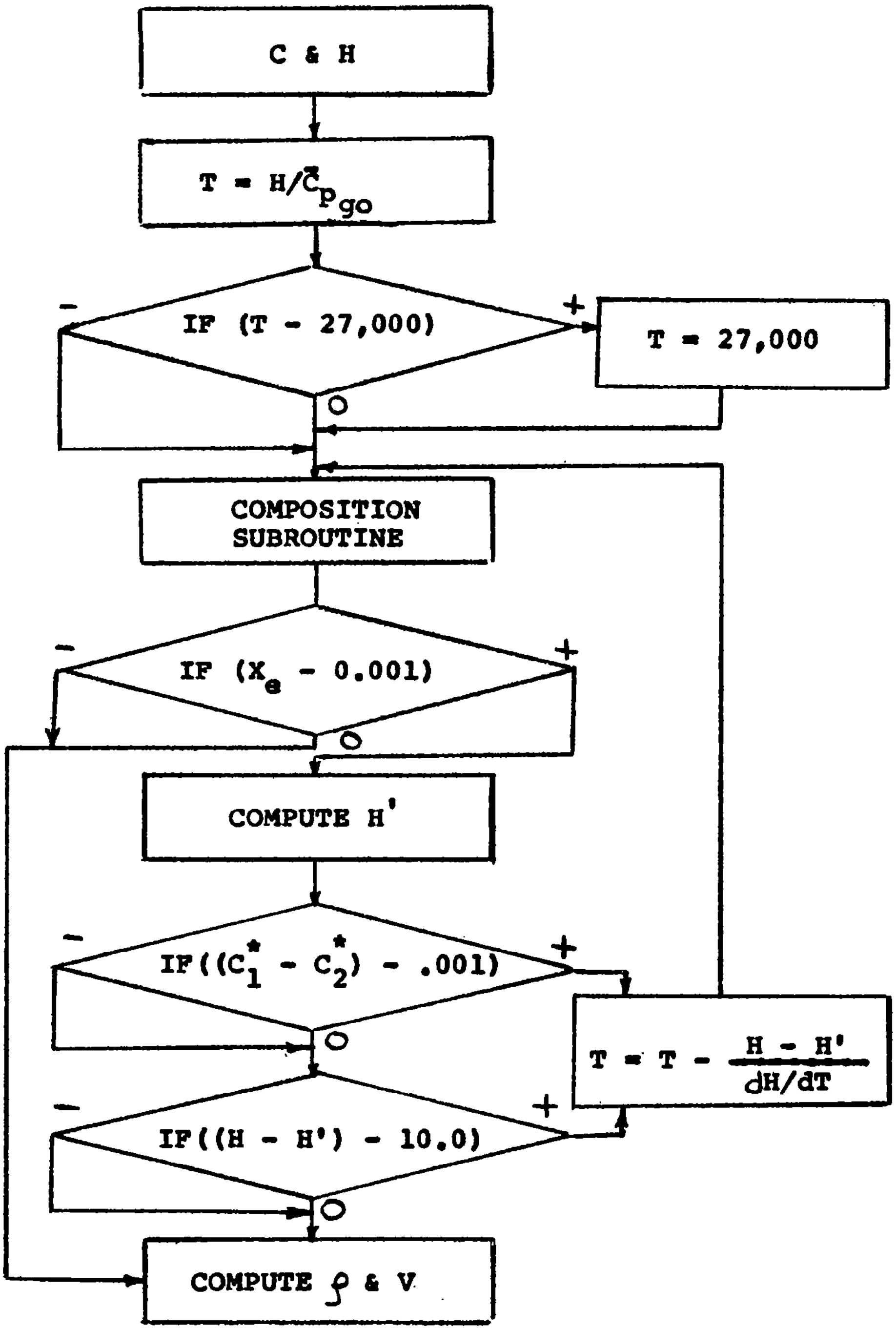

APPENDIX C: Mixing Data

Conditions for each experiment together with the coordinates used in obtaining average characteristics are tabulated separately, mixing profiles for each run are then presented.

Runs E-1, G-4, G-5, H-1, and H-2 were not used in the correlation developed and are not listed in Table I. These mixing profiles are included, however, for information purposes.

DATA SUMMARY, JET - COAXIAL FLOW MIXING EXPERIMENTS

RUN NO. A-1

NOZZLE DIAMETER= 1. CM ARGON MASS FLOW= .10GM/SEC
COAXIAL FLOW GAS-NITROGEN NOMINAL COAXIAL VELOCITY= 100.FT/SEC
FLOW STRAIGHTENOR TUBE DIAM.,1/16 IN.

NOMINAL INITIAL CONDITIONS

JET VELOCITY 1.4FT/SEC JET REYNOLDS NO. 238.
VELOCITY RATIO 71.39

PROFILE COORDINATES

AXIAL POSITION NOZZLE (DIAMETERS)	P	Q	S	T	A	G	B
EXIT	0.	0.	0.000	0.	.890	.011	.200
1/2	0.	0.	0.000	0.	.905	.010	.330
1	0.	0.	0.000	0.	.925	.008	.220
2	0.	0.	0.000	0.	.980	.002	.100

AVERAGE CHARACTERISTICS OF JET COLUMN

AXIAL POSITION (NOZZLE DIAMS)	EXIT	1/2	1	2
VELOCITY, FT/SEC	96.	96.	97.	99.
LOCAL SEPARATION RATIO	.96	.96	.97	.99
ARGON MOLE FRACTION	.05403	.05401	.03790	.00883
TEMPERATURE, R	550.	550.	550.	550.
TEMPERATURE RATIO	1.00000	1.00000	1.00000	1.00000

DATA SUMMARY, JET - COAXIAL FLOW MIXING EXPERIMENTS

RUN NO. A-2

NOZZLE DIAMETER= 1. CM ARGON MASS FLOW= 2.32GM/SEC
COAXIAL FLOW GAS-NITROGEN NOMINAL COAXIAL VELOCITY= 100.FT/SEC
FLOW STRAIGHTENOR TUBE DIAM.,1/16 IN.

NOMINAL INITIAL CONDITIONS

JET VELOCITY 60.9FT/SEC JET REYNOLDS NO. 7577.
VELOCITY RATIO 1.63

PROFILE COORDINATES

AXIAL POSITION NOZZLE (DIAMETERS)	P	Q	S	T	A	G	B
EXIT	0.	0.	0.000	0.	.110	.089	.410
1/2	0.	0.	0.000	0.	.285	.071	.450
1	0.	0.	0.000	0.	.535	.046	.520
2	0.	0.	0.000	0.	.825	.017	.380

AVERAGE CHARACTERISTICS OF JET COLUMN

AXIAL POSITION (NOZZLE DIAMS)	EXIT	1/2	1	2
VELOCITY, FT/SEC	77.	80.	86.	95.
LOCAL SEPARATION RATIO	.77	.80	.86	.95
ARGON MOLE FRACTION	.55133	.46300	.32544	.10471
TEMPERATURE, R	550.	550.	550.	550.
TEMPERATURE RATIO	1.00000	1.00000	1.00000	1.00000

DATA SUMMARY, JET - COAXIAL FLOW MIXING EXPERIMENTS

RUN NO. A-3

NOZZLE DIAMETER= 1. CM   ARGON MASS FLOW= 5.74GM/SEC
COAXIAL FLOW GAS-NITROGEN   NOMINAL COAXIAL VELOCITY= 100.FT/SEC
FLOW STRAIGHTENOR TUBE DIAM.,1/16   IN.

NOMINAL INITIAL CONDITIONS

JET VELOCITY 150.9FT/SEC   JET REYNOLDS NO. 18748.
VELOCITY RATIO   .66

PROFILE COORDINATES

AXIAL POSITION NOZZLE (DIAMETERS)	P	Q	S	T	A	G	B
EXIT	0.	0.	0.000	0.	.005	.099	.480
1/2	0.	0.	0.000	0.	.010	.099	.440
1	0.	0.	0.000	0.	.015	.098	.390
2	0.	0.	0.000	0.	.200	.080	.190

AVERAGE CHARACTERISTICS OF JET COLUMN

AXIAL POSITION (NOZZLE DIAMS)	EXIT	1/2	1	2
VELOCITY, FT/SEC	139.	138.	136.	126.
LOCAL SEPARATION RATIO	1.39	1.38	1.36	1.26
ARGON MOLE FRACTION	.66619	.63409	.59661	.38878
TEMPERATURE, R	550.	550.	550.	550.
TEMPERATURE RATIO	1.00000	1.00000	1.00000	1.00000

DATA SUMMARY, JET - COAXIAL FLOW MIXING EXPERIMENTS

RUN NO. A-4

NOZZLE DIAMETER= 1. CM   ARGON MASS FLOW=   .40GM/SEC
COAXIAL FLOW GAS-NITROGEN   NOMINAL COAXIAL VELOCITY= 308.FT/SEC
FLOW STRAIGHTENOR TUBE DIAM.,1/8   IN.

NOMINAL INITIAL CONDITIONS

JET VELOCITY   5.6FT/SEC   JET REYNOLDS NO.   953.
VELOCITY RATIO 54.97

PROFILE COORDINATES

AXIAL POSITION NOZZLE (DIAMETERS)	P	Q	S	T	A	G	B
EXIT	0.	0.	0.000	0.	.730	.027	.270
1/2	0.	0.	0.000	0.	.807	.019	.250
1	0.	0.	0.000	0.	.865	.014	.195
2	0.	0.	0.000	0.	.967	.003	.100

AVERAGE CHARACTERISTICS OF JET COLUMN

AXIAL POSITION (NOZZLE DIAMS)	EXIT	1/2	1	2
VELOCITY, FT/SEC	276.	286.	293.	304.
LOCAL SEPARATION RATIO	.89	.92	.95	.98
ARGON MOLE FRACTION	.14318	.09998	.06622	.01439
TEMPERATURE, R	550.	550.	550.	550.
TEMPERATURE RATIO	1.00000	1.00000	1.00000	1.00000

DATA SUMMARY, JET - COAXIAL FLOW MIXING EXPERIMENTS

RUN NO. A-5

NOZZLE DIAMETER= 1. CM   ARGON MASS FLOW=   .90GM/SEC
COAXIAL FLOW GAS-NITROGEN   NOMINAL COAXIAL VELOCITY= 305.FT/SEC
FLOW STRAIGHTENOR TUBE DIAM.,1/8   IN.

NOMINAL INITIAL CONDITIONS

JET VELOCITY   23.6FT/SEC   JET REYNOLDS NO. 2939.
VELOCITY RATIO 12.89

PROFILE COORDINATES

AXIAL POSITION NOZZLE (DIAMETERS)	P	Q	S	T	A	G	B
EXIT	0.	0.	0.000	0.	.485	.052	.190
1/2	0.	0.	0.000	0.	.650	.035	.190
1	0.	0.	0.000	0.	.707	.029	.195
2	0.	0.	0.000	0.	.930	.007	.175

AVERAGE CHARACTERISTICS OF JET COLUMN

AXIAL POSITION (NOZZLE DIAMS)	EXIT	1/2	1	2
VELOCITY, FT/SEC	251.	268.	274.	297.
LOCAL SEPARATION RATIO	.82	.88	.89	.97
ARGON MOLE FRACTION	.25054	.17009	.14300	.03347
TEMPERATURE, R	550.	550.	550.	550.
TEMPERATURE RATIO	1.00000	1.00000	1.00000	1.00000

DATA SUMMARY, JET - COAXIAL FLOW MIXING EXPERIMENTS

RUN NO. A-6

NOZZLE DIAMETER= 1. CM ARGON MASS FLOW= 4.10GM/SEC
COAXIAL FLOW GAS-NITROGEN NOMINAL COAXIAL VELOCITY= 308.FT/SEC
FLOW STRAIGHTENOR TUBE DIAM.,1/8 IN.

NOMINAL INITIAL CONDITIONS

JET VELOCITY 107.7FT/SEC JET REYNOLDS NO. 13391.
VELOCITY RATIO 2.85

PROFILE COORDINATES

AXIAL POSITION NOZZLE (DIAMETERS)	P	Q	S	T	A	G	B
EXIT	0.	0.	0.000	0.	0.000	.100	.517
1/2	0.	0.	0.000	0.	.018	.098	.480
1	0.	0.	0.000	0.	.135	.087	.395
2	0.	0.	0.000	0.	.775	.023	.390

AVERAGE CHARACTERISTICS OF JET COLUMN

AXIAL POSITION (NOZZLE DIAMS)	EXIT	1/2	1	2
VELOCITY, FT/SEC	176.	184.	209.	282.
LOCAL SEPARATION RATIO	.57	.59	.67	.91
ARGON MOLE FRACTION	.69756	.65751	.52709	.13644
TEMPERATURE, R	550.	550.	550.	550.
TEMPERATURE RATIO	1.00000	1.00000	1.00000	1.00000

DATA SUMMARY, JET - COAXIAL FLOW MIXING EXPERIMENTS

RUN NO. A-7

NOZZLE DIAMETER= 1. CM   ARGON MASS FLOW= 4.40GM/SEC
COAXIAL FLOW GAS-NITROGEN   NOMINAL COAXIAL VELOCITY= 573.FT/SEC
FLOW STRAIGHTENOR TUBE DIAM.,1/8   IN.

NOMINAL INITIAL CONDITIONS

JET VELOCITY 61.6FT/SEC   JET REYNOLDS NO. 10490.
VELOCITY RATIO 9.29

PROFILE COORDINATES

AXIAL POSITION NOZZLE (DIAMETERS)	P	Q	S	T	A	G	B
EXIT	0.	0.	0.000	0.	.860	.014	.100
1/2	0.	0.	0.000	0.	.957	.004	.025
1	0.	0.	0.000	0.	.965	.004	.550
2	0.	0.	0.000	0.	.990	.001	.550

AVERAGE CHARACTERISTICS OF JET COLUMN

AXIAL POSITION (NOZZLE DIAMS)	EXIT	1/2	1	2
VELOCITY, FT/SEC	548.	565.	562.	570.
LOCAL SEPARATION RATIO	.95	.98	.98	.99
ARGON MOLE FRACTION	.06186	.01742	.02529	.00723
TEMPERATURE, R	550.	550.	550.	550.
TEMPERATURE RATIO	1.00000	1.00000	1.00000	1.00000

DATA SUMMARY, JET - COAXIAL FLOW MIXING EXPERIMENTS

RUN NO. A-8

NOZZLE DIAMETER= 1. CM   ARGON MASS FLOW= 2.20GM/SEC
COAXIAL FLOW GAS-NITROGEN   NOMINAL COAXIAL VELOCITY= 563.FT/SEC
FLOW STRAIGHTENOR TUBE DIAM.,1/8 IN.

NOMINAL INITIAL CONDITIONS

JET VELOCITY 57.8FT/SEC   JET REYNOLDS NO. 7185.
VELOCITY RATIO 9.73

PROFILE COORDINATES

AXIAL POSITION NOZZLE (DIAMETERS)	P	Q	S	T	A	G	B
EXIT	0.	0.	0.000	0.	.346	.065	.530
1/2	0.	0.	0.000	0.	.732	.027	.720
1	0.	0.	0.000	0.	.808	.019	.460
2	0.	0.	0.000	0.	.907	.009	.560

AVERAGE CHARACTERISTICS OF JET COLUMN

AXIAL POSITION (NOZZLE DIAMS)	EXIT	1/2	1	2
VELOCITY, FT/SEC	379.	471.	513.	536.
LOCAL SEPARATION RATIO	.67	.83	.91	.95
ARGON MOLE FRACTION	.46280	.23290	.12571	.06804
TEMPERATURE, R	550.	550.	550.	550.
TEMPERATURE RATIO	1.00000	1.00000	1.00000	1.00000

DATA SUMMARY, JET - COAXIAL FLOW MIXING EXPERIMENTS

RUN NO. A-9

NOZZLE DIAMETER= 1. CM   ARGON MASS FLOW= 4.10GM/SEC
COAXIAL FLOW GAS-NITROGEN   NOMINAL COAXIAL VELOCITY= 560.FT/SEC
FLOW STRAIGHTENOR TUBE DIAM.,1/8   IN.

NOMINAL INITIAL CONDITIONS

JET VELOCITY 107.7FT/SEC   JET REYNOLDS NO. 13391.
VELOCITY RATIO 5.19

PROFILE COORDINATES

AXIAL POSITION NOZZLE (DIAMETERS)	P	Q	S	T	A	G	B
EXIT	0.	0.	0.000	0.	.040	.096	.520
1/2	0.	0.	0.000	0.	.330	.067	.500
1	0.	0.	0.000	0.	.650	.035	.540
2	0.	0.	0.000	0.	.830	.017	.470

AVERAGE CHARACTERISTICS OF JET COLUMN

AXIAL POSITION (NOZZLE DIAMS)	EXIT	1/2	1	2
VELOCITY, FT/SEC	297.	385.	464.	516.
LOCAL SEPARATION RATIO	.53	.68	.83	.92
ARGON MOLE FRACTION	.67188	.45867	.25041	.11257
TEMPERATURE, R	550.	550.	550.	550.
TEMPERATURE RATIO	1.00000	1.00000	1.00000	1.00000

DATA SUMMARY, JET - COAXIAL FLOW MIXING EXPERIMENTS

RUN NO. B-1

NOZZLE DIAMETER= 1. CM   ARGON MASS FLOW=   .10GM/SEC
COAXIAL FLOW GAS-HELIUM   NOMINAL COAXIAL VELOCITY= 10.FT/SEC
FLOW STRAIGHTENOR TUBE DIAM.,1/8   IN.

NOMINAL INITIAL CONDITIONS

JET VELOCITY   1.4FT/SEC   JET REYNOLDS NO.   238.
VELOCITY RATIO   7.13

PROFILE COORDINATES

AXIAL POSITION NOZZLE (DIAMETERS)	P	Q	S	T	A	G	B
EXIT	0.	0.	0.000	0.	.257	.074	.275
1/2	0.	0.	0.000	0.	.295	.071	.210
1	0.	0.	0.000	0.	.345	.066	.185
2	0.	0.	0.000	0.	.675	.033	.170

AVERAGE CHARACTERISTICS OF JET COLUMN

AXIAL POSITION (NOZZLE DIAMS)	EXIT	1/2	1	2
VELOCITY, FT/SEC	3.	4.	4.	6.
LOCAL SEPARATION RATIO	.38	.41	.43	.60
ARGON MOLE FRACTION	.39606	.35036	.31687	.15485
TEMPERATURE, R	550.	550.	550.	550.
TEMPERATURE RATIO	1.00000	1.00000	1.00000	1.00000

DATA SUMMARY, JET - COAXIAL FLOW MIXING EXPERIMENTS

RUN NO. B-2

NOZZLE DIAMETER= 1. CM   ARGON MASS FLOW= 2.15GM/SEC
COAXIAL FLOW GAS-HELIUM   NOMINAL COAXIAL VELOCITY= 10.FT/SEC
FLOW STRAIGHTENOR TUBE DIAM.,1/8 IN.

NOMINAL INITIAL CONDITIONS

JET VELOCITY 56.5FT/SEC   JET REYNOLDS NO. 7022.
VELOCITY RATIO .17

PROFILE COORDINATES

AXIAL POSITION NOZZLE (DIAMETERS)	P	Q	S	T	A	G	B
EXIT	0.	0.	0.000	0.	0.000	.100	.280
1/2	0.	0.	0.000	0.	0.000	.100	.250
1	0.	0.	0.000	0.	.005	.099	.220
2	0.	0.	0.000	0.	.060	.094	.210

AVERAGE CHARACTERISTICS OF JET COLUMN

AXIAL POSITION (NOZZLE DIAMS)	EXIT	1/2	1	2
VELOCITY, FT/SEC	54.	54.	53.	53.
LOCAL SEPARATION RATIO	5.43	5.41	5.39	5.36
ARGON MOLE FRACTION	.53618	.51877	.49927	.46681
TEMPERATURE, R	550.	550.	550.	550.
TEMPERATURE RATIO	1.00000	1.00000	1.00000	1.00000

DATA SUMMARY, JET - COAXIAL FLOW MIXING EXPERIMENTS

RUN NO. B-3

NOZZLE DIAMETER= 1. CM   ARGON MASS FLOW=   .10GM/SEC
COAXIAL FLOW GAS-HELIUM   NOMINAL COAXIAL VELOCITY= 49.FT/SEC
FLOW STRAIGHTENOR TUBE DIAM.,1/8   IN.

NOMINAL INITIAL CONDITIONS

JET VELOCITY   1.4FT/SEC   JET REYNOLDS NO.   238.
VELOCITY RATIO 34.98

PROFILE COORDINATES

AXIAL POSITION NOZZLE (DIAMETERS)	P	Q	S	T	A	G	B
EXIT	0.	0.	0.000	0.	.680	.032	.170
1/2	0.	0.	0.000	0.	.725	.028	.180
1	0.	0.	0.000	0.	.775	.023	.190
2	0.	0.	0.000	0.	.965	.004	.550

AVERAGE CHARACTERISTICS OF JET COLUMN

AXIAL POSITION (NOZZLE DIAMS)	EXIT	1/2	1	2
VELOCITY, FT/SEC	29.	30.	32.	43.
LOCAL SEPARATION RATIO	.59	.62	.66	.89
ARGON MOLE FRACTION	.15220	.13248	.10960	.02529
TEMPERATURE, R	550.	550.	550.	550.
TEMPERATURE RATIO	1.00000	1.00000	1.00000	1.00000

DATA SUMMARY, JET - COAXIAL FLOW MIXING EXPERIMENTS

RUN NO. B-4

NOZZLE DIAMETER= 1. CM ARGON MASS FLOW= .80GM/SEC
COAXIAL FLOW GAS-HELIUM NOMINAL COAXIAL VELOCITY= 48.FT/SEC
FLOW STRAIGHTENOR TUBE DIAM.,1/8 IN.

NOMINAL INITIAL CONDITIONS

JET VELOCITY 21.0FT/SEC JET REYNOLDS NO. 2612.
VELOCITY RATIO 2.31

PROFILE COORDINATES

AXIAL POSITION NOZZLE (DIAMETERS)	P	Q	S	T	A	G	B
EXIT	0.	0.	0.000	0.	0.000	.100	.310
1/2	0.	0.	0.000	0.	0.000	.100	.200
1	0.	0.	0.000	0.	0.000	.100	.250
2	0.	0.	0.000	0.	.023	.098	.190

AVERAGE CHARACTERISTICS OF JET COLUMN

AXIAL POSITION (NOZZLE DIAMS)	EXIT	1/2	1	2
VELOCITY, FT/SEC	24.	24.	24.	25.
LOCAL SEPARATION RATIO	.49	.51	.50	.51
ARGON MOLE FRACTION	.55427	.49125	.51877	.47495
TEMPERATURE, R	550.	550.	550.	550.
TEMPERATURE RATIO	1.00000	1.00000	1.00000	1.0000(

DATA SUMMARY, JET - COAXIAL FLOW MIXING EXPERIMENTS

RUN NO. C-1

NOZZLE DIAMETER= 1. CM ARGON MASS FLOW= .10GM/SEC
COAXIAL FLOW GAS-HELIUM NOMINAL COAXIAL VELOCITY= 10.FT/SEC
FLOW STRAIGHTENOR TUBE DIAM.,1/16 IN.

NOMINAL INITIAL CONDITIONS

JET VELOCITY 1.4FT/SEC JET REYNOLDS NO. 238.
VELOCITY RATIO 7.13

PROFILE COORDINATES

AXIAL POSITION NOZZLE (DIAMETERS)	P	Q	S	T	A	G	B
EXIT	0.	0.	0.000	0.	.187	.081	.210
1/2	0.	0.	0.000	0.	.275	.073	.170
1	0.	0.	0.000	0.	.297	.070	.160
2	0.	0.	0.000	0.	.575	.043	.160

AVERAGE CHARACTERISTICS OF JET COLUMN

AXIAL POSITION (NOZZLE DIAMS)	EXIT	1/2	1	2
VELOCITY, FT/SEC	3.	4.	4.	5.
LOCAL SEPARATION RATIO	.38	.41	.42	.54
ARGON MOLE FRACTION	.40358	.34511	.33066	.20028
TEMPERATURE, R	550.	550.	550.	550.
TEMPERATURE RATIO	1.00000	1.00000	1.00000	1.00000

DATA SUMMARY, JET - COAXIAL FLOW MIXING EXPERIMENTS

RUN NO. C-2

NOZZLE DIAMETER= 1. CM   ARGON MASS FLOW=   .90GM/SEC
COAXIAL FLOW GAS-HELIUM   NOMINAL COAXIAL VELOCITY= 49.FT/SEC
FLOW STRAIGHTENOR TUBE DIAM.,1/16   IN.

NOMINAL INITIAL CONDITIONS

JET VELOCITY   23.6FT/SEC   JET REYNOLDS NO. 2939.
VELOCITY RATIO   2.07

PROFILE COORDINATES

AXIAL POSITION NOZZLE (DIAMETERS)	P	Q	S	T	A	G	B
EXIT	0.	0.	0.000	0.	0.000	.100	.370
1/2	0.	0.	0.000	0.	0.000	.100	.350
1	0.	0.	0.000	0.	.007	.099	.260
2	0.	0.	0.000	0.	.123	.088	.170

AVERAGE CHARACTERISTICS OF JET COLUMN

AXIAL POSITION (NOZZLE DIAMS)	EXIT	1/2	1	2
VELOCITY, FT/SEC	26.	26.	26.	28.
LOCAL SEPARATION RATIO	.52	.53	.54	.57
ARGON MOLE FRACTION	.59249	.57945	.52069	.41730
TEMPERATURE, R	550.	550.	550.	550.
TEMPERATURE RATIO	1.00000	1.00000	1.00000	1.00000

DATA SUMMARY, JET - COAXIAL FLOW MIXING EXPERIMENTS

RUN NO. D-1

NOZZLE DIAMETER= 1. CM   ARGON MASS FLOW= 2.20GM/SEC
COAXIAL FLOW GAS-NITROGEN   NOMINAL COAXIAL VELOCITY= 565.FT/SEC
FLOW STRAIGHTENOR TUBE DIAM.,1/16   IN.

NOMINAL INITIAL CONDITIONS

JET VELOCITY   57.8FT/SEC   JET REYNOLDS NO. 7185.
VELOCITY RATIO   9.76

PROFILE COORDINATES

AXIAL POSITION NOZZLE (DIAMETERS)	P	Q	S	T	A	G	B
EXIT	0.	0.	0.000	0.	.228	.077	.540
1/2	0.	0.	0.000	0.	.567	.043	.090
1	0.	0.	0.000	0.	.626	.037	.095
2	0.	0.	0.000	0.	.626	.037	.095

AVERAGE CHARACTERISTICS OF JET COLUMN

AXIAL POSITION (NOZZLE DIAMS)	EXIT	1/2	1	2
VELOCITY, FT/SEC	343.	490.	500.	500.
LOCAL SEPARATION RATIO	.60	.86	.88	.88
ARGON MOLE FRACTION	.55235	.18918	.16416	.16416
TEMPERATURE, R	550.	550.	550.	550.
TEMPERATURE RATIO	1.00000	1.00000	1.00000	1.00000

DATA SUMMARY, JET - COAXIAL FLOW MIXING EXPERIMENTS

RUN NO. E-2

NOZZLE DIAMETER= 1. CM   ARGON MASS FLOW=   .90GM/SEC
COAXIAL FLOW GAS-NITROGEN   NOMINAL COAXIAL VELOCITY= 780.FT/SEC
FLOW STRAIGHTENOR TUBE DIAM.,1/16   IN.

NOMINAL INITIAL CONDITIONS

JET VELOCITY   23.6FT/SEC   JET REYNOLDS NO.   2939.
VELOCITY RATIO   32.96

PROFILE COORDINATES

AXIAL POSITION NOZZLE (DIAMETERS)	P	Q	S	T	A	G	B
EXIT	0.	0.	0.000	0.	.769	.023	.340
1/2	0.	0.	0.000	0.	.809	.019	.250
1	0.	0.	0.000	0.	.857	.014	.140
2	0.	0.	0.000	0.	.980	.020	.430

AVERAGE CHARACTERISTICS OF JET COLUMN

AXIAL POSITION (NOZZLE DIAMS)	EXIT	1/2	1	2
VELOCITY, FT/SEC	706.	725.	743.	771.
LOCAL SEPARATION RATIO	.90	.92	.95	.98
ARGON MOLE FRACTION	.13233	.09903	.06570	.01602
TEMPERATURE, R	550.	550.	550.	550.
TEMPERATURE RATIO	1.00000	1.00000	1.00000	1.00000

DATA SUMMARY, JET - COAXIAL FLOW MIXING EXPERIMENTS

RUN NO. E-3

NOZZLE DIAMETER= 1. CM   ARGON MASS FLOW= 4.00GM/SEC
COAXIAL FLOW GAS-NITROGEN   NOMINAL COAXIAL VELOCITY= 780.FT/SEC
FLOW STRAIGHTENOR TUBE DIAM.,1/16   IN.

NOMINAL INITIAL CONDITIONS

JET VELOCITY 105.1FT/SEC   JET REYNOLDS NO. 13064.
VELOCITY RATIO   7.41

PROFILE COORDINATES

AXIAL POSITION NOZZLE (DIAMETERS)	P	Q	S	T	A	G	B
EXIT	0.	0.	0.000	0.	.157	.084	.500
1/2	0.	0.	0.000	0.	.397	.060	.280
1	0.	0.	0.000	0.	.516	.048	.230
2	0.	0.	0.000	0.	.820	.036	.380

AVERAGE CHARACTERISTICS OF JET COLUMN

AXIAL POSITION (NOZZLE DIAMS)	EXIT	1/2	1	2
VELOCITY, FT/SEC	462.	605.	647.	718.
LOCAL SEPARATION RATIO	.59	.77	.82	.92
ARGON MOLE FRACTION	.57709	.32319	.24545	.11275
TEMPERATURE, R	550.	550.	550.	550.
TEMPERATURE RATIO	1.00000	1.00000	1.00000	1.00000

DATA SUMMARY, JET - COAXIAL FLOW MIXING EXPERIMENTS

RUN NO. F-1

NOZZLE DIAMETER= 1. CM   ARGON MASS FLOW= 1.20GM/SEC
COAXIAL FLOW GAS-HELIUM   NOMINAL COAXIAL VELOCITY= 0.FT/SEC
FLOW STRAIGHTENOR TUBE DIAM.,1/16 IN.

NOMINAL INITIAL CONDITIONS

JET VELOCITY 31.5FT/SEC   JET REYNOLDS NO. 3919.
VELOCITY RATIO 0.00

PROFILE COORDINATES

AXIAL POSITION NOZZLE (DIAMETERS)	P	Q	S	T	A	G	B
EXIT	0.	0.	0.000	0.	0.000	.100	.390
1/2	0.	0.	0.000	0.	0.000	.100	.370
1	0.	0.	0.000	0.	0.000	.100	.315
2	0.	0.	0.000	0.	.020	.098	.185

AVERAGE CHARACTERISTICS OF JET COLUMN

AXIAL POSITION (NOZZLE DIAMS)	EXIT	1/2	1	2
VELOCITY, FT/SEC	30.	30.	30.	29.
LOCAL SEPARATION RATIO	3.05	3.05	3.03	2.98
ARGON MOLE FRACTION	.60583	.59249	.55735	.46229
TEMPERATURE, R	550.	550.	550.	550.
TEMPERATURE RATIO	1.00000	1.00000	1.00000	1.00000

DATA SUMMARY, JET - COAXIAL FLOW MIXING EXPERIMENTS

RUN NO. F-2

NOZZLE DIAMETER= 1. CM   ARGON MASS FLOW= 2.40GM/SEC
COAXIAL FLOW GAS-HELIUM   NOMINAL COAXIAL VELOCITY=   0.FT/SEC
FLOW STRAIGHTENOR TUBE DIAM.,1/16   IN.

NOMINAL INITIAL CONDITIONS

JET VELOCITY   63.0FT/SEC   JET REYNOLDS NO. 7838.
VELOCITY RATIO   0.00

PROFILE COORDINATES

AXIAL POSITION NOZZLE (DIAMETERS)	P	Q	S	T	A	G	B
EXIT	0.	0.	0.000	0.	0.000	.100	.430
1/2	0.	0.	0.000	0.	0.000	.100	.375
1	0.	0.	0.000	0.	0.000	.100	.260
2	0.	0.	0.000	0.	.055	.095	.175

AVERAGE CHARACTERISTICS OF JET COLUMN

AXIAL POSITION (NOZZLE DIAMS)	EXIT	1/2	1	2
VELOCITY, FT/SEC	61.	61.	60.	59.
LOCAL SEPARATION RATIO	6.13	6.10	6.04	5.91
ARGON MOLE FRACTION	.63341	.59579	.52450	.42048
TEMPERATURE, R	550.	550.	550.	550.
TEMPERATURE RATIO	1.00000	1.00000	1.00000	1.00000

DATA SUMMARY, JET - COAXIAL FLOW MIXING EXPERIMENTS

RUN NO. F-3

NOZZLE DIAMETER= 1. CM   ARGON MASS FLOW= 2.40GM/SEC
COAXIAL FLOW GAS-HELIUM   NOMINAL COAXIAL VELOCITY= 29.FT/SEC
FLOW STRAIGHTENOR TUBE DIAM.,1/16   IN.

NOMINAL INITIAL CONDITIONS

JET VELOCITY 63.0FT/SEC   JET REYNOLDS NO. 7838.
VELOCITY RATIO   .46

PROFILE COORDINATES

AXIAL POSITION NOZZLE (DIAMETERS)	P	Q	S	T	A	G	B
EXIT	0.	0.	0.000	0.	0.000	.100	.320
1/2	0.	0.	0.000	0.	0.000	.100	.285
1	0.	0.	0.000	0.	0.000	.100	.225
2	0.	0.	0.000	0.	.135	.087	.170

AVERAGE CHARACTERISTICS OF JET COLUMN

AXIAL POSITION (NOZZLE DIAMS)	EXIT	1/2	1	2
VELOCITY, FT/SEC	61.	61.	60.	59.
LOCAL SEPARATION RATIO	2.09	2.09	2.08	2.05
ARGON MOLE FRACTION	.56045	.53915	.50477	.41170
TEMPERATURE, R	550.	550.	550.	550.
TEMPERATURE RATIO	1.00000	1.00000	1.00000	1.00000

DATA SUMMARY, JET - COAXIAL FLOW MIXING EXPERIMENTS

RUN NO. F-4

NOZZLE DIAMETER= 1. CM ARGON MASS FLOW= .10GM/SEC
COAXIAL FLOW GAS-HELIUM NOMINAL COAXIAL VELOCITY= 1.FT/SEC
FLOW STRAIGHTENOR TUBE DIAM.,1/16 IN.

NOMINAL INITIAL CONDITIONS

JET VELOCITY 1.4FT/SEC JET REYNOLDS NO. 238.
VELOCITY RATIO .71

PROFILE COORDINATES

AXIAL POSITION NOZZLE (DIAMETERS)	P	Q	S	T	A	G	B
EXIT	0.	0.	0.000	0.	.052	.095	.100
1/2	0.	0.	0.000	0.	.130	.087	.085
1	0.	0.	0.000	0.	.252	.075	.100
2	0.	0.	0.000	0.	.467	.053	.095

AVERAGE CHARACTERISTICS OF JET COLUMN

AXIAL POSITION (NOZZLE DIAMS)	EXIT	1/2	1	2
VELOCITY, FT/SEC	1.	1.	1.	1.
LOCAL SEPARATION RATIO	1.35	1.35	1.34	1.31
ARGON MOLE FRACTION	.41900	.37854	.33063	.23411
TEMPERATURE, R	550.	550.	550.	550.
TEMPERATURE RATIO	1.00000	1.00000	1.00000	1.00000

DATA SUMMARY, JET - COAXIAL FLOW MIXING EXPERIMENTS

RUN NO. F-5

NOZZLE DIAMETER= 1. CM   ARGON MASS FLOW=   .20GM/SEC
COAXIAL FLOW GAS-HELIUM   NOMINAL COAXIAL VELOCITY=   3.FT/SEC
FLOW STRAIGHTENOR TUBE DIAM.,1/16   IN.

NOMINAL INITIAL CONDITIONS

JET VELOCITY   2.8FT/SEC   JET REYNOLDS NO.   476.
VELOCITY RATIO   1.07

PROFILE COORDINATES

AXIAL POSITION NOZZLE (DIAMETERS)	P	Q	S	T	A	G	B
EXIT	0.	0.	0.000	0.	0.000	.100	.190
1/2	0.	0.	0.000	0.	0.000	.100	.185
1	0.	0.	0.000	0.	0.000	.100	.185
2	0.	0.	0.000	0.	.027	.097	.150

AVERAGE CHARACTERISTICS OF JET COLUMN

AXIAL POSITION (NOZZLE DIAMS)	EXIT	1/2	1	2
VELOCITY, FT/SEC	2.	2.	2.	2.
LOCAL SEPARATION RATIO	.94	.94	.94	.94
ARGON MOLE FRACTION	.48597	.48336	.48336	.45287
TEMPERATURE, R	550.	550.	550.	550.
TEMPERATURE RATIO	1.00000	1.00000	1.00000	1.00000

DATA SUMMARY, JET - COAXIAL FLOW MIXING EXPERIMENTS

RUN NO. G-1

NOZZLE DIAMETER= 1. CM   ARGON MASS FLOW= 2.40GM/SEC
COAXIAL FLOW GAS-NITROGEN   NOMINAL COAXIAL VELOCITY= 0.FT/SEC
FLOW STRAIGHTENOR TUBE DIAM.,1/16 IN.

NOMINAL INITIAL CONDITIONS

JET VELOCITY 63.0FT/SEC   JET REYNOLDS NO. 7838.
VELOCITY RATIO 0.00

PROFILE COORDINATES

AXIAL POSITION NOZZLE (DIAMETERS)	P	Q	S	T	A	G	B
EXIT	0.	0.	0.000	0.	0.000	.111	.320
1/2	0.	0.	0.000	0.	0.000	.100	.220
1	0.	0.	0.000	0.	.010	.099	.230
2	0.	0.	0.000	0.	.100	.090	.170

AVERAGE CHARACTERISTICS OF JET COLUMN

AXIAL POSITION (NOZZLE DIAMS)	EXIT	1/2	1	2
VELOCITY, FT/SEC	50.	48.	48.	42.
LOCAL SEPARATION RATIO	5.08	4.84	4.82	4.26
ARGON MOLE FRACTION	.56448	.50203	.49705	.37016
TEMPERATURE, R	550.	550.	550.	550.
TEMPERATURE RATIO	1.00000	1.00000	1.00000	1.00000

DATA SUMMARY, JET - COAXIAL FLOW MIXING EXPERIMENTS

RUN NO. G-2

NOZZLE DIAMETER= 1. CM   ARGON MASS FLOW= .10GM/SEC
COAXIAL FLOW GAS-NITROGEN   NOMINAL COAXIAL VELOCITY= 1.FT/SEC
FLOW STRAIGHTENOR TUBE DIAM.,1/16   IN.

NOMINAL INITIAL CONDITIONS

JET VELOCITY 1.4FT/SEC   JET REYNOLDS NO. 238.
VELOCITY RATIO .71

PROFILE COORDINATES

AXIAL POSITION NOZZLE (DIAMETERS)	P	Q	S	T	A	G	B
EXIT	0.	0.	0.000	0.	.005	.099	.125
1/2	0.	0.	0.000	0.	.040	.096	.120
1	0.	0.	0.000	0.	.100	.090	.105
2	0.	0.	0.000	0.	.324	.068	.110

AVERAGE CHARACTERISTICS OF JET COLUMN

AXIAL POSITION (NOZZLE DIAMS)	EXIT	1/2	1	2
VELOCITY, FT/SEC	1.	1.	1.	1.
LOCAL SEPARATION RATIO	1.23	1.22	1.21	1.16
ARGON MOLE FRACTION	.44791	.43309	.39973	.30204
TEMPERATURE, R	550.	550.	550.	550.
TEMPERATURE RATIO	1.00000	1.00000	1.00000	1.00000

DATA SUMMARY, JET - COAXIAL FLOW MIXING EXPERIMENTS

RUN NO. G-3

NOZZLE DIAMETER= 1. CM   ARGON MASS FLOW=   .20GM/SEC
COAXIAL FLOW GAS-NITROGEN   NOMINAL COAXIAL VELOCITY=   3.FT/SEC
FLOW STRAIGHTENOR TUBE DIAM.,1/16   IN.

NOMINAL INITIAL CONDITIONS

JET VELOCITY   2.8FT/SEC   JET REYNOLDS NO.   476.
VELOCITY RATIO   1.07

PROFILE COORDINATES

AXIAL POSITION NOZZLE (DIAMETERS)	P	Q	S	T	A	G	B
EXIT	0.	0.	0.000	0.	0.000	.100	.240
1/2	0.	0.	0.000	0.	0.000	.100	.240
1	0.	0.	0.000	0.	0.000	.100	.200
2	0.	0.	0.000	0.	.040	.096	.195

AVERAGE CHARACTERISTICS OF JET COLUMN

AXIAL POSITION (NOZZLE DIAMS)	EXIT	1/2	1	2
VELOCITY, FT/SEC	2.	2.	2.	2.
LOCAL SEPARATION RATIO	.96	.96	.96	.96
ARGON MOLE FRACTION	.51311	.51311	.49125	.46906
TEMPERATURE, R	550.	550.	550.	550.
TEMPERATURE RATIO	1.00000	1.00000	1.00000	1.00000

DATA SUMMARY, JET - COAXIAL FLOW MIXING EXPERIMENTS

RUN NO. P-2

NOZZLE DIAMETER= 1. CM   ARGON MASS FLOW= 2.20GM/SEC
COAXIAL FLOW GAS-NITROGEN   NOMINAL COAXIAL VELOCITY= 100.FT/SEC
FLOW STRAIGHTENOR TUBE DIAM.,POROUS

NOMINAL INITIAL CONDITIONS

JET VELOCITY   57.8FT/SEC   JET REYNOLDS NO. 7185.
VELOCITY RATIO   1.72

PROFILE COORDINATES

AXIAL POSITION NOZZLE (DIAMETERS)	P	Q	S	T	A	G	B
EXIT	0.	0.	0.000	0.	.007	.099	.320
1/2	0.	0.	0.000	0.	.120	.088	.345
1	0.	0.	0.000	0.	.545	.046	.350
2	0.	0.	0.000	0.	.567	.043	.185

AVERAGE CHARACTERISTICS OF JET COLUMN

AXIAL POSITION (NOZZLE DIAMS)	EXIT	1/2	1	2
VELOCITY, FT/SEC	75.	77.	88.	90.
LOCAL SEPARATION RATIO	.75	.77	.88	.90
ARGON MOLE FRACTION	.55642	.50709	.26381	.20913
TEMPERATURE, R	550.	550.	550.	550.
TEMPERATURE RATIO	1.00000	1.00000	1.00000	1.00000

DATA SUMMARY, JET - COAXIAL FLOW MIXING EXPERIMENTS

RUN NO. P-3

NOZZLE DIAMETER= 1. CM   ARGON MASS FLOW= 2.20GM/SEC
COAXIAL FLOW GAS-NITROGEN   NOMINAL COAXIAL VELOCITY= 100.FT/SEC
FLOW STRAIGHTENOR TUBE DIAM.,POROUS

NOMINAL INITIAL CONDITIONS

JET VELOCITY   57.8FT/SEC   JET REYNOLDS NO. 7185.
VELOCITY RATIO   1.72

PROFILE COORDINATES

AXIAL POSITION NOZZLE (DIAMETERS)	P	Q	S	T	A	G	B
EXIT	0.	0.	0.000	0.	.020	.098	.380
1/2	0.	0.	0.000	0.	.195	.080	.520
1	0.	0.	0.000	0.	.482	.052	.390
2	0.	0.	0.000	0.	.735	.027	.185

AVERAGE CHARACTERISTICS OF JET COLUMN

AXIAL POSITION (NOZZLE DIAMS)	EXIT	1/2	1	2
VELOCITY, FT/SEC	74.	75.	85.	94.
LOCAL SEPARATION RATIO	.74	.75	.85	.94
ARGON MOLE FRACTION	.58714	.56340	.31387	.12835
TEMPERATURE, R	550.	550.	550.	550.
TEMPERATURE RATIO	1.00000	1.00000	1.00000	1.00000

DATA SUMMARY, JET - COAXIAL FLOW MIXING EXPERIMENTS

RUN NO. 2CA

NOZZLE DIAMETER= 2. CM   ARGON MASS FLOW=   .39GM/SEC
COAXIAL FLOW GAS-NITROGEN   NOMINAL COAXIAL VELOCITY=   1.FT/SEC
FLOW STRAIGHTENOR TUBE DIAM.,1/16   IN.

NOMINAL INITIAL CONDITIONS

JET VELOCITY   2.5FT/SEC   JET REYNOLDS NO.   636.
VELOCITY RATIO   .67

PROFILE COORDINATES

AXIAL POSITION NOZZLE (DIAMETERS)	P	Q	S	T	A	G	B
EXIT	0.	0.	0.000	0.	0.000	.100	1.750
1/2	0.	0.	0.000	0.	0.000	.100	1.320
1	0.	0.	0.000	0.	.020	.100	1.050
2	0.	0.	0.000	0.	.125	.087	.790

AVERAGE CHARACTERISTICS OF JET COLUMN

AXIAL POSITION (NOZZLE DIAMS)	EXIT	1/2	1	2
VELOCITY, FT/SEC	2.	2.	2.	2.
LOCAL SEPARATION RATIO	1.44	1.39	1.35	1.30
ARGON MOLE FRACTION	.84114	.69964	.60980	.48535
TEMPERATURE, R	550.	550.	550.	550.
TEMPERATURE RATIO	1.00000	1.00000	1.00000	1.0000

DATA SUMMARY, JET - COAXIAL FLOW MIXING EXPERIMENTS

RUN NO. 2CB

NOZZLE DIAMETER= 2. CM   ARGON MASS FLOW= 1.96GM/SEC
COAXIAL FLOW GAS-NITROGEN   NOMINAL COAXIAL VELOCITY= 37.FT/SEC
FLOW STRAIGHTENOR TUBE DIAM.,1/16   IN.

NOMINAL INITIAL CONDITIONS

JET VELOCITY   12.8FT/SEC   JET REYNOLDS NO. 3200.
VELOCITY RATIO   2.87

PROFILE COORDINATES

AXIAL POSITION NOZZLE (DIAMETERS)	P	Q	S	T	A	G	B
EXIT	0.	0.	0.000	0.	.050	.095	1.999
1/2	0.	0.	0.000	0.	.500	.050	1.999
1	0.	0.	0.000	0.	.620	.040	1.999
2	0.	0.	0.000	0.	.750	.025	1.320

AVERAGE CHARACTERISTICS OF JET COLUMN

AXIAL POSITION (NOZZLE DIAMS)	EXIT	1/2	1	2
VELOCITY, FT/SEC	16.	26.	29.	33.
LOCAL SEPARATION RATIO	.44	.71	.78	.89
ARGON MOLE FRACTION	.88631	.46648	.35319	.17491
TEMPERATURE, R	550.	550.	550.	550.
TEMPERATURE RATIO	1.00000	1.00000	1.00000	1.00000

DATA SUMMARY, JET - COAXIAL FLOW MIXING EXPERIMENTS

RUN NO. 2CC

NOZZLE DIAMETER= 2. CM   ARGON MASS FLOW= 6.30GM/SEC
COAXIAL FLOW GAS-NITROGEN   NOMINAL COAXIAL VELOCITY= 176.FT/SEC
FLOW STRAIGHTENOR TUBE DIAM.,1/16   IN.

NOMINAL INITIAL CONDITIONS

JET VELOCITY 41.4FT/SEC   JET REYNOLDS NO. 10288.
VELOCITY RATIO 4.25

PROFILE COORDINATES

AXIAL POSITION NOZZLE (DIAMETERS)	P	Q	S	T	A	G	B
EXIT	0.	0.	0.000	0.	.900	.010	1.999
1/2	0.	0.	0.000	0.	.920	.008	1.999
1	0.	0.	0.000	0.	.960	.004	1.000
2	0.	0.	0.000	0.	.980	.002	1.000

AVERAGE CHARACTERISTICS OF JET COLUMN

AXIAL POSITION (NOZZLE DIAMS)	EXIT	1/2	1	2
VELOCITY, FT/SEC	165.	167.	173.	174.
LOCAL SEPARATION RATIO	.93	.94	.98	.99
ARGON MOLE FRACTION	.09329	.07463	.02433	.01216
TEMPERATURE, R	550.	550.	550.	550.
TEMPERATURE RATIO	1.00000	1.00000	1.00000	1.0000(

DATA SUMMARY, JET - COAXIAL FLOW MIXING EXPERIMENTS

RUN NO. HA 3

NOZZLE DIAMETER= 1. CM   ARGON MASS FLOW= 1.00GM/SEC
COAXIAL FLOW GAS-NITROGEN   NOMINAL COAXIAL VELOCITY= 200.FT/SEC
FLOW STRAIGHTENOR TUBE DIAM.,1/16   IN.

NOMINAL INITIAL CONDITIONS

JET VELOCITY 167.1FT/SEC   JET REYNOLDS NO. 1295.
VELOCITY RATIO 1.19

PROFILE COORDINATES

AXIAL POSITION NOZZLE (DIAMETERS)	P	Q	S	T	A	G	B
EXIT	9150.	8200.	.270	550.	0.000	.100	1.800
1/2	8460.	7510.	.300	550.	0.000	.100	1.050
1	7250.	6300.	.350	550.	0.000	.100	.750
2	3720.	2770.	.950	550.	.625	.375	.375

AVERAGE CHARACTERISTICS OF JET COLUMN

AXIAL POSITION (NOZZLE DIAMS)	EXIT	1/2	1	2
VELOCITY, FT/SEC	170.	174.	170.	169.
LOCAL SEPARATION RATIO	.85	.87	.85	.84
ARGON MOLE FRACTION	.85900	.62181	.54531	.36621
TEMPERATURE, R	3496.	3277.	2870.	1879.
TEMPERATURE RATIO	6.35726	5.95877	5.21905	3.41801

DATA SUMMARY, JET - COAXIAL FLOW MIXING EXPERIMENTS

RUN NO. HA 4

NOZZLE DIAMETER= 1. CM   ARGON MASS FLOW= 1.00GM/SEC
COAXIAL FLOW GAS-NITROGEN   NOMINAL COAXIAL VELOCITY= 135.FT/SEC
FLOW STRAIGHTENOR TUBE DIAM.,1/16   IN.

NOMINAL INITIAL CONDITIONS

JET VELOCITY 139.6FT/SEC   JET REYNOLDS NO. 1416.
VELOCITY RATIO   .96

PROFILE COORDINATES

AXIAL POSITION NOZZLE (DIAMETERS)	P	Q	S	T	A	G	B
EXIT	7340.	6606.	.300	550.	0.000	.100	1.200
1/2	6550.	5895.	.300	550.	0.000	.100	1.050
1	7000.	6300.	.200	550.	0.000	.100	.600
2	3325.	2992.	.250	550.	.315	.068	.250

AVERAGE CHARACTERISTICS OF JET COLUMN

AXIAL POSITION (NOZZLE DIAMS)	EXIT	1/2	1	2
VELOCITY, FT/SEC	138.	133.	134.	122.
LOCAL SEPARATION RATIO	1.02	.98	.99	.90
ARGON MOLE FRACTION	.66400	.62181	.51100	.30188
TEMPERATURE, R	2922.	2643.	2679.	1480.
TEMPERATURE RATIO	5.31343	4.80712	4.87242	2.69127

DATA SUMMARY, JET - COAXIAL FLOW MIXING EXPERIMENTS

RUN NO. HA 5

NOZZLE DIAMETER= 1. CM ARGON MASS FLOW= 1.00GM/SEC
COAXIAL FLOW GAS-NITROGEN NOMINAL COAXIAL VELOCITY= 67.FT/SEC
FLOW STRAIGHTENOR TUBE DIAM.,1/16 IN.

NOMINAL INITIAL CONDITIONS

JET VELOCITY 144.6FT/SEC JET REYNOLDS NO. 1392.
VELOCITY RATIO .46

PROFILE COORDINATES

AXIAL POSITION NOZZLE (DIAMETERS)	P	Q	S	T	A	G	B
EXIT	6500.	5850.	.600	550.	0.000	.100	1.000
1/2	6250.	5625.	.500	550.	0.000	.100	1.025
1	6100.	5590.	.400	550.	0.000	.100	.775
2	4600.	4140.	.250	550.	.100	.090	.275

AVERAGE CHARACTERISTICS OF JET COLUMN

AXIAL POSITION (NOZZLE DIAMS)	EXIT	1/2	1	2
VELOCITY, FT/SEC	125.	121.	115.	93.
LOCAL SEPARATION RATIO	1.87	1.81	1.71	1.39
ARGON MOLE FRACTION	.60833	.61503	.55128	.40109
TEMPERATURE, R	3025.	2783.	2640.	1917.
TEMPERATURE RATIO	5.50030	5.06060	4.80000	3.48607

DATA SUMMARY, JET - COAXIAL FLOW MIXING EXPERIMENTS

RUN NO. HA 6

NOZZLE DIAMETER= 1. CM   ARGON MASS FLOW= 1.00GM/SEC
COAXIAL FLOW GAS-NITROGEN   NOMINAL COAXIAL VELOCITY= 130.FT/SEC
FLOW STRAIGHTENOR TUBE DIAM.,1/16   IN.

NOMINAL INITIAL CONDITIONS

JET VELOCITY   58.3FT/SEC   JET REYNOLDS NO. 2191.
VELOCITY RATIO   2.22

PROFILE COORDINATES

AXIAL POSITION NOZZLE (DIAMETERS)	P	Q	S	T	A	G	B
EXIT	2300.	2170.	.400	550.	.020	.098	.680
1/2	2180.	1960.	.300	550.	.072	.093	.540
1	1950.	1750.	.300	550.	.150	.085	.560
2	1130.	1020.	.800	550.	.623	.038	.640

AVERAGE CHARACTERISTICS OF JET COLUMN

AXIAL POSITION (NOZZLE DIAMS)	EXIT	1/2	1	2
VELOCITY, FT/SEC	93.	96.	98.	114.
LOCAL SEPARATION RATIO	.71	.74	.75	.88
ARGON MOLE FRACTION	.51839	.46225	.42694	.19613
TEMPERATURE, R	1221.	1102.	1020.	800.
TEMPERATURE RATIO	2.22060	2.00495	1.85545	1.45503

DATA SUMMARY, JET - COAXIAL FLOW MIXING EXPERIMENTS

RUN NO. HA 7

NOZZLE DIAMETER= 1. CM ARGON MASS FLOW= 1.00GM/SEC
COAXIAL FLOW GAS-HELIUM NOMINAL COAXIAL VELOCITY= 67.FT/SEC
FLOW STRAIGHTENOR TUBE DIAM.,1/16 IN.

NOMINAL INITIAL CONDITIONS

JET VELOCITY 158.2FT/SEC JET REYNOLDS NO. 1331.
VELOCITY RATIO .42

PROFILE COORDINATES

AXIAL POSITION NOZZLE (DIAMETERS)	P	Q	S	T	A	G	B
EXIT	7580.	6822.	.500	550.	0.000	.100	.880
1/2	6800.	6120.	.400	550.	0.000	.100	.880
1	6570.	5913.	.400	550.	.040	.096	.840
2	4250.	3830.	.320	550.	.350	.065	.300

AVERAGE CHARACTERISTICS OF JET COLUMN

AXIAL POSITION (NOZZLE DIAMS)	EXIT	1/2	1	2
VELOCITY, FT/SEC	153.	143.	140.	110.
LOCAL SEPARATION RATIO	2.29	2.13	2.09	1.64
ARGON MOLE FRACTION	.57717	.57717	.54447	.29266
TEMPERATURE, R	3309.	2861.	2775.	1849.
TEMPERATURE RATIO	6.01780	5.20242	5.04630	3.36334

DATA SUMMARY, JET - COAXIAL FLOW MIXING EXPERIMENTS

RUN NO. HA 8

NOZZLE DIAMETER= 1. CM ARGON MASS FLOW= 1.00GM/SEC
COAXIAL FLOW GAS-NITROGEN NOMINAL COAXIAL VELOCITY= 170.FT/SEC
FLOW STRAIGHTENOR TUBE DIAM.,1/16 IN.

NOMINAL INITIAL CONDITIONS

JET VELOCITY 139.8FT/SEC JET REYNOLDS NO. 1416.
VELOCITY RATIO 1.21

PROFILE COORDINATES

AXIAL POSITION NOZZLE (DIAMETERS)	P	Q	S	T	A	G	B
EXIT	5625.	5062.	.800	550.	.010	.099	.800
1/2	5050.	4545.	.800	550.	.030	.097	.540
1	4550.	4095.	.400	550.	.115	.088	.360
2	1750.	1680.	1.100	550.	.635	.036	.360

AVERAGE CHARACTERISTICS OF JET COLUMN

AXIAL POSITION (NOZZLE DIAMS)	EXIT	1/2	1	2
VELOCITY, FT/SEC	151.	150.	145.	155.
LOCAL SEPARATION RATIO	.89	.88	.85	.91
ARGON MOLE FRACTION	.55176	.48306	.40819	.16818
TEMPERATURE, R	2926.	2654.	2021.	1254.
TEMPERATURE RATIO	5.32048	4.82606	3.67515	2.28151

DATA SUMMARY, JET - COAXIAL FLOW MIXING EXPERIMENTS

RUN NO. HA 9

NOZZLE DIAMETER= 1. CM   ARGON MASS FLOW= 3.00GM/SEC
COAXIAL FLOW GAS-NITROGEN   NOMINAL COAXIAL VELOCITY= 355.FT/SEC
FLOW STRAIGHTENOR TUBE DIAM.,1/16   IN.

NOMINAL INITIAL CONDITIONS

JET VELOCITY 289.2FT/SEC   JET REYNOLDS NO. 5116.
VELOCITY RATIO   1.22

PROFILE COORDINATES

AXIAL POSITION NOZZLE (DIAMETERS)	P	Q	S	T	A	G	B
EXIT	4100.	3690.	.600	550.	0.000	.100	1.000
1/2	3650.	3300.	.600	550.	.010	.099	.680
1	3150.	2840.	.400	550.	.092	.090	.600
2	2000.	1800.	.200	550.	.380	.062	.280

AVERAGE CHARACTERISTICS OF JET COLUMN

AXIAL POSITION (NOZZLE DIAMS)	EXIT	1/2	1	2
VELOCITY, FT/SEC	311.	309.	301.	310.
LOCAL SEPARATION RATIO	.87	.87	.84	.87
ARGON MOLE FRACTION	.60833	.52368	.46360	.27687
TEMPERATURE, R	2017.	1834.	1500.	1013.
TEMPERATURE RATIO	3.66757	3.33575	2.72848	1.84212

DATA SUMMARY, JET - COAXIAL FLOW MIXING EXPERIMENTS

RUN NO. HA10

NOZZLE DIAMETER= 1. CM   ARGON MASS FLOW= 3.00GM/SEC
COAXIAL FLOW GAS-NITROGEN   NOMINAL COAXIAL VELOCITY= 530.FT/SEC
FLOW STRAIGHTENOR TUBE DIAM.,1/16   IN.

NOMINAL INITIAL CONDITIONS

JET VELOCITY 473.6FT/SEC   JET REYNOLDS NO. 3998.
VELOCITY RATIO 1.11

PROFILE COORDINATES

AXIAL POSITION NOZZLE (DIAMETERS)	P	Q	S	T	A	G	B
EXIT	7650.	6880.	.480	550.	0.000	.100	1.100
1/2	5950.	5350.	.440	550.	.030	.100	.760
1	4850.	4360.	.480	550.	.080	.090	.600
2	3600.	3240.	.360	550.	.320	.065	.280

AVERAGE CHARACTERISTICS OF JET COLUMN

AXIAL POSITION (NOZZLE DIAMS)	EXIT	1/2	1	2
VELOCITY, FT/SEC	490.	464.	455.	464.
LOCAL SEPARATION RATIO	.92	.87	.86	.87
ARGON MOLE FRACTION	.63558	.53244	.46916	.30186
TEMPERATURE, R	3302.	2589.	2207.	1641.
TEMPERATURE RATIO	6.00494	4.70749	4.01338	2.98364

DATA SUMMARY, JET - COAXIAL FLOW MIXING EXPERIMENTS

RUN NO. HA12

NOZZLE DIAMETER= 1. CM ARGON MASS FLOW= .80GM/SEC
COAXIAL FLOW GAS-NITROGEN NOMINAL COAXIAL VELOCITY= 300.FT/SEC
FLOW STRAIGHTENOR TUBE DIAM.,1/16 IN.

NOMINAL INITIAL CONDITIONS

JET VELOCITY 82.5FT/SEC JET REYNOLDS NO. 1319.
VELOCITY RATIO 3.63

PROFILE COORDINATES

AXIAL POSITION NOZZLE (DIAMETERS)	P	Q	S	T	A	G	B
EXIT	4350.	3910.	.640	550.	.180	.082	1.120
1/2	3600.	3240.	.600	550.	.200	.080	.960
1	3050.	2700.	.600	550.	.125	.087	.840
2	800.	740.	.600	550.	.885	.011	.780

AVERAGE CHARACTERISTICS OF JET COLUMN

AXIAL POSITION (NOZZLE DIAMS)	EXIT	1/2	1	2
VELOCITY, FT/SEC	197.	205.	200.	286.
LOCAL SEPARATION RATIO	.65	.68	.66	.95
ARGON MOLE FRACTION	.52576	.47820	.49608	.06334
TEMPERATURE, R	2158.	1807.	1556.	639.
TEMPERATURE RATIO	3.92383	3.28575	2.83030	1.16333

DATA SUMMARY, JET - COAXIAL FLOW MIXING EXPERIMENTS

RUN NO. HA13

NOZZLE DIAMETER= 1. CM ARGON MASS FLOW= .80GM/SEC
COAXIAL FLOW GAS-NITROGEN NOMINAL COAXIAL VELOCITY= 780.FT/SEC
FLOW STRAIGHTENOR TUBE DIAM.,1/16 IN.

NOMINAL INITIAL CONDITIONS

JET VELOCITY 51.2FT/SEC JET REYNOLDS NO. 1673.
VELOCITY RATIO 15.21

PROFILE COORDINATES

AXIAL POSITION NOZZLE (DIAMETERS)	P	Q	S	T	A	G	B
EXIT	2650.	2400.	.450	550.	.515	.048	1.600
1/2	1900.	1700.	.580	550.	.660	.034	1.600
1	1250.	1130.	.380	550.	.805	.019	.900
2	550.	550.	1.990	550.	.930	.007	.550

AVERAGE CHARACTERISTICS OF JET COLUMN

AXIAL POSITION (NOZZLE DIAMS)	EXIT	1/2	1	2
VELOCITY, FT/SEC	568.	632.	717.	760.
LOCAL SEPARATION RATIO	.72	.81	.91	.97
ARGON MOLE FRACTION	.38294	.26837	.11338	.03501
TEMPERATURE, R	1340.	1082.	788.	550.
TEMPERATURE RATIO	2.43791	1.96790	1.43361	1.00000

DATA SUMMARY, JET - COAXIAL FLOW MIXING EXPERIMENTS

RUN NO. 2HA1

NOZZLE DIAMETER= 2. CM   ARGON MASS FLOW= 2.60GM/SEC
COAXIAL FLOW GAS-NITROGEN   NOMINAL COAXIAL VELOCITY= 74.FT/SEC
FLOW STRAIGHTENOR TUBE DIAM.,1/16   IN.

NOMINAL INITIAL CONDITIONS

JET VELOCITY 139.6FT/SEC   JET REYNOLDS NO. 1485.
VELOCITY RATIO .52

PROFILE COORDINATES

AXIAL POSITION NOZZLE (DIAMETERS)	P	Q	S	T	A	G	B
EXIT	8000.	7200.	1.000	550.	0.000	.100	1.580
1/2	7150.	6435.	.800	550.	0.000	.100	1.560
1	7700.	6930.	.600	550.	.010	.090	.760
2	5250.	4725.	.600	550.	.172	.083	.600

AVERAGE CHARACTERISTICS OF JET COLUMN

AXIAL POSITION (NOZZLE DIAMS)	EXIT	1/2	1	2
VELOCITY, FT/SEC	131.	118.	107.	90.
LOCAL SEPARATION RATIO	1.77	1.60	1.45	1.22
ARGON MOLE FRACTION	.78262	.77596	.53865	.42320
TEMPERATURE, R	4495.	3648.	3529.	2500.
TEMPERATURE RATIO	8.17424	6.63333	6.41666	4.54575

DATA SUMMARY, JET - COAXIAL FLOW MIXING EXPERIMENTS

RUN NO. 2HB1

NOZZLE DIAMETER= 2. CM   ARGON MASS FLOW= 1.83GM/SEC
COAXIAL FLOW GAS-NITROGEN   NOMINAL COAXIAL VELOCITY= 45.FT/SEC
FLOW STRAIGHTENOR TUBE DIAM.,1/16   IN.

NOMINAL INITIAL CONDITIONS

JET VELOCITY 105.8FT/SEC   JET REYNOLDS NO. 1007.
VELOCITY RATIO .42

PROFILE COORDINATES

AXIAL POSITION NOZZLE (DIAMETERS)	P	Q	S	T	A	G	B
EXIT	8650.	7785.	1.000	550.	0.000	.100	1.520
1/2	8600.	7740.	.760	550.	0.000	.100	1.360
1	8250.	7425.	.760	550.	.028	.097	.740
2	3850.	3465.	.640	550.	.280	.072	.680

AVERAGE CHARACTERISTICS OF JET COLUMN

AXIAL POSITION (NOZZLE DIAMS)	EXIT	1/2	1	2
VELOCITY, FT/SEC	97.	90.	81.	56.
LOCAL SEPARATION RATIO	2.17	2.00	1.80	1.25
ARGON MOLE FRACTION	.76277	.71189	.52765	.38086
TEMPERATURE, R	4842.	4244.	4083.	1945.
TEMPERATURE RATIO	8.80454	7.71795	7.42386	3.53680

DATA SUMMARY, JET - COAXIAL FLOW MIXING EXPERIMENTS

RUN NO. 2HB2

NOZZLE DIAMETER= 2. CM   ARGON MASS FLOW= 1.83GM/SEC
COAXIAL FLOW GAS-NITROGEN   NOMINAL COAXIAL VELOCITY= 134.FT/SEC
FLOW STRAIGHTENOR TUBE DIAM.,1/16   IN.

NOMINAL INITIAL CONDITIONS

JET VELOCITY   94.6FT/SEC   JET REYNOLDS NO.   1065.
VELOCITY RATIO   1.41

PROFILE COORDINATES

AXIAL POSITION NOZZLE (DIAMETERS)	P	Q	S	T	A	G	B
EXIT	8400.	7560.	.840	550.	0.000	.100	.760
1/2	6450.	5800.	.880	550.	.010	.099	.840
1	6450.	5800.	.720	550.	.197	.083	1.080
2	1900.	1700.	.800	550.	.570	.043	.480

AVERAGE CHARACTERISTICS OF JET COLUMN

AXIAL POSITION (NOZZLE DIAMS)	EXIT	1/2	1	2
VELOCITY, FT/SEC	110.	104.	105.	117.
LOCAL SEPARATION RATIO	.82	.78	.78	.87
ARGON MOLE FRACTION	.54769	.56148	.50644	.20873
TEMPERATURE, R	4329.	3450.	3184.	1158.
TEMPERATURE RATIO	7.87208	6.27408	5.79069	2.10666

DATA SUMMARY, JET - COAXIAL FLOW MIXING EXPERIMENTS

RUN NO. 2HB3

NOZZLE DIAMETER= 2. CM   ARGON MASS FLOW= 1.83GM/SEC
COAXIAL FLOW GAS-NITROGEN   NOMINAL COAXIAL VELOCITY= 450.FT/SEC
FLOW STRAIGHTENOR TUBE DIAM.,1/16 IN.

NOMINAL INITIAL CONDITIONS

JET VELOCITY 51.4FT/SEC   JET REYNOLDS NO. 1445.
VELOCITY RATIO 8.74

PROFILE COORDINATES

AXIAL POSITION NOZZLE (DIAMETERS)	P	Q	S	T	A	G	B
EXIT	4600.	4140.	.720	550.	.385	.062	1.560
1/2	2000.	1800.	1.600	550.	.720	.028	1.760
1	975.	900.	1.900	550.	.880	.012	1.560
2	770.	700.	1.000	550.	.947	.005	.720

AVERAGE CHARACTERISTICS OF JET COLUMN

AXIAL POSITION (NOZZLE DIAMS)	EXIT	1/2	1	2
VELOCITY, FT/SEC	299.	375.	420.	440.
LOCAL SEPARATION RATIO	.66	.83	.93	.97
ARGON MOLE FRACTION	.47711	.23651	.09311	.02840
TEMPERATURE, R	2352.	1609.	905.	643.
TEMPERATURE RATIO	4.27713	2.92606	1.64609	1.16969

DATA SUMMARY, JET - COAXIAL FLOW MIXING EXPERIMENTS

RUN NO. 2HC1

NOZZLE DIAMETER= 2. CM   ARGON MASS FLOW= 1.04GM/SEC
COAXIAL FLOW GAS-NITROGEN   NOMINAL COAXIAL VELOCITY= 27.FT/SEC
FLOW STRAIGHTENOR TUBE DIAM.,1/16   IN.

NOMINAL INITIAL CONDITIONS

JET VELOCITY   39.2FT/SEC   JET REYNOLDS NO.   708.
VELOCITY RATIO   .68

PROFILE COORDINATES

AXIAL POSITION NOZZLE (DIAMETERS)	P	Q	S	T	A	G	B
EXIT	7200.	6660.	.450	550.	0.000	.100	.300
1/2	6500.	5850.	.400	550.	.025	.100	.420
1	5070.	4570.	.600	550.	.160	.084	.200
2	2200.	1980.	.480	550.	.590	.060	.280

AVERAGE CHARACTERISTICS OF JET COLUMN

AXIAL POSITION (NOZZLE DIAMS)	EXIT	1/2	1	2
VELOCITY, FT/SEC	34.	32.	30.	26.
LOCAL SEPARATION RATIO	1.26	1.20	1.13	.97
ARGON MOLE FRACTION	.45025	.46283	.36316	.19450
TEMPERATURE, R	3157.	2749.	2427.	1172.
TEMPERATURE RATIO	5.74024	4.99878	4.41381	2.13226

DATA SUMMARY, JET - COAXIAL FLOW MIXING EXPERIMENTS

RUN NO. HP 1

NOZZLE DIAMETER= 1. CM   ARGON MASS FLOW= 1.00GM/SEC
COAXIAL FLOW GAS-NITROGEN   NOMINAL COAXIAL VELOCITY= 130.FT/SEC
FLOW STRAIGHTENOR TUBE DIAM.,POROUS

NOMINAL INITIAL CONDITIONS

JET VELOCITY 128.3FT/SEC   JET REYNOLDS NO. 1478.
VELOCITY RATIO 1.01

PROFILE COORDINATES

AXIAL POSITION NOZZLE (DIAMETERS)	P	Q	S	T	A	G	B
EXIT	6000.	5400.	.500	550.	.005	.099	1.000
1/2	4750.	4275.	.400	550.	.007	.099	.840
1	3550.	3195.	.640	550.	.425	.057	.640
2	3200.	2880.	.400	550.	.682	.032	.440

AVERAGE CHARACTERISTICS OF JET COLUMN

AXIAL POSITION (NOZZLE DIAMS)	EXIT	1/2	1	2
VELOCITY, FT/SEC	128.	119.	121.	123.
LOCAL SEPARATION RATIO	.99	.91	.93	.95
ARGON MOLE FRACTION	.60516	.56308	.29870	.15188
TEMPERATURE, R	2684.	2096.	1816.	1517.
TEMPERATURE RATIO	4.88068	3.81090	3.30218	2.7587

APPENDIX D: Mixing Data Reduction Procedure

Average values of composition and temperature were computed from the mixing profile data by a simplified integration technique deemed adequate within the accuracy of the experiments. Figure Appendix D-1 identifies the quantities obtained from composition and temperature profiles, respectively. It is seen that data curves have been approximated by fitted triangular and trapezoidal regions which are identified as regions I and II respectively.

For the case of the composition profiles it was observed (see Table II) that no measurable amount of argon was found exterior to the cylindrical column formed by the jet nozzle. Thus the expression for the average composition of the profile $\bar{y}$ is found by the present technique as follows:

$$\bar{y} = \frac{\int_{-1}^{1} y(x)\, 2\pi x\, dx}{\int_{-1}^{1} 2\pi x\, dx}$$

where the $2\pi x$ term appears because the plane representation must be rotated to provide a three-dimensional average.

$$y(x) = a + y_{I}(x) + y_{II}(x)$$

where $y_{I}(x) = \frac{2gx}{b}$, $\left|\frac{b}{2}\right| \leq |x| \geq 0$

$= 0$, $|x| > \left|\frac{b}{2}\right|$

$$y_{II}(x) = \frac{(x-\frac{b}{2})(c-g)}{(1-\frac{b}{2})} \quad , \quad 1 \geq |x| > |\frac{b}{2}|$$

$$= 0 \quad , \quad |x| < |\frac{b}{2}|$$

The result is:

$$\bar{y} = a + \frac{b^2 g}{6} + \frac{[1-(a+g)]}{(1-\frac{b}{2})}\left[\frac{2}{3} - \frac{b}{2} + \frac{b^3}{24}\right]$$

By a similar argument it may be readily shown that the average temperature $\bar{T}$ is,

$$\bar{T} = \frac{s^2}{12}(p-q) + \frac{q-t}{1-\frac{s}{2}}\left(\frac{s^3}{12} - \frac{1}{6} - \frac{s^2}{8}\right) + q$$

The velocities used in calculating the separation ratio were computed from the composition data. As mentioned in the text, velocity data were not obtainable at many conditions of interest, and thus a formulation utilizing the composition data was developed from the following momentum considerations:

$$\overline{\rho U^2} = \bar{\rho}\bar{U}^2 = x\rho_c^\circ U_c^{\circ 2} + \rho_e(1-x)U_e^2$$

Assuming the equation of state for a perfect gas, it can readily be shown that:

$$\frac{U_c}{U_c^\circ} = \left\{\frac{1}{x+(1-x)\frac{M_e}{M_{Ar}}}\left[x\frac{T}{T_c^\circ} + (1-x)\frac{M_e}{M_{Ar}}\left(V_R\right)^2\right]\right\}^{1/2}$$

In most cases of high velocity ratio experiments, velocity data are not available in the core at and near the exit plane, as discussed earlier, but velocity data are generally available at two jet diameters downstream. The agreement between the above method of computation and measured velocities two diameters downstream is good.

The data summary sheet prepared for each run defines the complete test conditions. Computation techniques for quantities appearing in this summary and not discussed elsewhere were as follows:

Nominal Initial Jet Velocity, U_c^o in ft/sec

$$U_c^o = \frac{\dot{m}_{Ar}}{\rho_{Ar} \frac{\pi D^2}{4}} = \frac{4 \dot{m}_{Ar} R T_1}{\pi D^2 M_{Ar} P} = \frac{0.0475 T_1 \dot{m}_{Ar}}{D^2}$$

for D in cm, T in °R, P = 1 atm, $\dot{m}_{Ar}$ in gm/sec

Nominal Initial Jet Reynolds Number, R_c

$$R_c = \frac{4 \dot{m}_{Ar}}{\pi D \mu} = \frac{7.66 \times 10^4 \dot{m}_{Ar}}{D \sqrt{T_1}}$$

for D in cm, T in °R, $\dot{m}_{Ar}$ in gm/sec. Viscosity data from Sherman, M. P. and Grey, J., "Calculation of Transport Properties, Mixtures of Helium and Partially-Ionized Argon," Princeton University Aeronautical Engineering Report No. 673, December 1963.

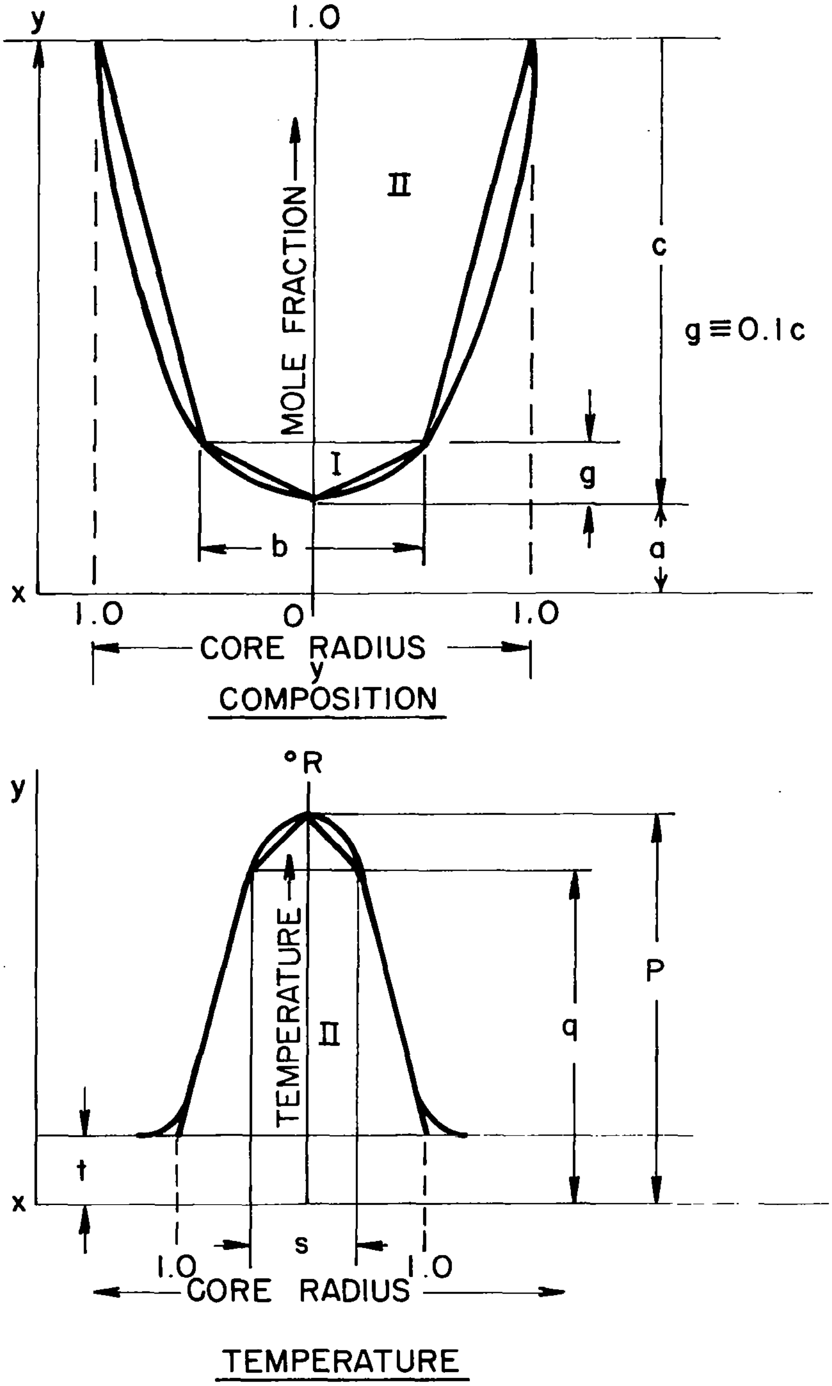

PROFILE INTEGRATION NOMENCLATURE

FIGURE D-1

APPENDIX E: Computation of Turbulent Wake Factor

RUN	$\frac{R_C}{1000}$	V_R	T_R	S_1	S_2	S_3	S_4	$\left(\frac{M_E}{M_C}\right)^{0.1}$	$\left[\frac{V_R R_C T_R}{1000}\right]$	$\left[\frac{V_R R_C T_R}{1000}\right]^{0.1}$	ϵ 1	ϵ 2	ϵ 3	ϵ 4	$\bar{\epsilon}$
2HB3	1.45	8.74	4.27	.66	.83	.93	.97	.965	54.5	1.49	.48	.53	.54	.48	.51
HA-13	1.7	15.21	2.44	.72	.81	.91	.97	"	63.0	1.51	.50	.52	.52	.47	.50
HA-12	1.3	3.63	3.90	.65	.68	.66	.95	"	18.5	1.34	.51	.49	.43	.53	.45
HA-6	2.2	2.22	2.2	.71	.74	.75	.88	"	10.8	1.28	.58	.55	.51	.51	.53
2CB	3.2	2.87	1.0	.44	.71	.78	.89	"	9.2	1.25	.37	.54	.54	.54	.49
E-3	13.0	7.41	1.0	.59	.77	.82	.92	"	9.7	1.25	.49	.58	.56	.54	.55
E-2	2.9	32.96	1.0	.90	.92	.95	.98	"	9.6	1.25	.75	.69	.56	.57	.61
D-1	7.2	9.76	1.0	.60	.86	.88	.88	"	7.0	1.22	.51	.66	.62	.53	.59
C-2	2.9	2.07	1.0	.52	.53	.54	.57	.79	6.0	1.20	.55	.56	.55	.57	.56
B-4	2.6	2.3	1.0	.49	.51	.50	.51	.79	6.0	1.20	.52	.53	.51	.51	.52
A-9	13.4	5.19	1.0	.53	.68	.83	.92	.92	7.0	1.22	.45	.53	.58	.55	.54
A-8	7.2	9.73	1.0	.67	.83	.91	.95	"	7.0	1.22	.57	.64	.64	.57	.61
A-6	13.4	2.85	1.0	.57	.59	.67	.91	"	38.0	1.44	.41	.39	.39	.46	.42
A-5	2.9	12.9	1.0	.82	.88	.89	.97	"	37.4	1.44	.59	.58	.53	.49	.53

$$\epsilon_n \approx \frac{S_{L,n}}{\left[1 + .3\alpha\left(\frac{z}{D}\right)_n\right]} \cdot \frac{1}{\alpha^{0.1}\left(\frac{V_R R_C T_R}{1000}\right)^{0.1}} \; ; \qquad \bar{\epsilon} = \frac{\frac{\epsilon_1 + \epsilon_2}{2} + \epsilon_3 + \epsilon_4}{3}$$

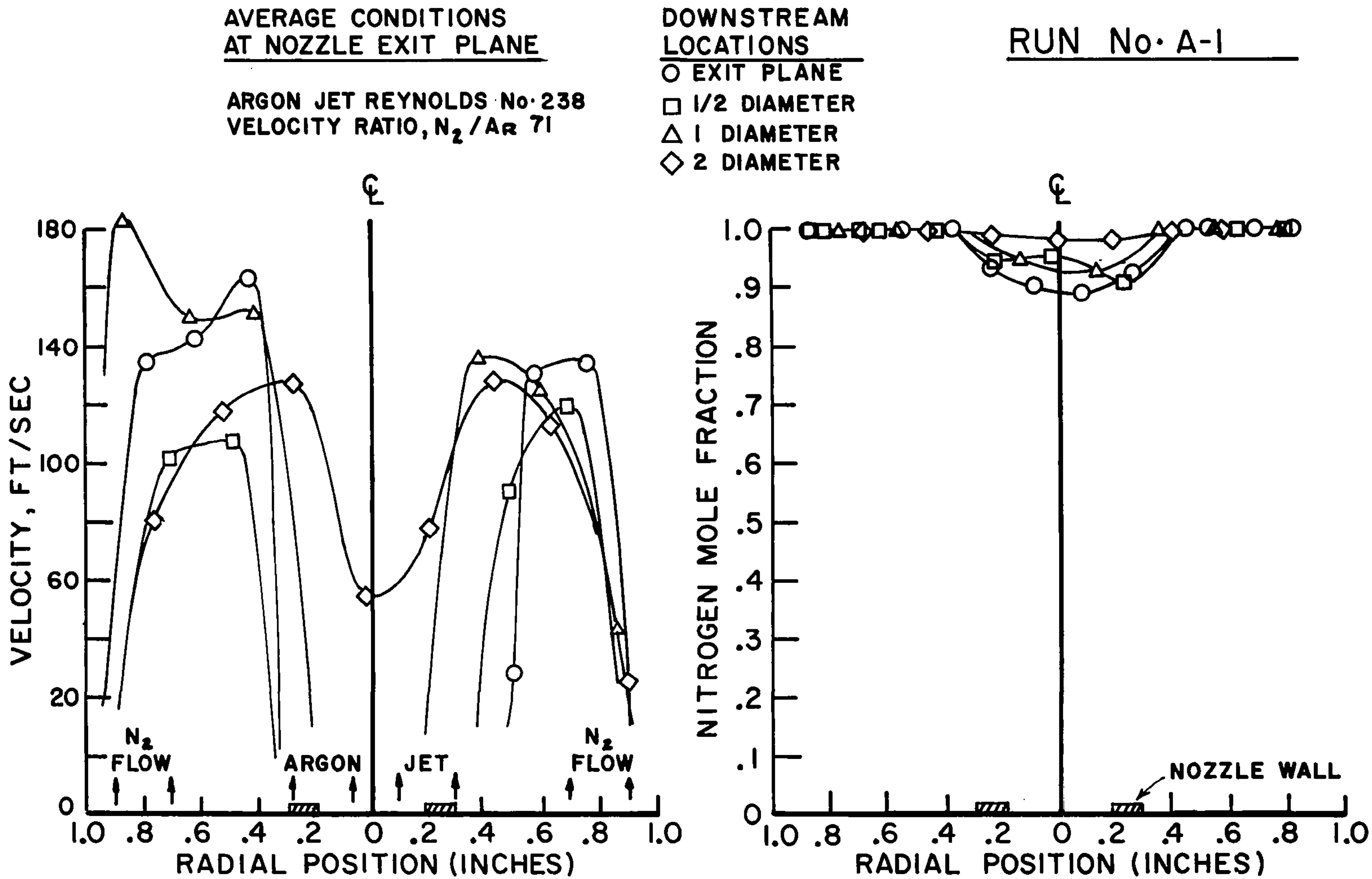

PROFILES OF ARGON JET MIXING ISOTHERMALLY WITH COAXIAL NITROGEN FLOW

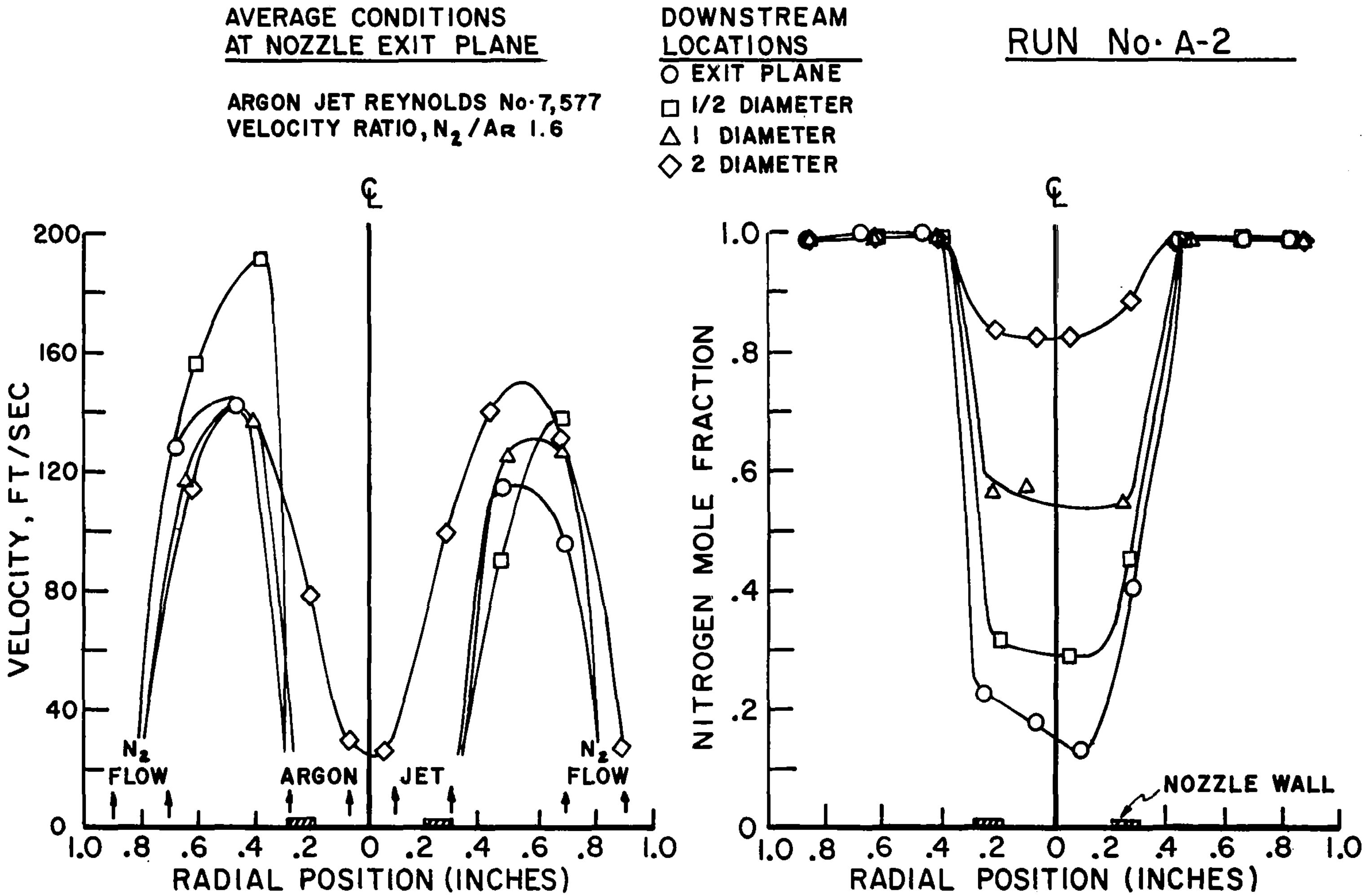

PROFILES OF ARGON JET MIXING ISOTHERMALLY WITH COAXIAL NITROGEN FLOW

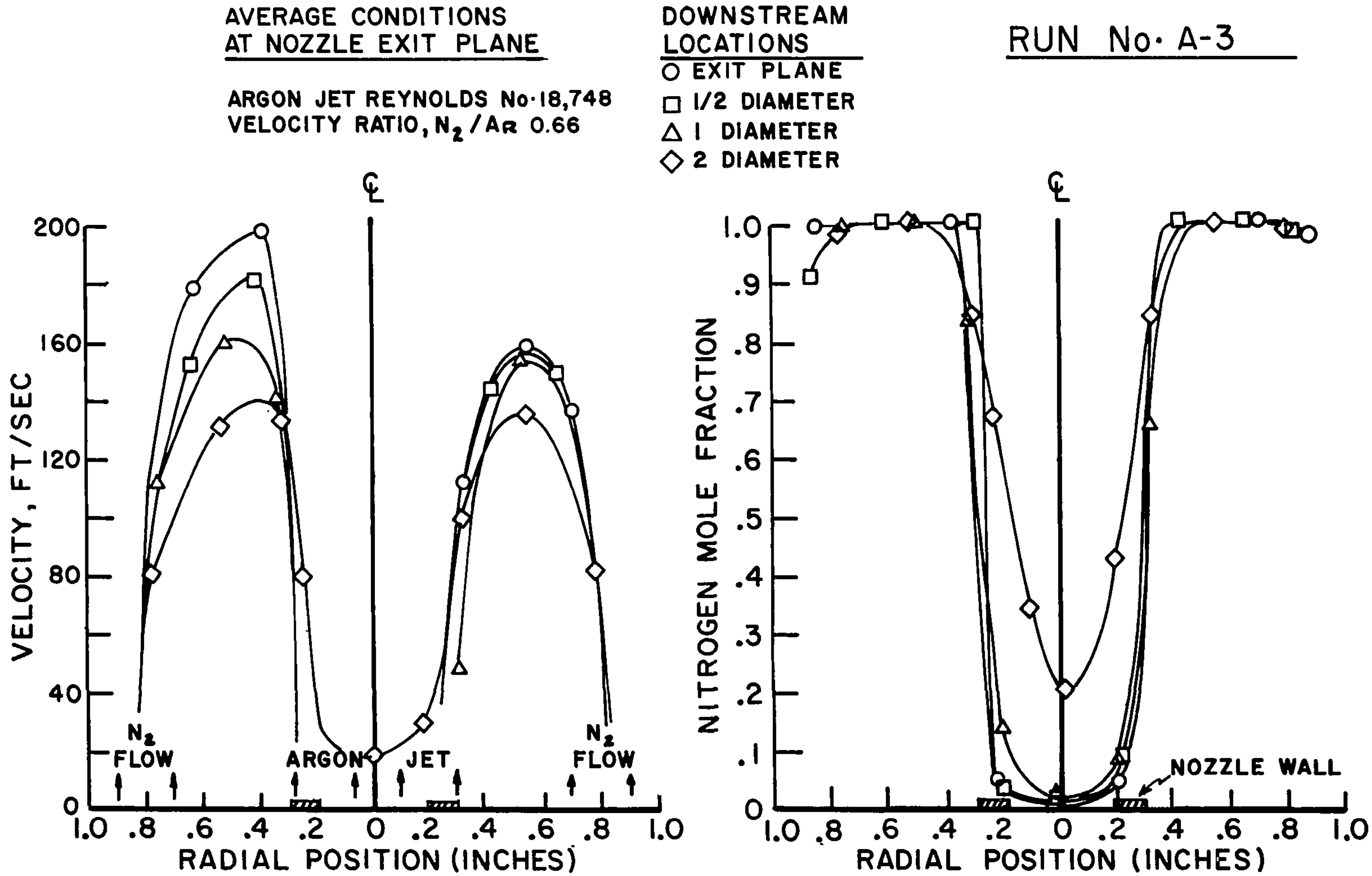

PROFILES OF ARGON JET MIXING ISOTHERMALLY WITH COAXIAL NITROGEN FLOW

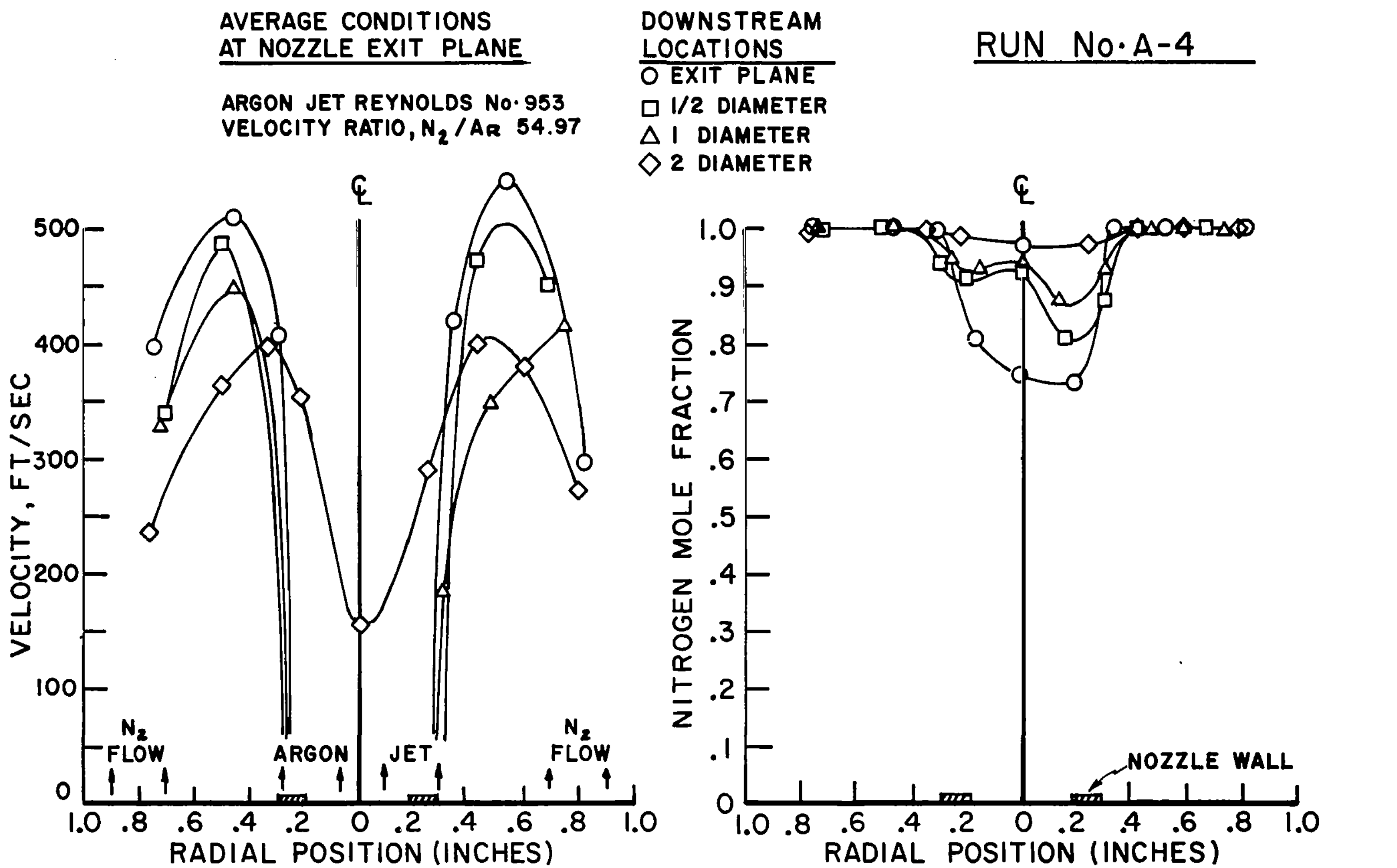

PROFILES OF ARGON JET MIXING ISOTHERMALLY WITH COAXIAL NITROGEN FLOW

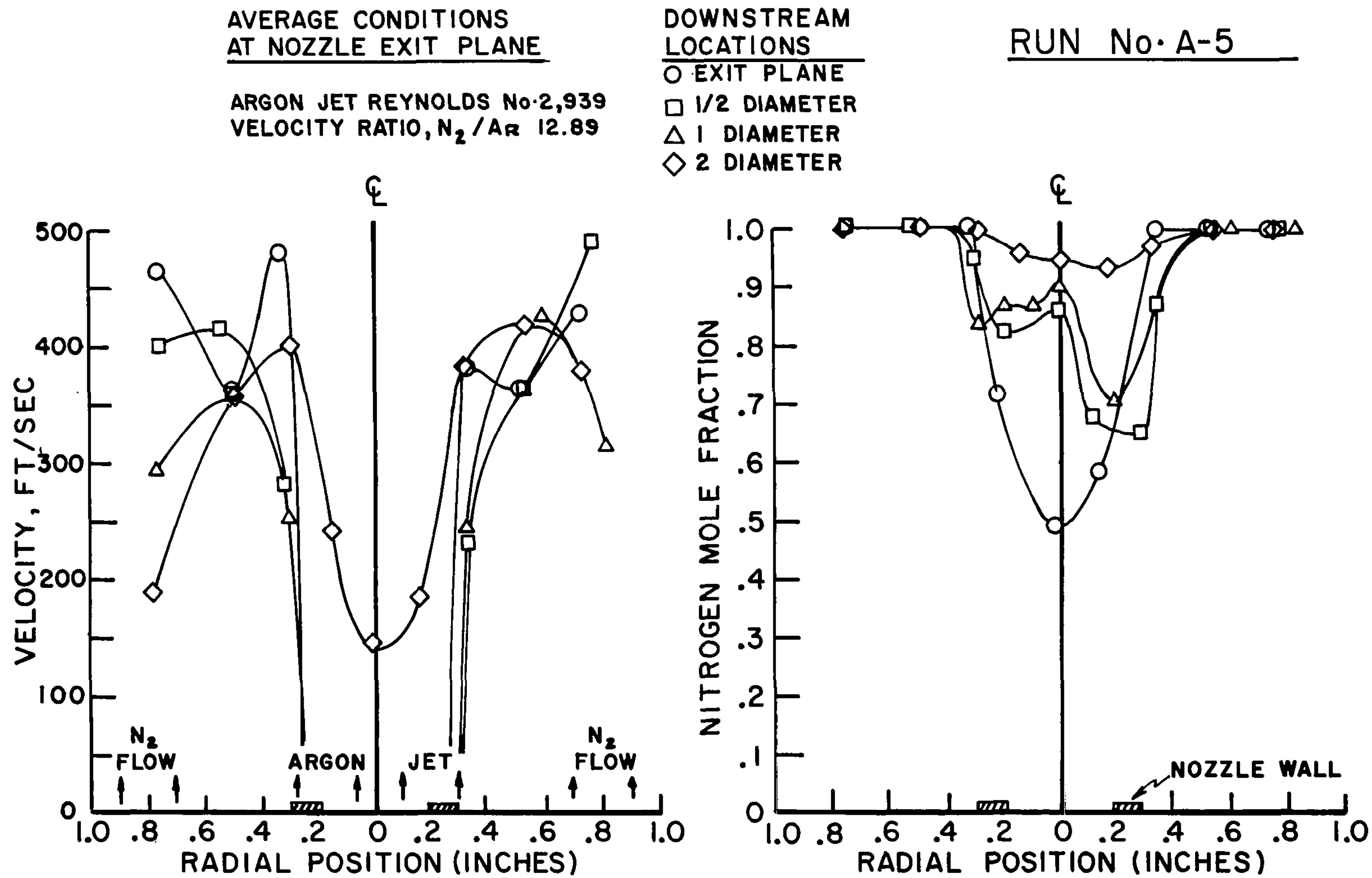

PROFILES OF ARGON JET MIXING ISOTHERMALLY WITH COAXIAL NITROGEN FLOW

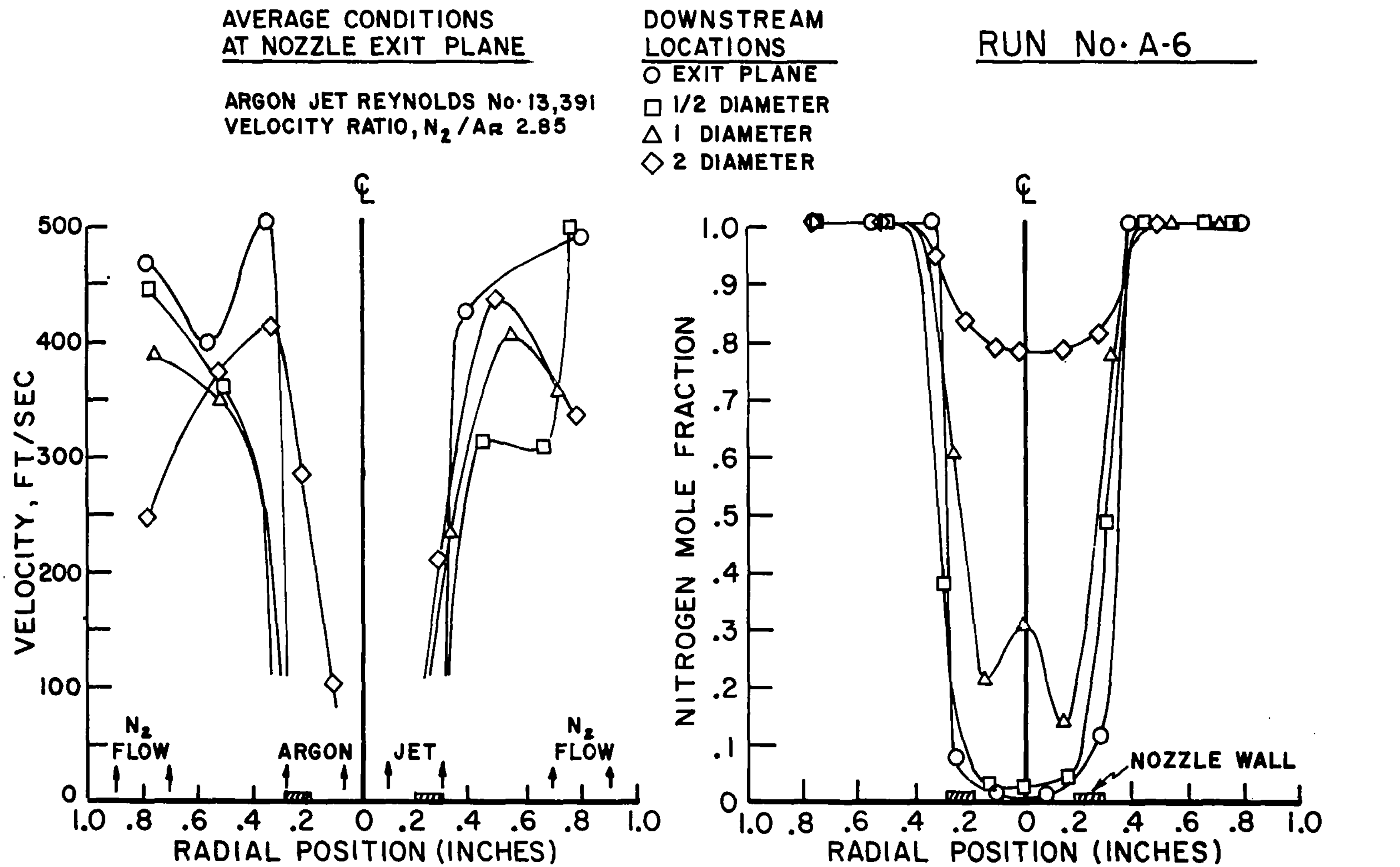

PROFILES OF ARGON JET MIXING ISOTHERMALLY WITH COAXIAL NITROGEN FLOW

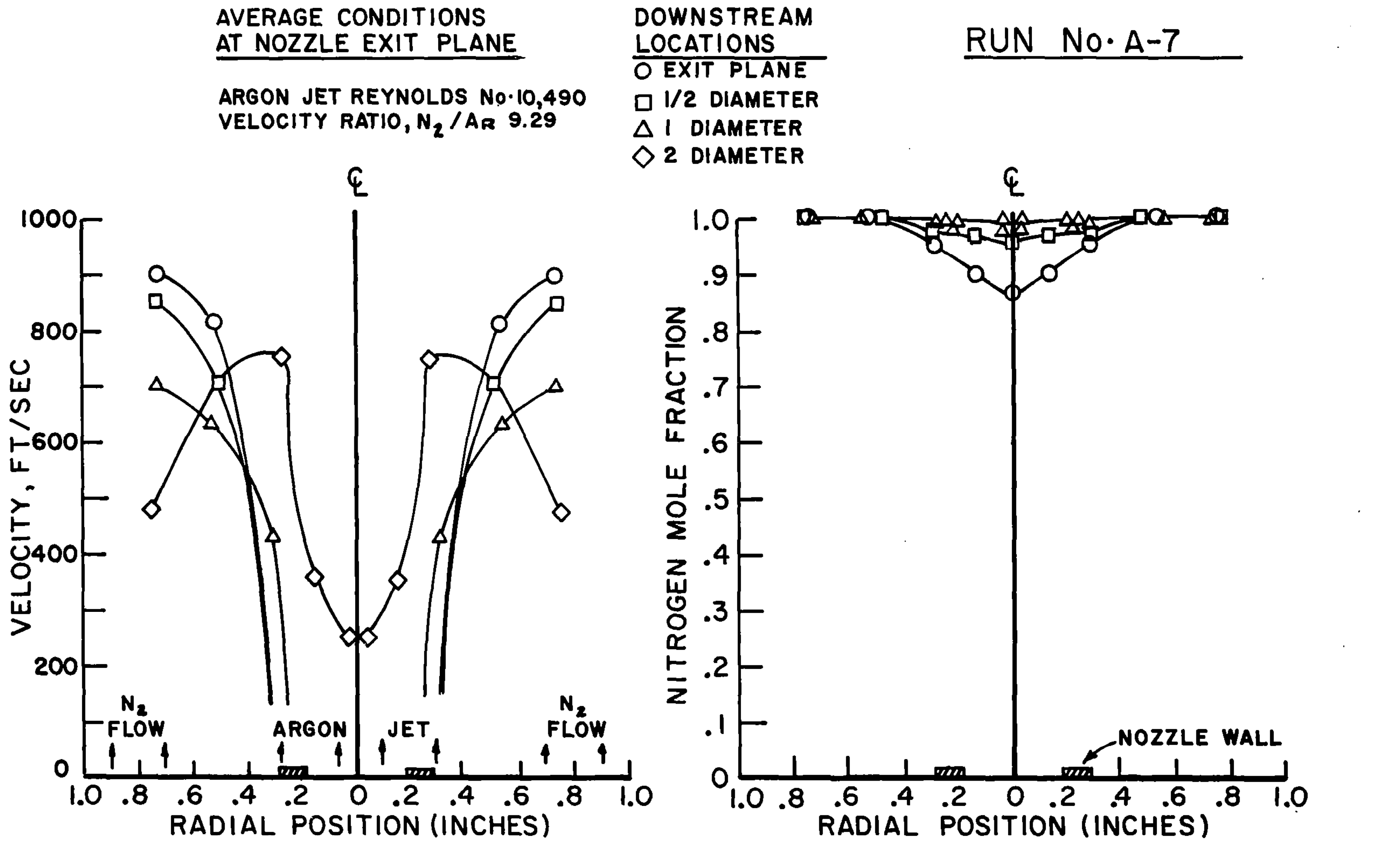

PROFILES OF ARGON JET MIXING ISOTHERMALLY WITH COAXIAL NITROGEN FLOW
(LEFT HAND PROFILE MEASURED, RIGHT HAND PROFILE DRAWN SYMETRICALLY)

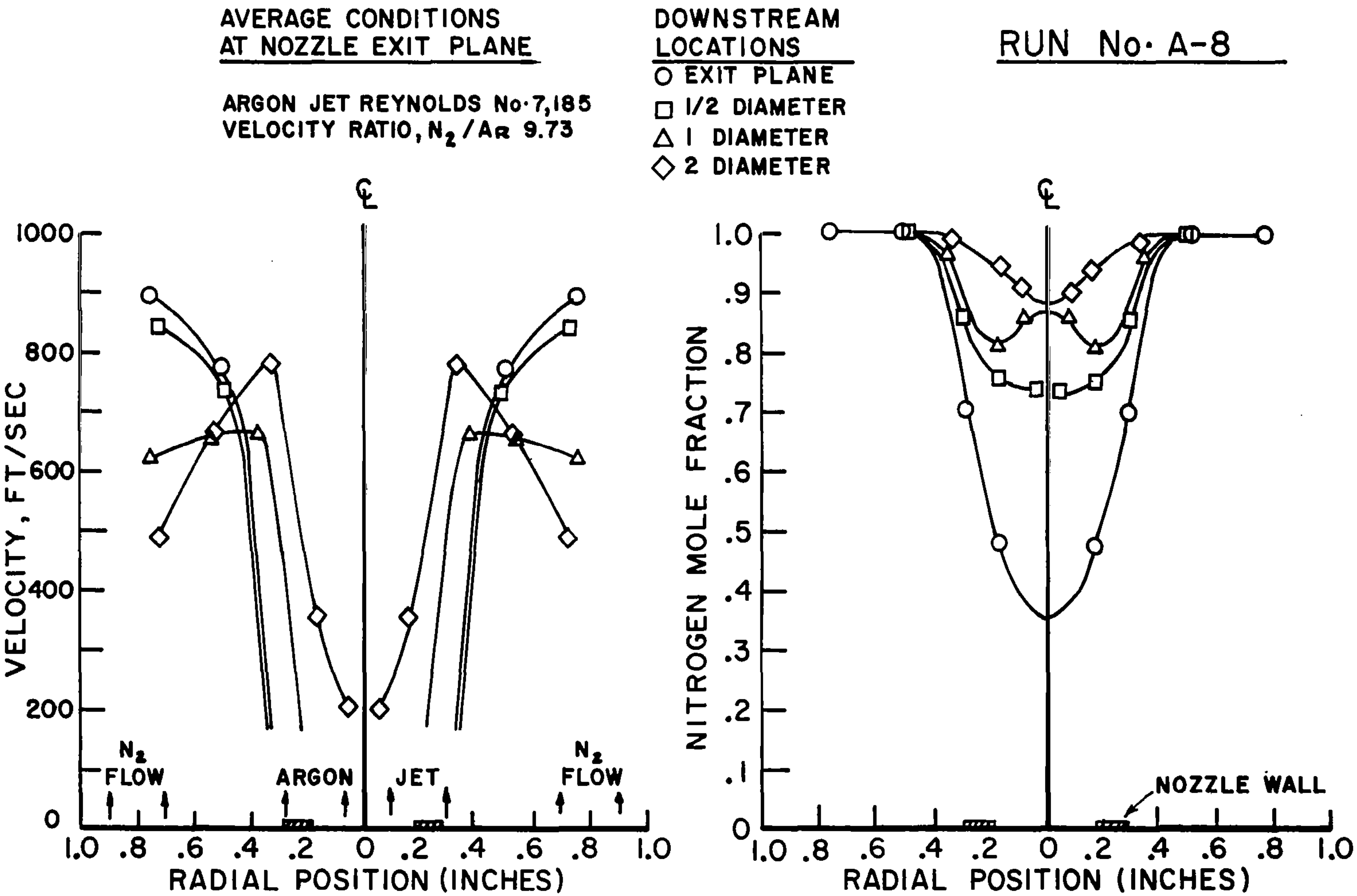

PROFILES OF ARGON JET MIXING ISOTHERMALLY WITH COAXIAL NITROGEN FLOW
(LEFT HAND PROFILE MEASURED, RIGHT HAND PROFILE DRAWN SYMETRICALLY)

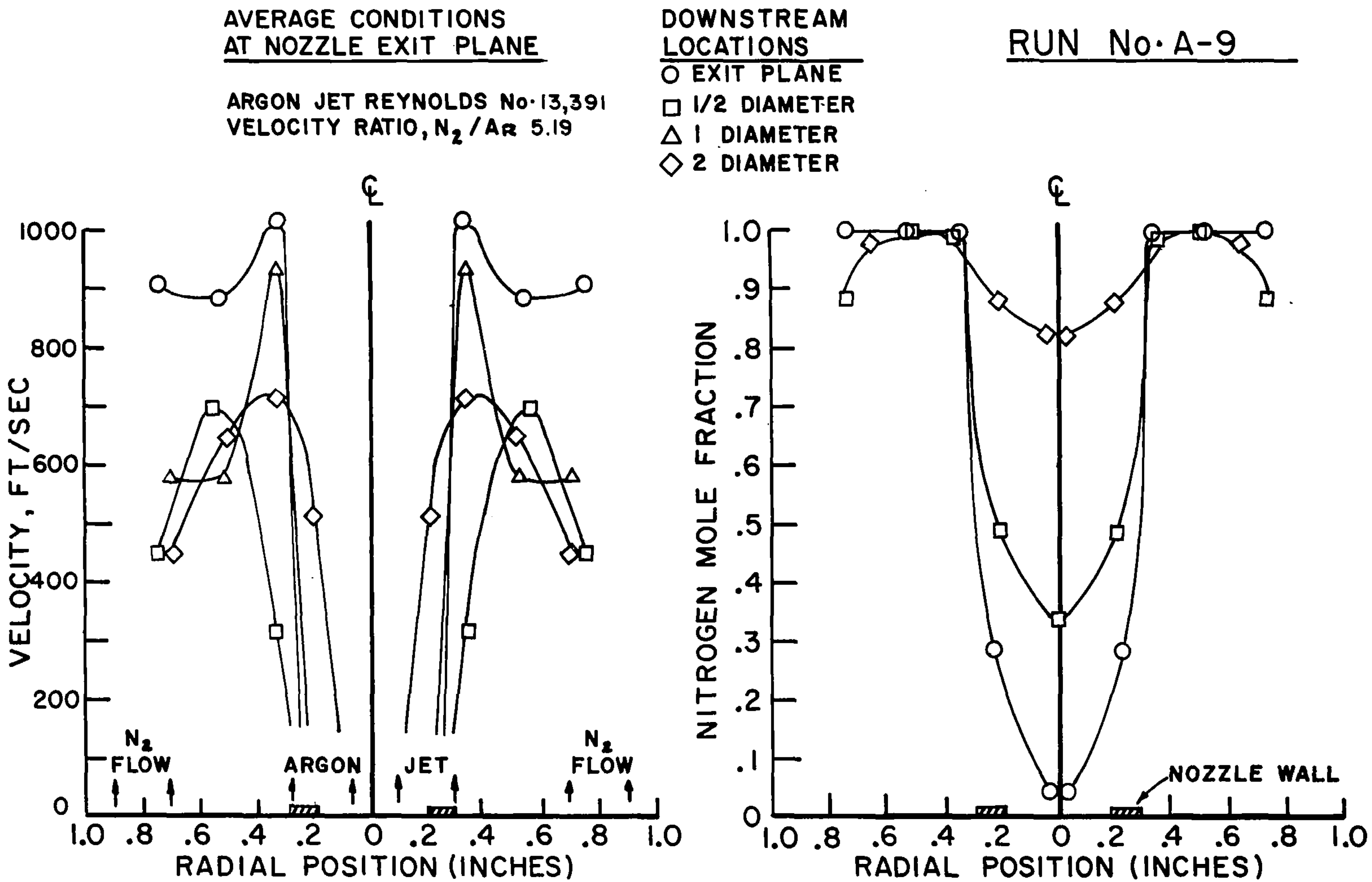

PROFILES OF ARGON JET MIXING ISOTHERMALLY WITH COAXIAL NITROGEN FLOW
(LEFT HAND PROFILE MEASURED, RIGHT HAND PROFILE DRAWN SYMETRICALLY)

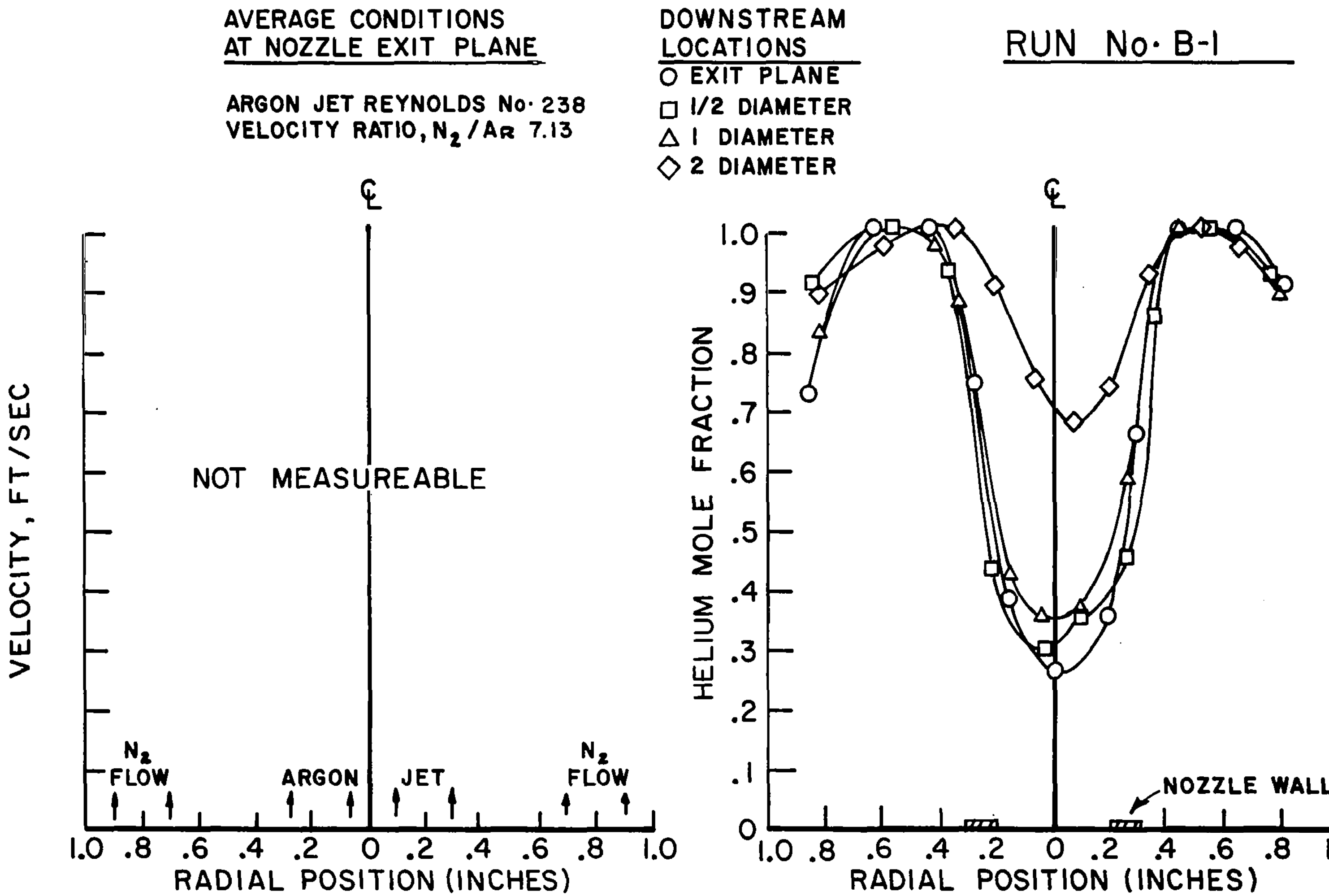

PROFILES OF ARGON JET MIXING ISOTHERMALLY WITH COAXIAL HELIUM FLOW

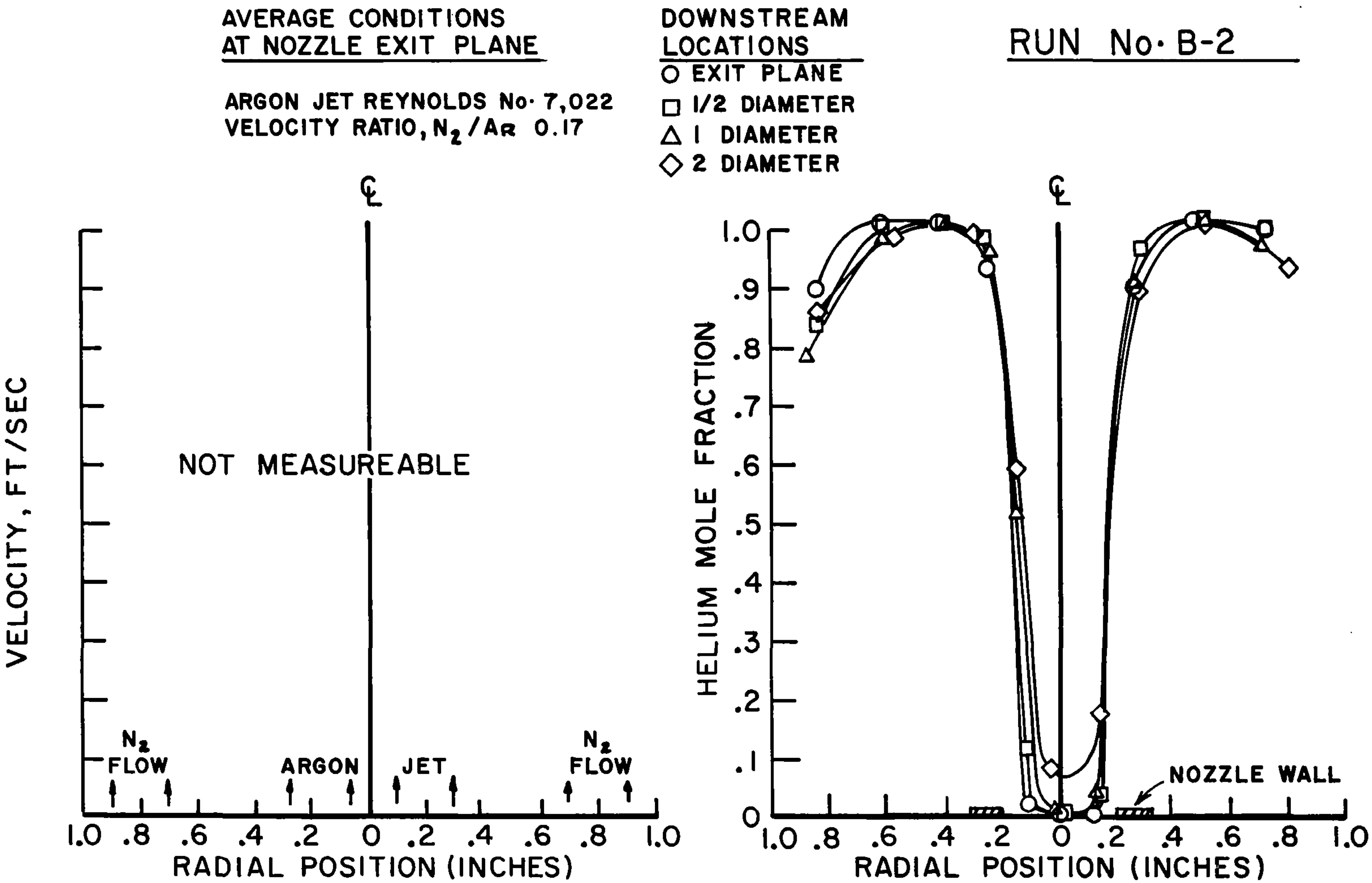

PROFILES OF ARGON JET MIXING ISOTHERMALLY WITH COAXIAL HELIUM FLOW

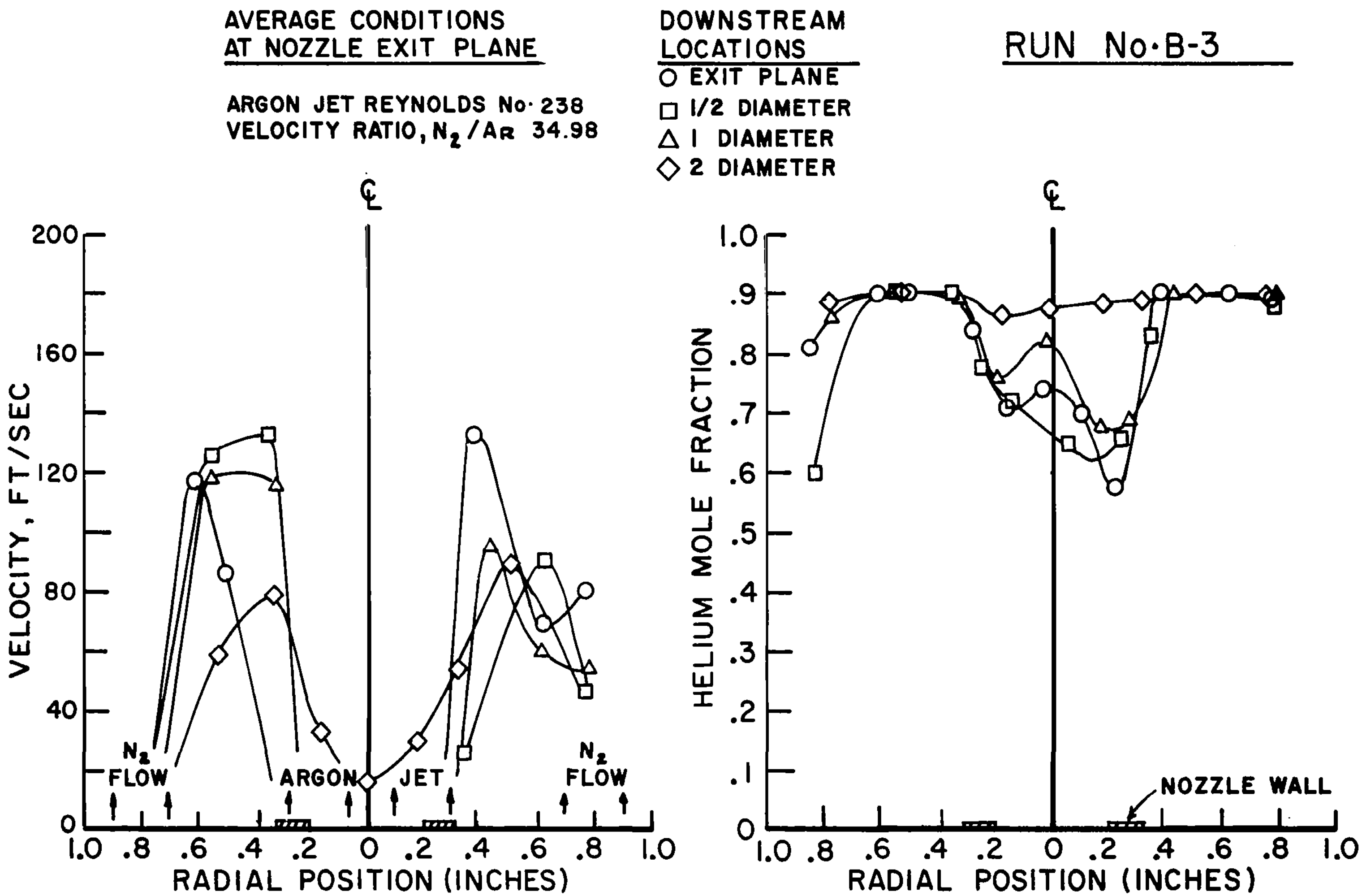

PROFILES OF ARGON JET MIXING ISOTHERMALLY WITH COAXIAL HELIUM FLOW

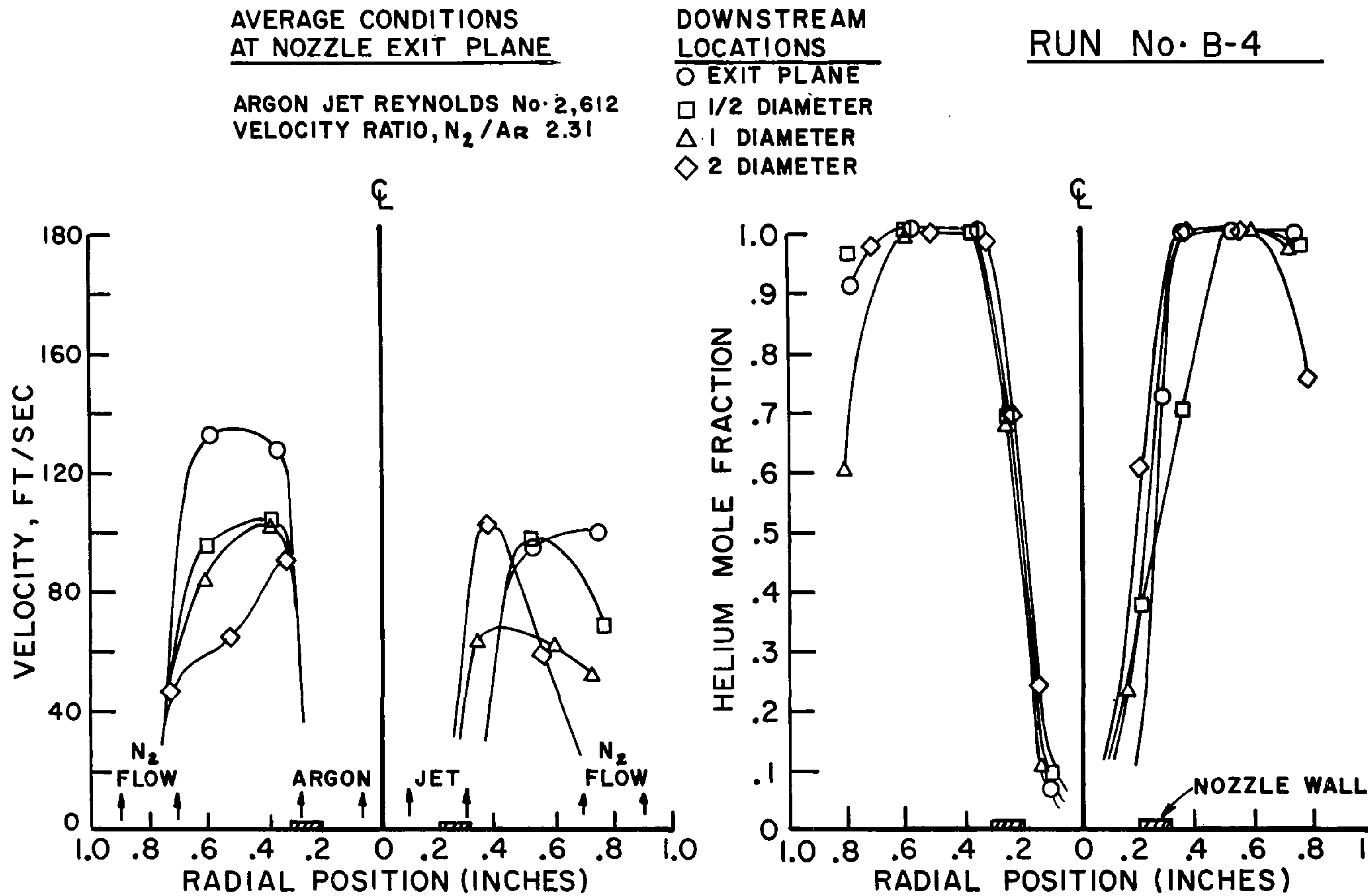

PROFILES OF ARGON JET MIXING ISOTHERMALLY WITH COAXIAL HELIUM FLOW

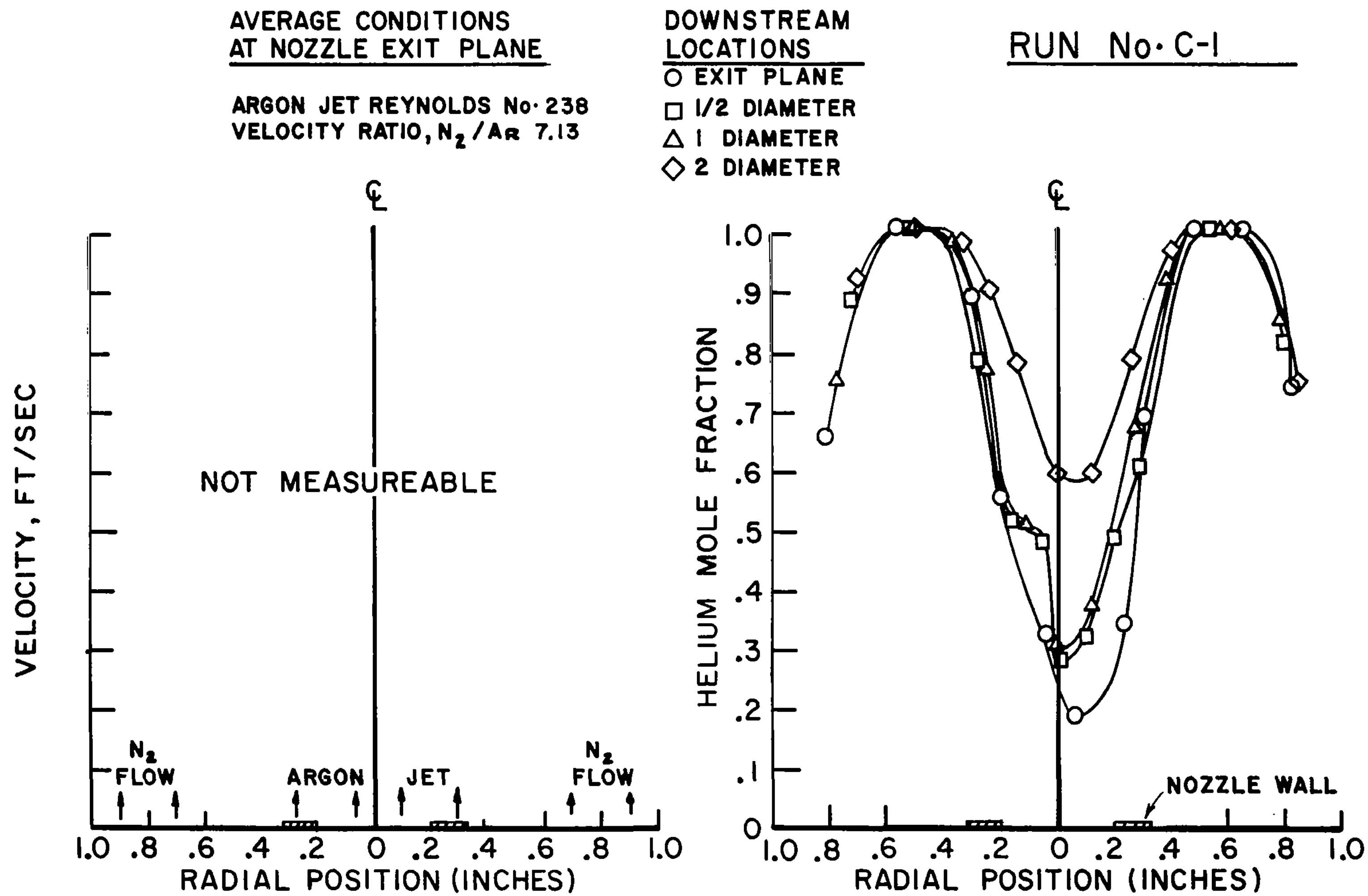

PROFILES OF ARGON JET MIXING ISOTHERMALLY WITH COAXIAL HELIUM FLOW

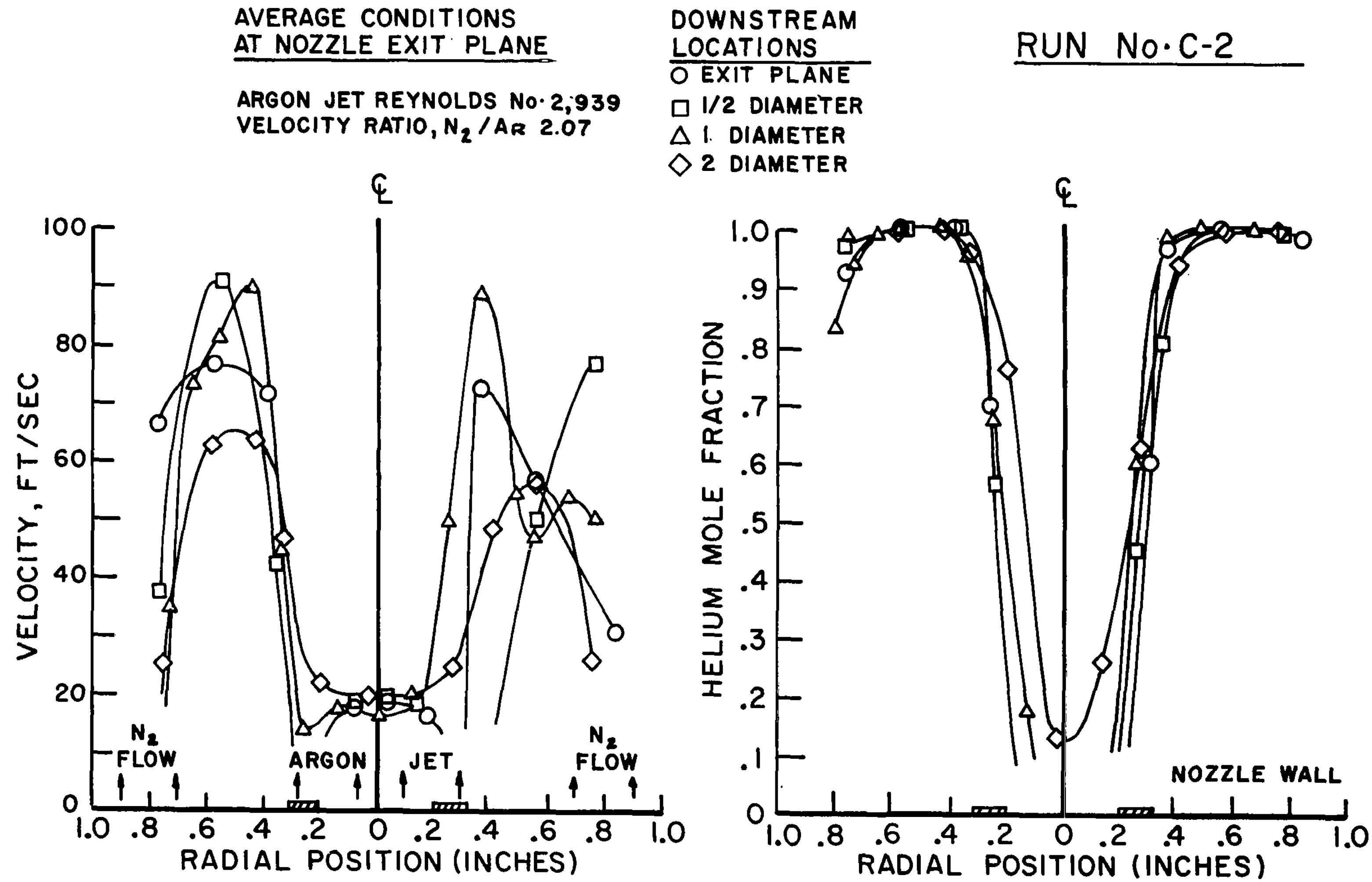

PROFILES OF ARGON JET MIXING ISOTHERMALLY WITH COAXIAL HELIUM FLOW

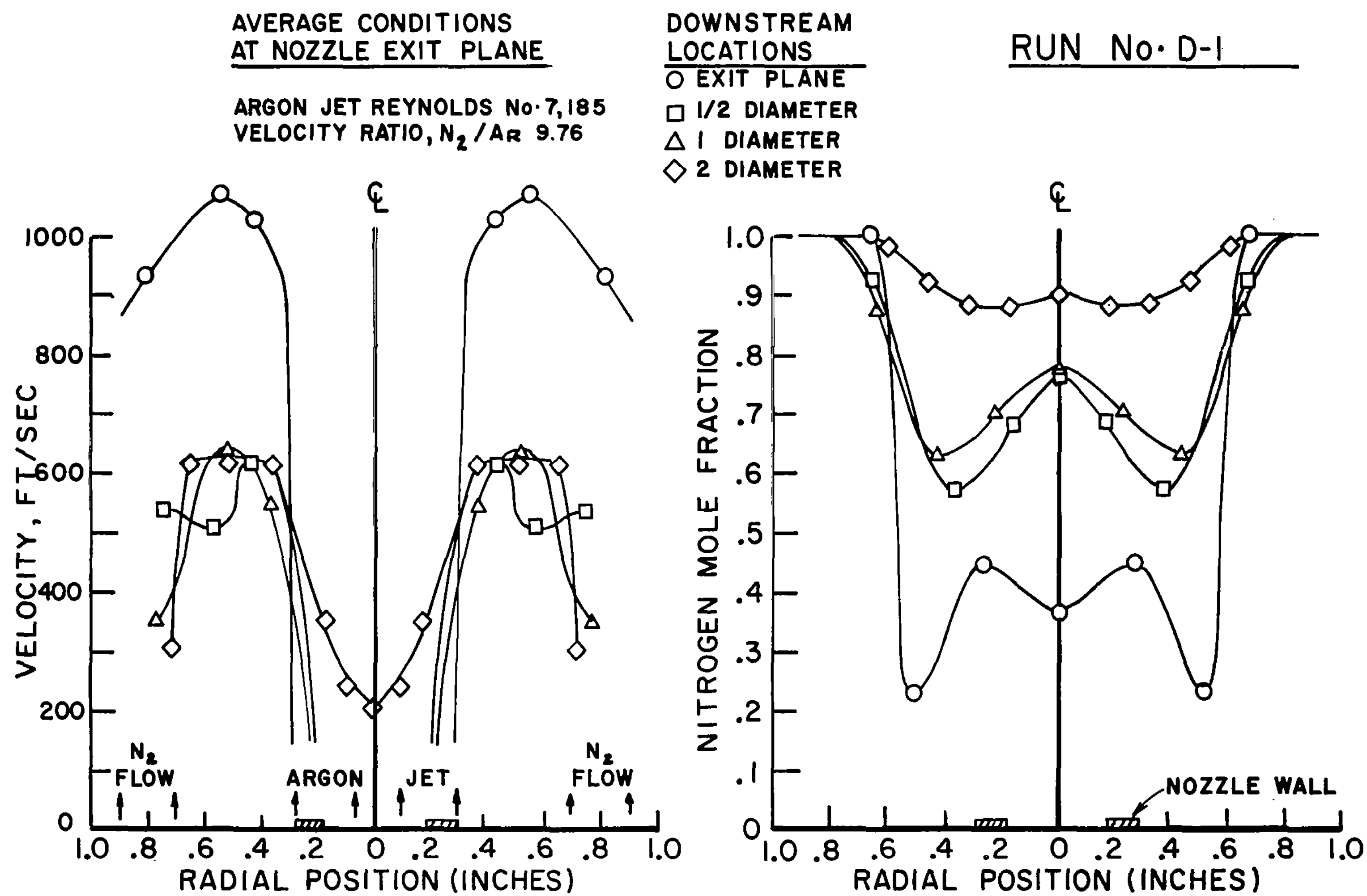

PROFILES OF ARGON JET MIXING ISOTHERMALLY WITH COAXIAL NITROGEN FLOW
(LEFT HAND PROFILE MEASURED, RIGHT HAND PROFILE DRAWN SYMETRICALLY)

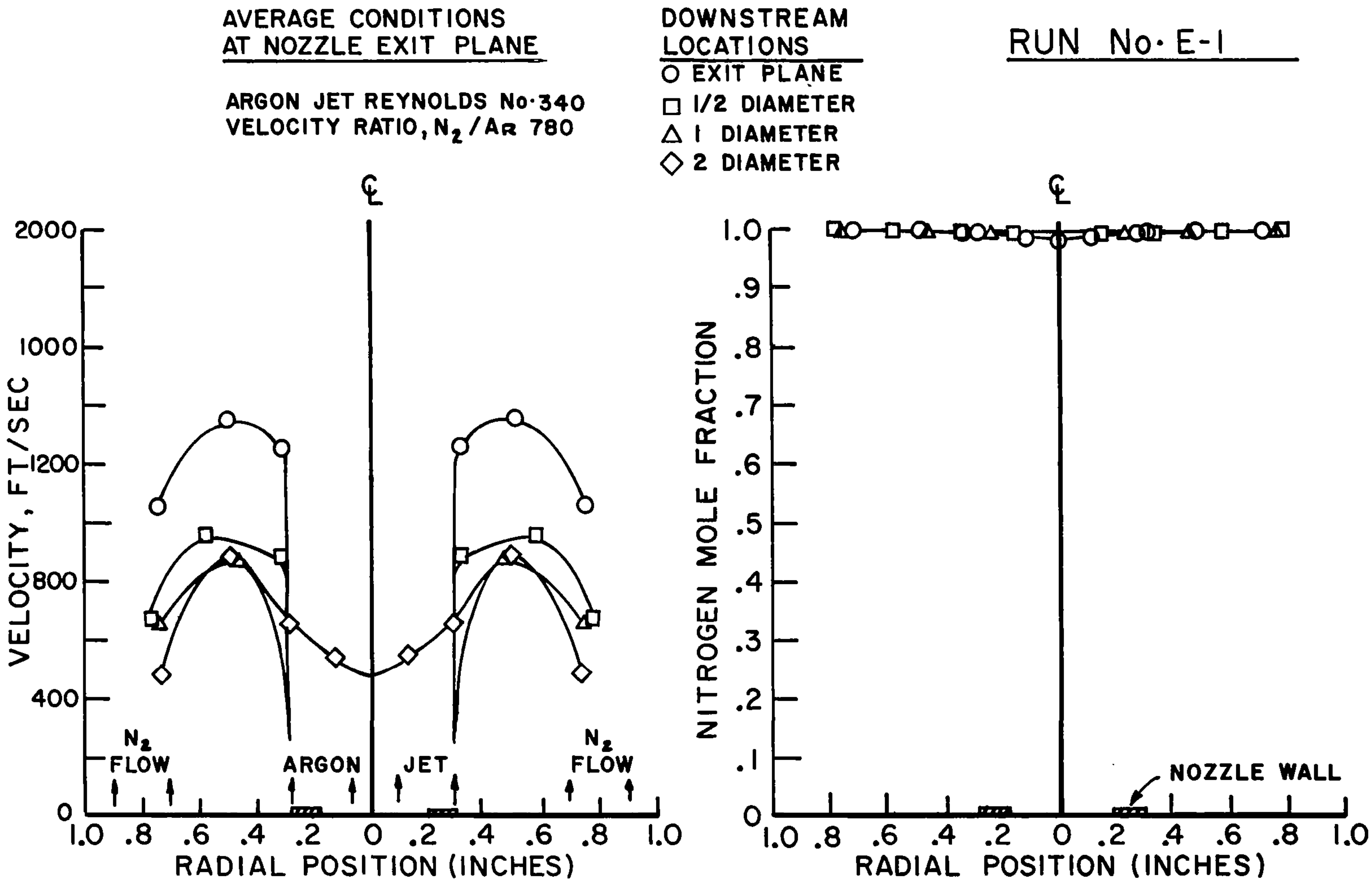

PROFILES OF ARGON JET MIXING ISOTHERMALLY WITH COAXIAL NITROGEN FLOW
(LEFT HAND PROFILE MEASURED, RIGHT HAND PROFILE DRAWN SYMETRICALLY)

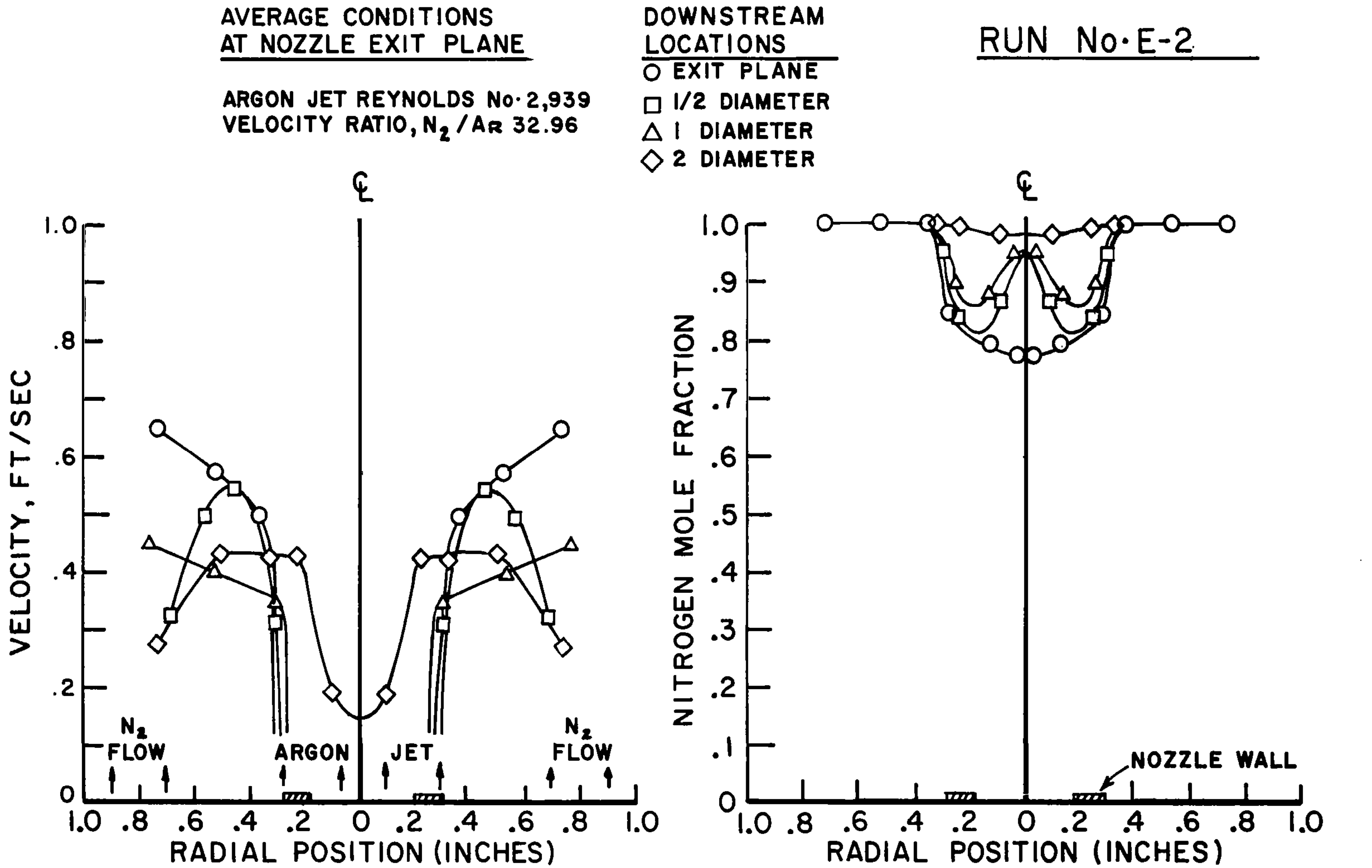

PROFILES OF ARGON JET MIXING ISOTHERMALLY WITH COAXIAL NITROGEN FLOW
(LEFT HAND PROFILE MEASURED, RIGHT HAND PROFILE DRAWN SYMETRICALLY)

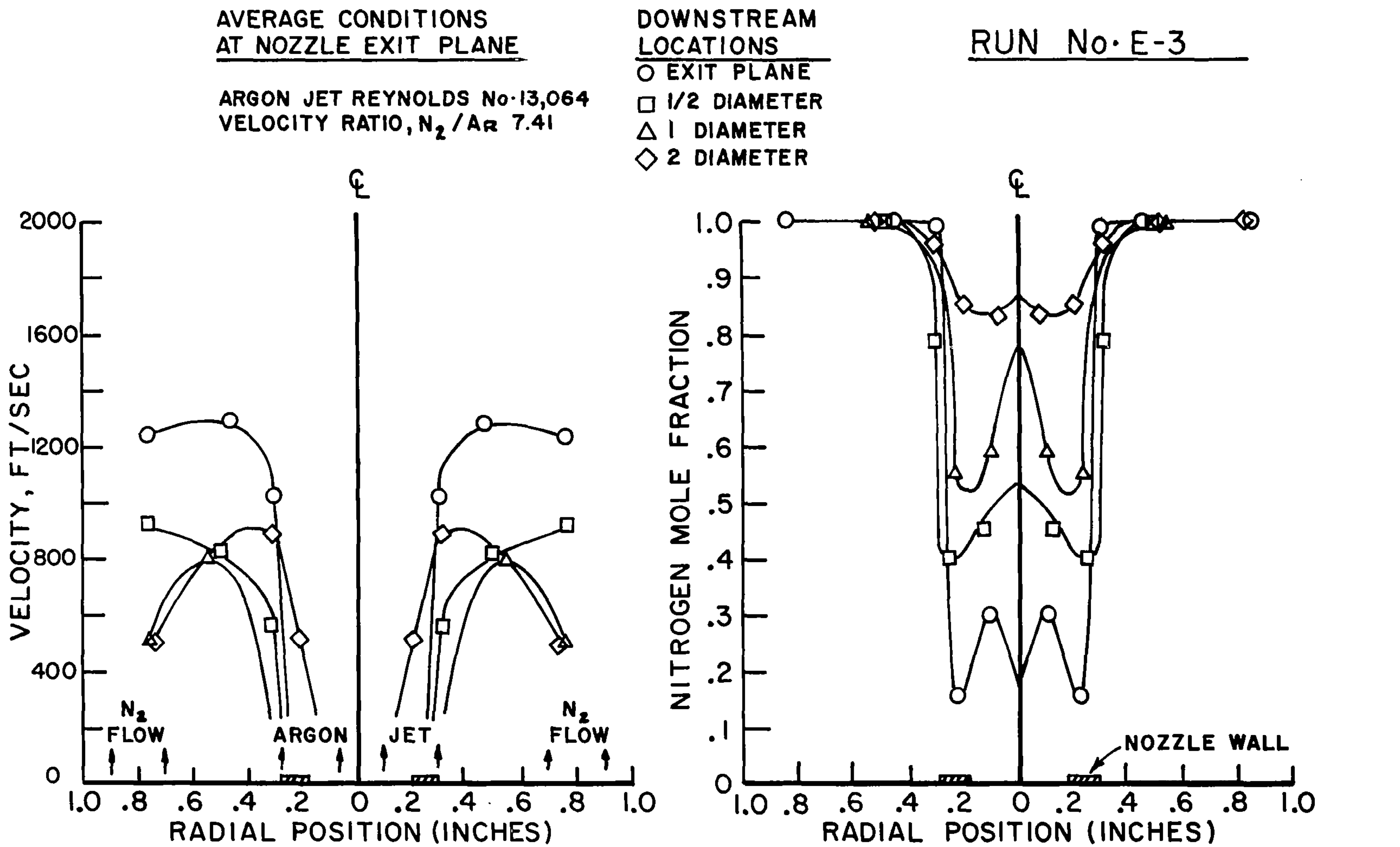

PROFILES OF ARGON JET MIXING ISOTHERMALLY WITH COAXIAL NITROGEN FLOW
(LEFT HAND PROFILE MEASURED, RIGHT HAND PROFILE DRAWN SYMETRICALLY)

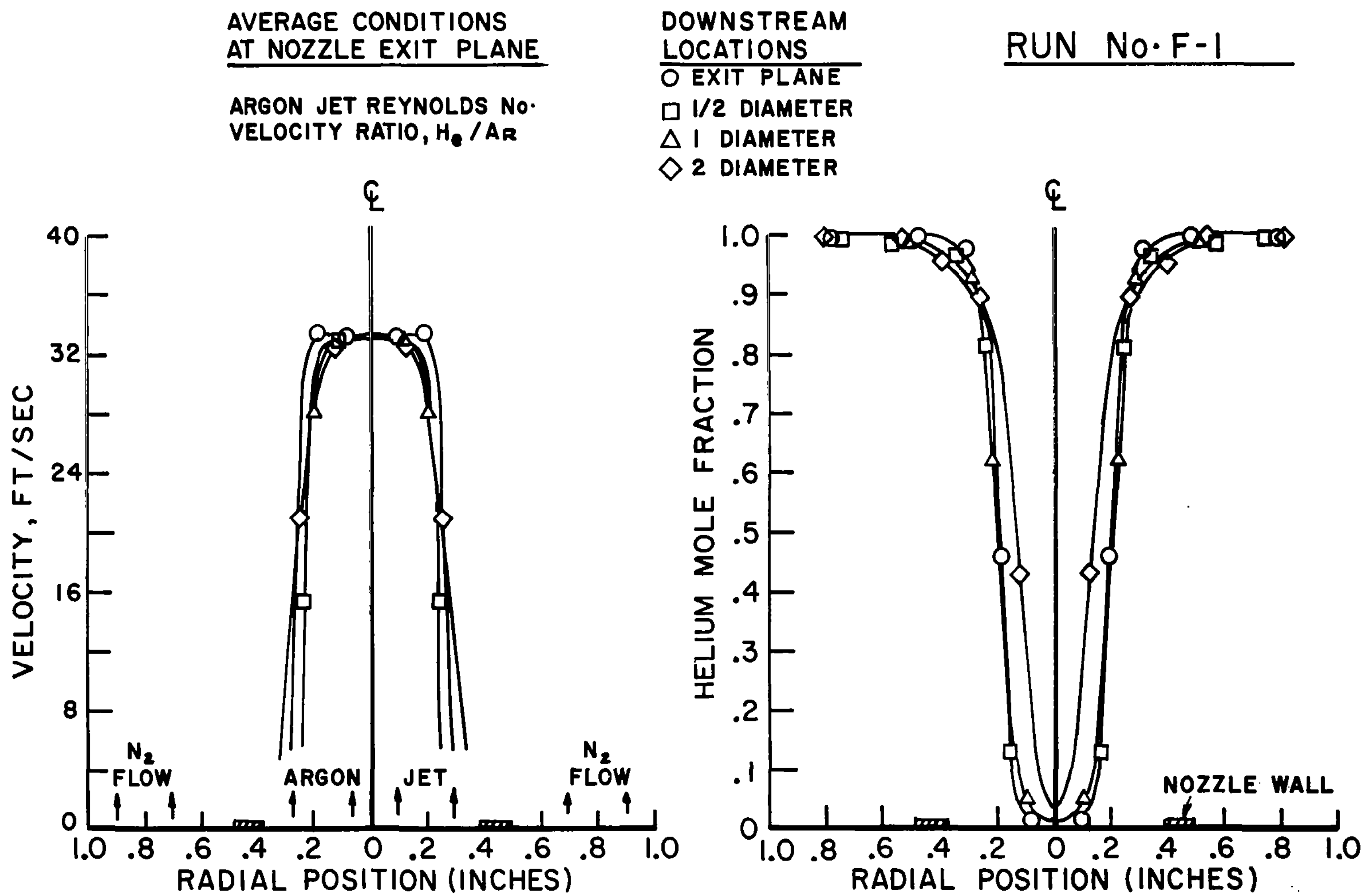

PROFILES OF ARGON JET MIXING ISOTHERMALLY WITH COAXIAL HELIUM FLOW

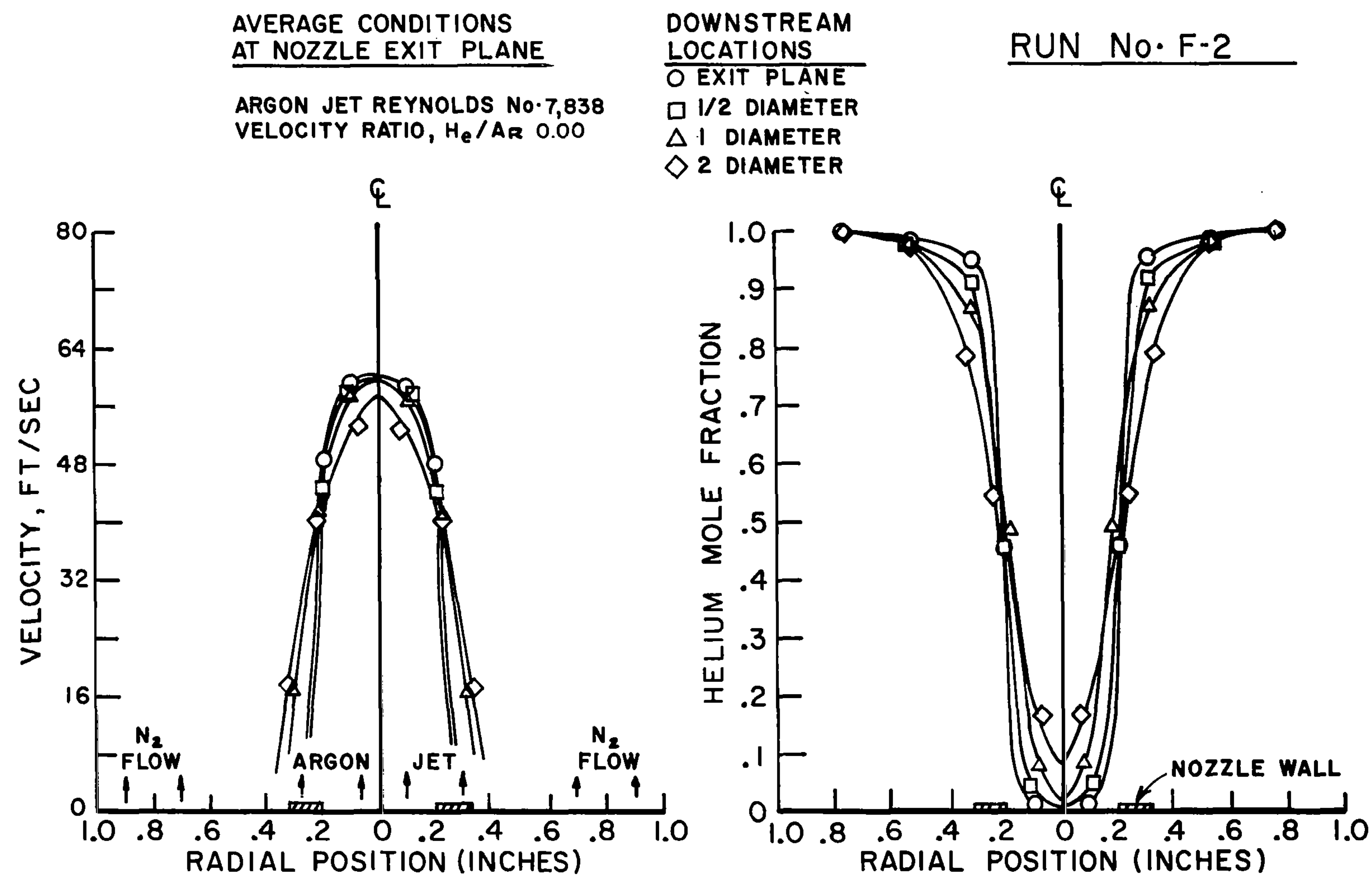

PROFILES OF ARGON JET MIXING ISOTHERMALLY WITH COAXIAL HELIUM FLOW
(LEFT HAND PROFILE MEASURED, RIGHT HAND PROFILE DRAWN SYMETRICALLY)

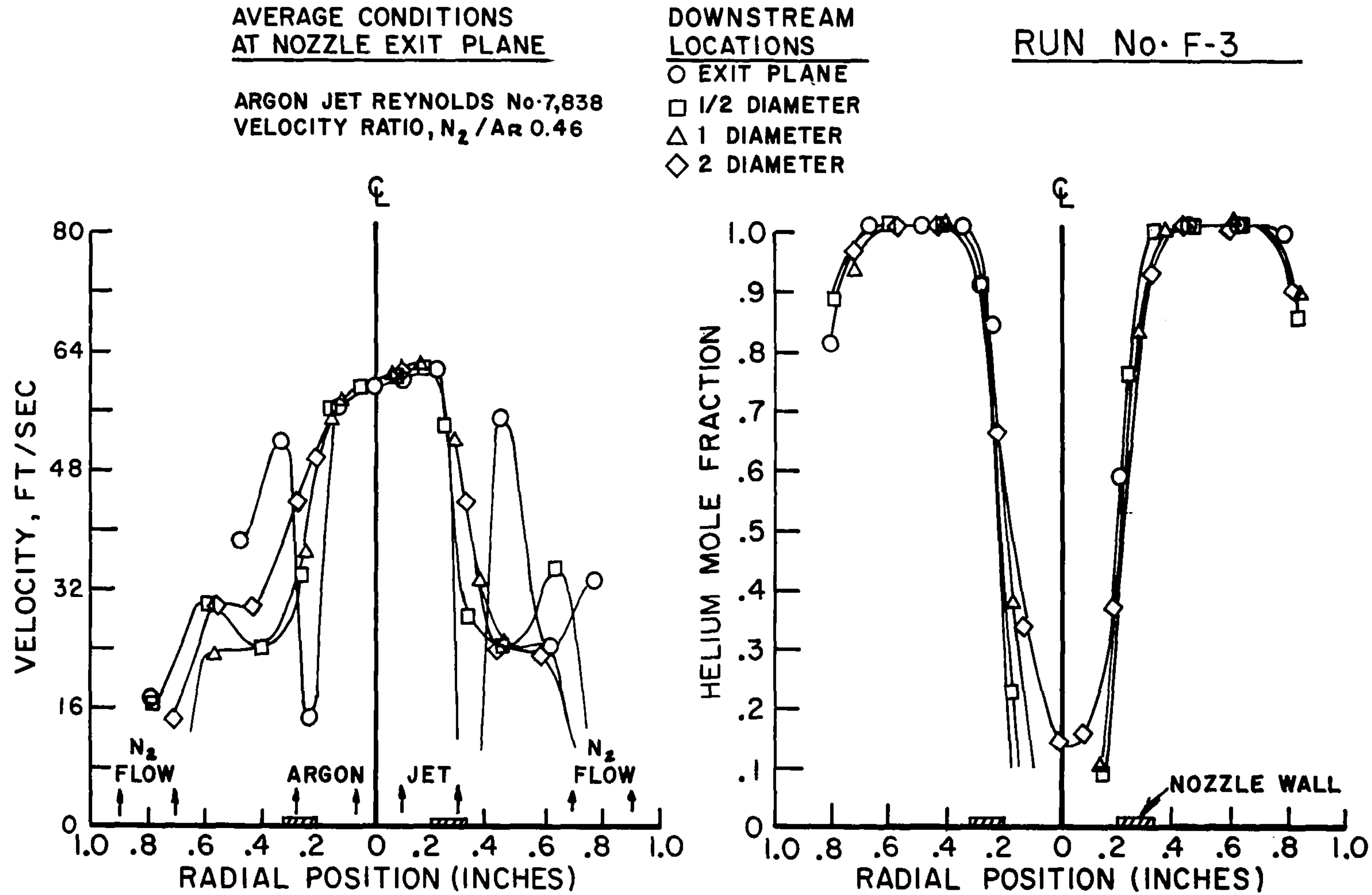

PROFILES OF ARGON JET MIXING ISOTHERMALLY WITH COAXIAL HELIUM FLOW

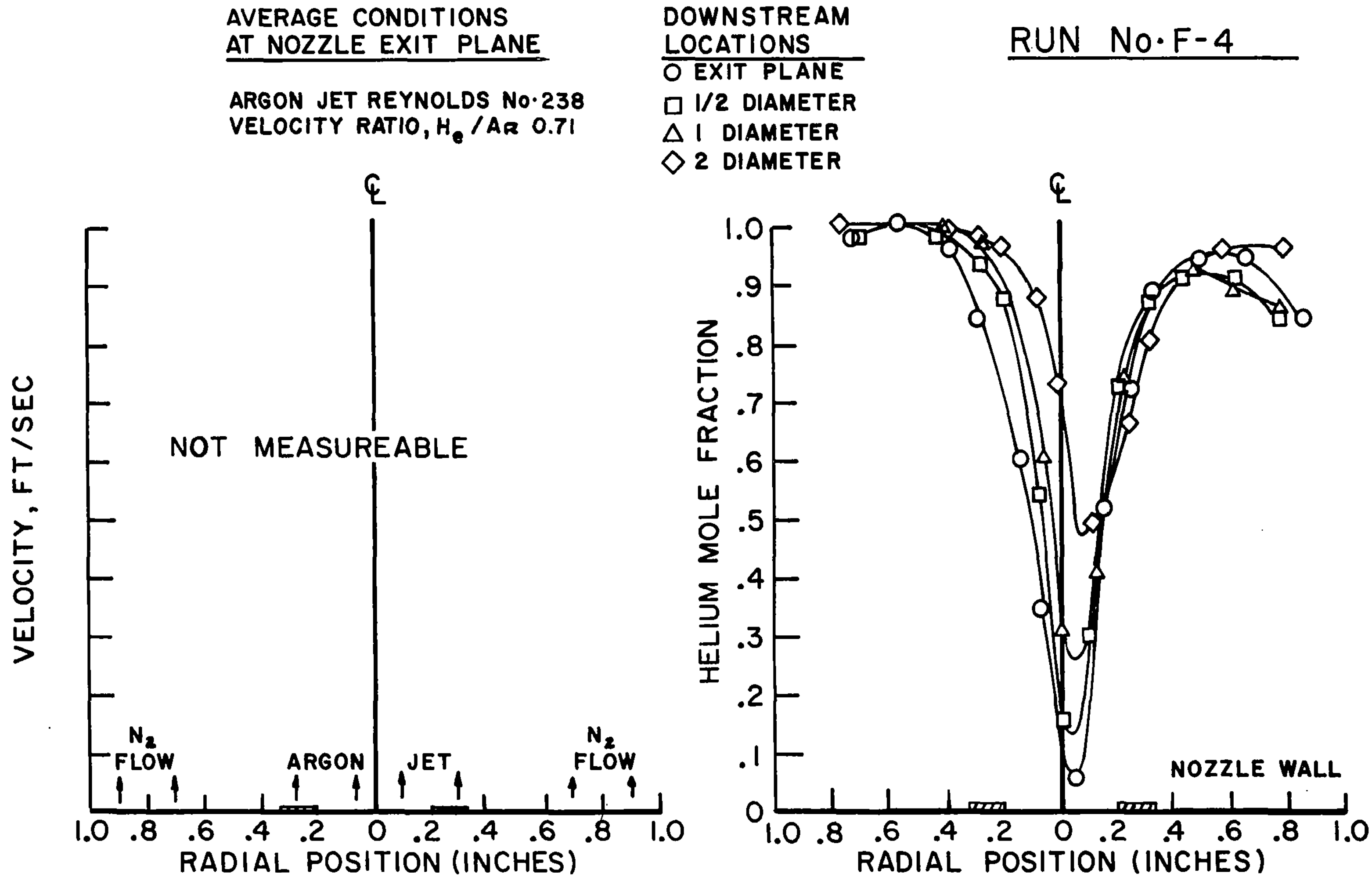

PROFILES OF ARGON JET MIXING ISOTHERMALLY WITH COAXIAL HELIUM FLOW

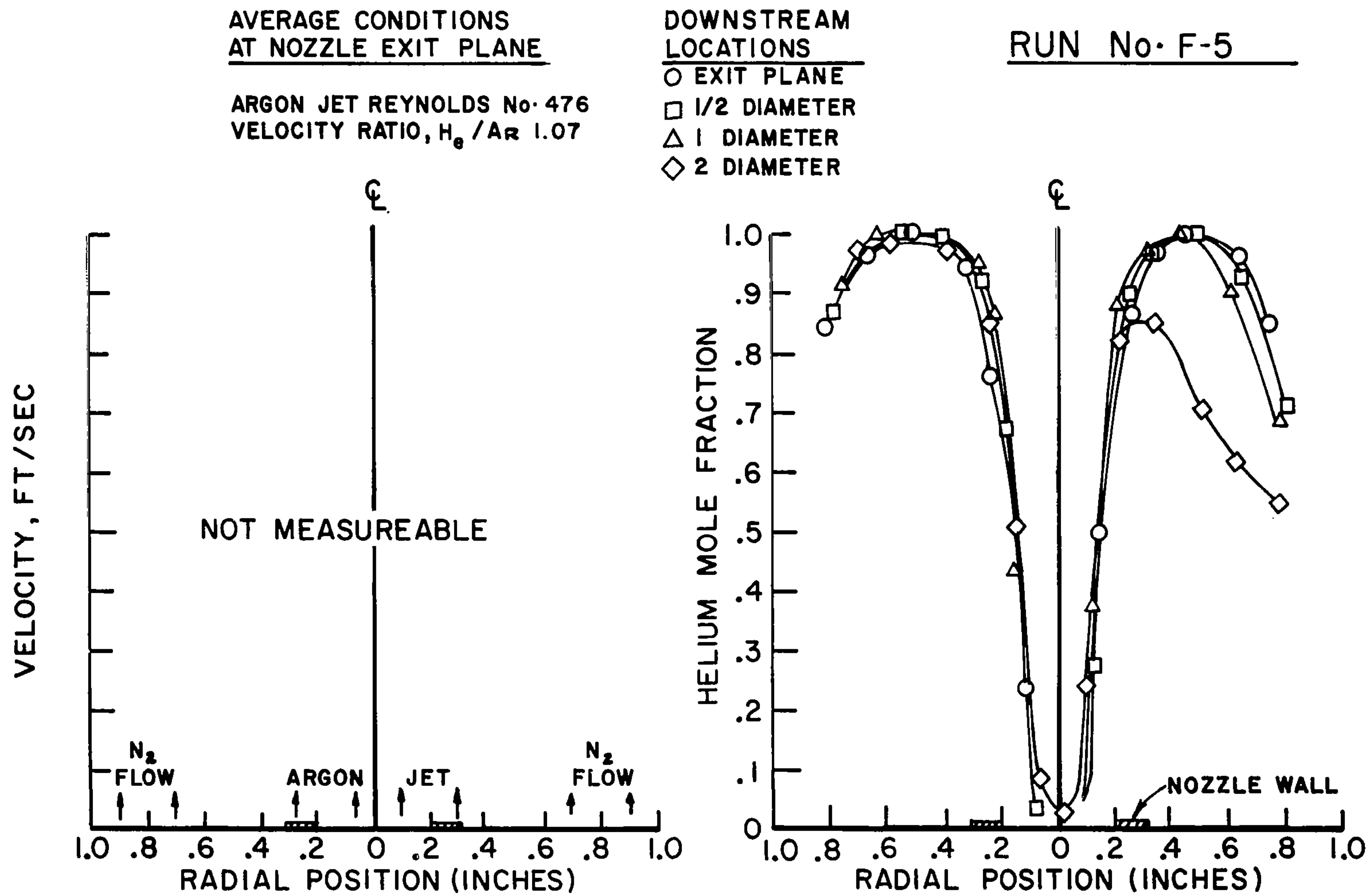

PROFILES OF ARGON JET MIXING ISOTHERMALLY WITH COAXIAL HELIUM FLOW

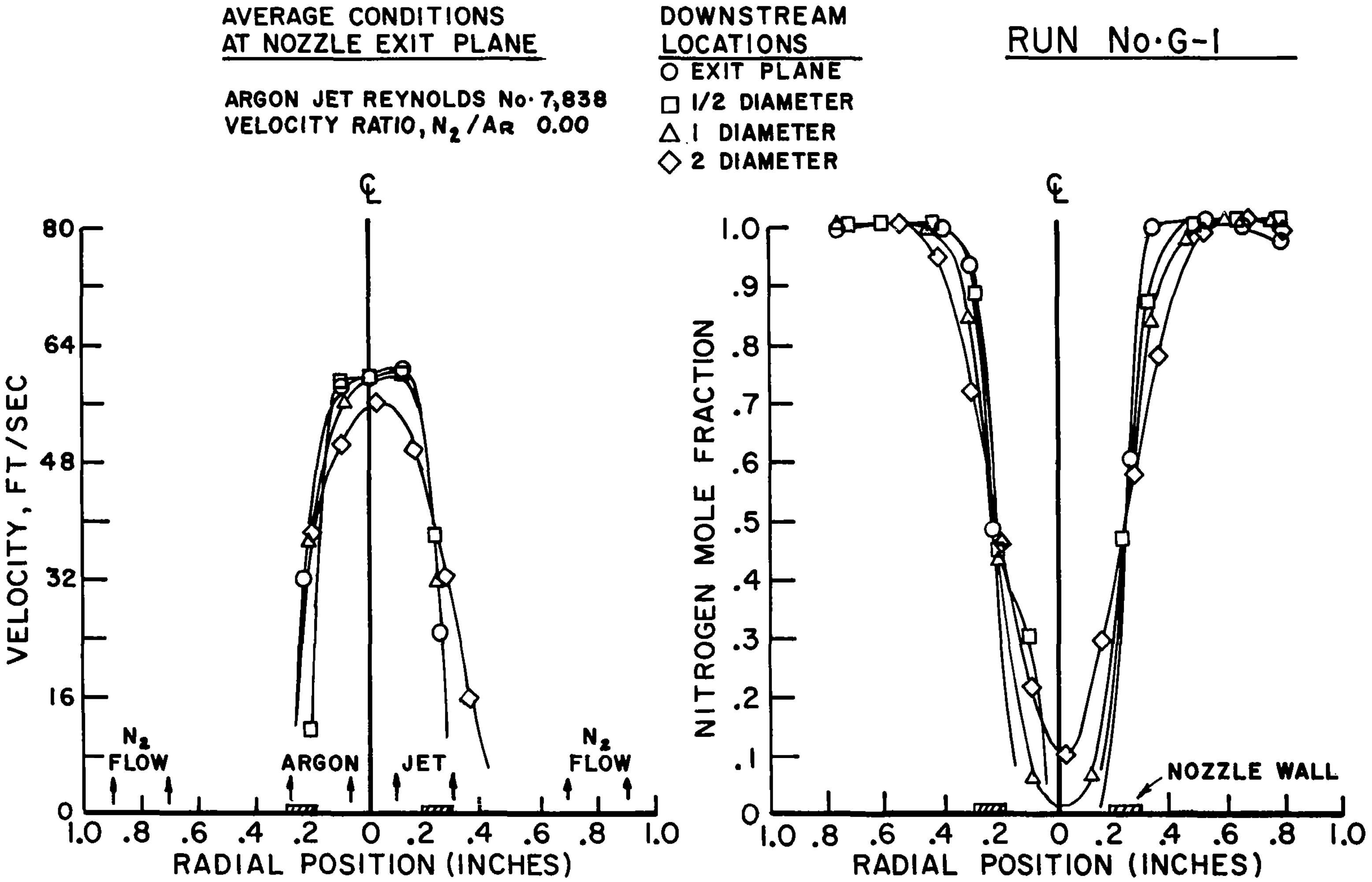

PROFILES OF ARGON JET MIXING ISOTHERMALLY WITH COAXIAL NITROGEN FLOW

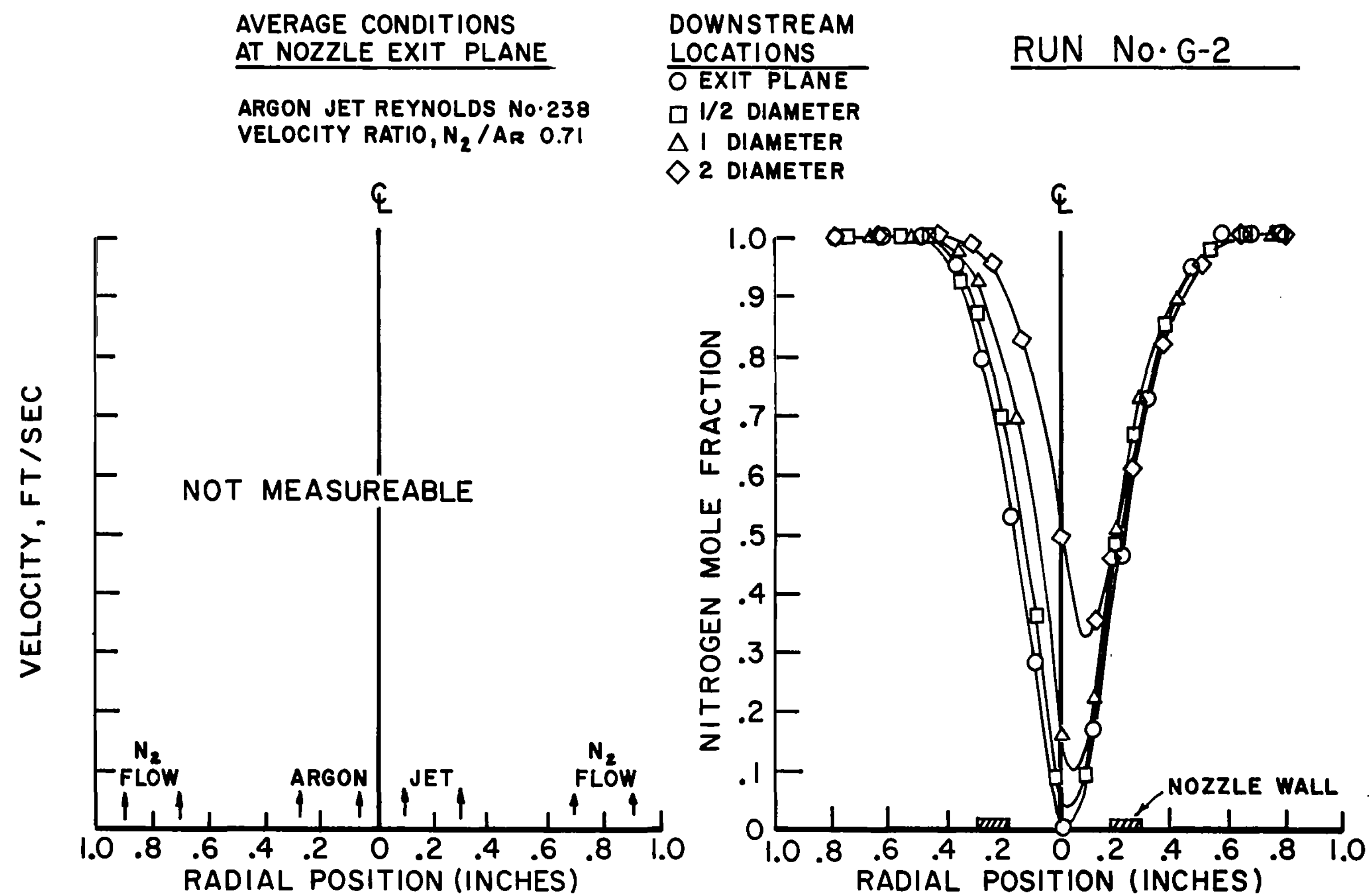

PROFILES OF ARGON JET MIXING ISOTHERMALLY WITH COAXIAL NITROGEN FLOW

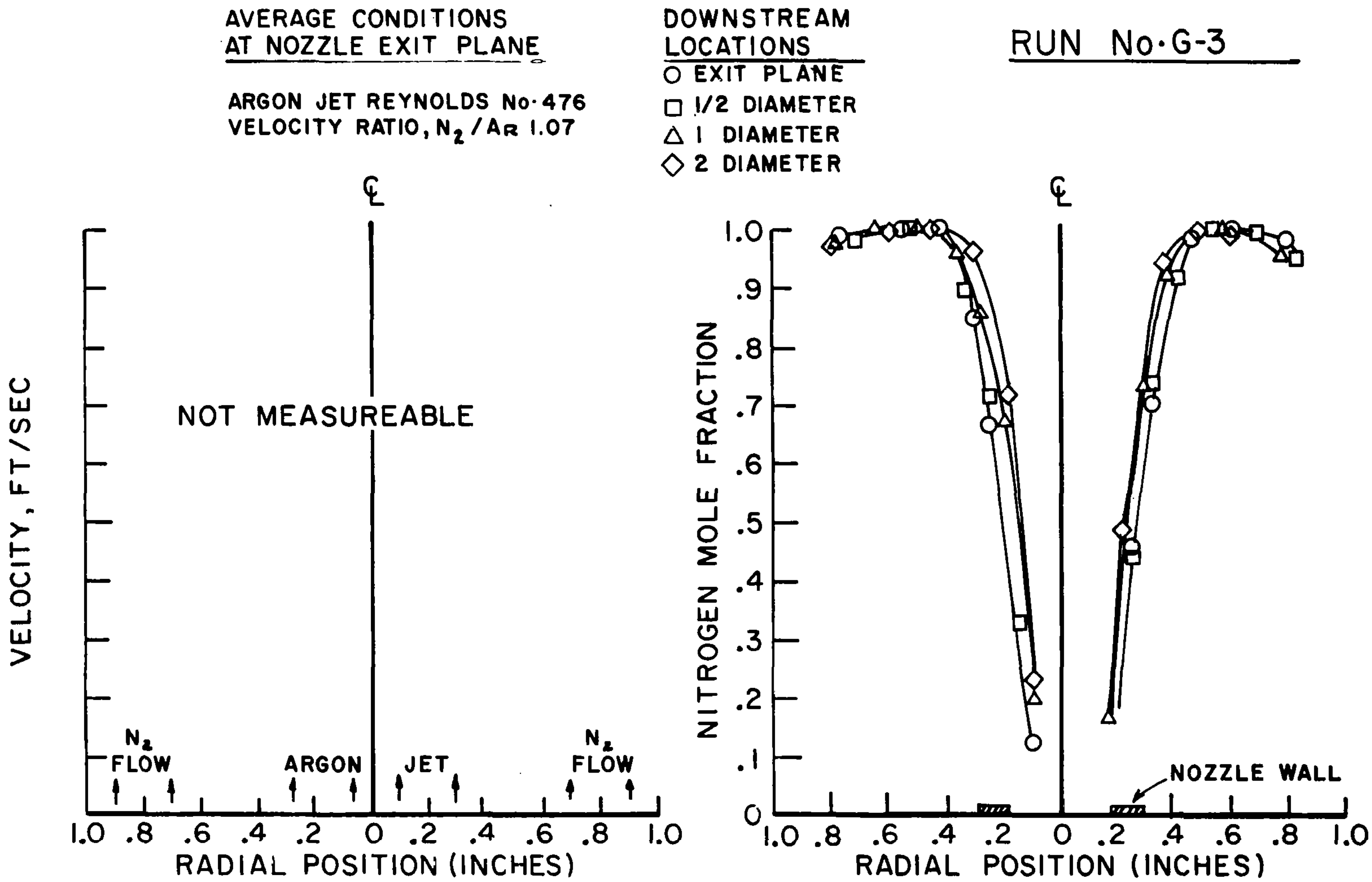

PROFILES OF ARGON JET MIXING ISOTHERMALLY WITH COAXIAL NITROGEN FLOW

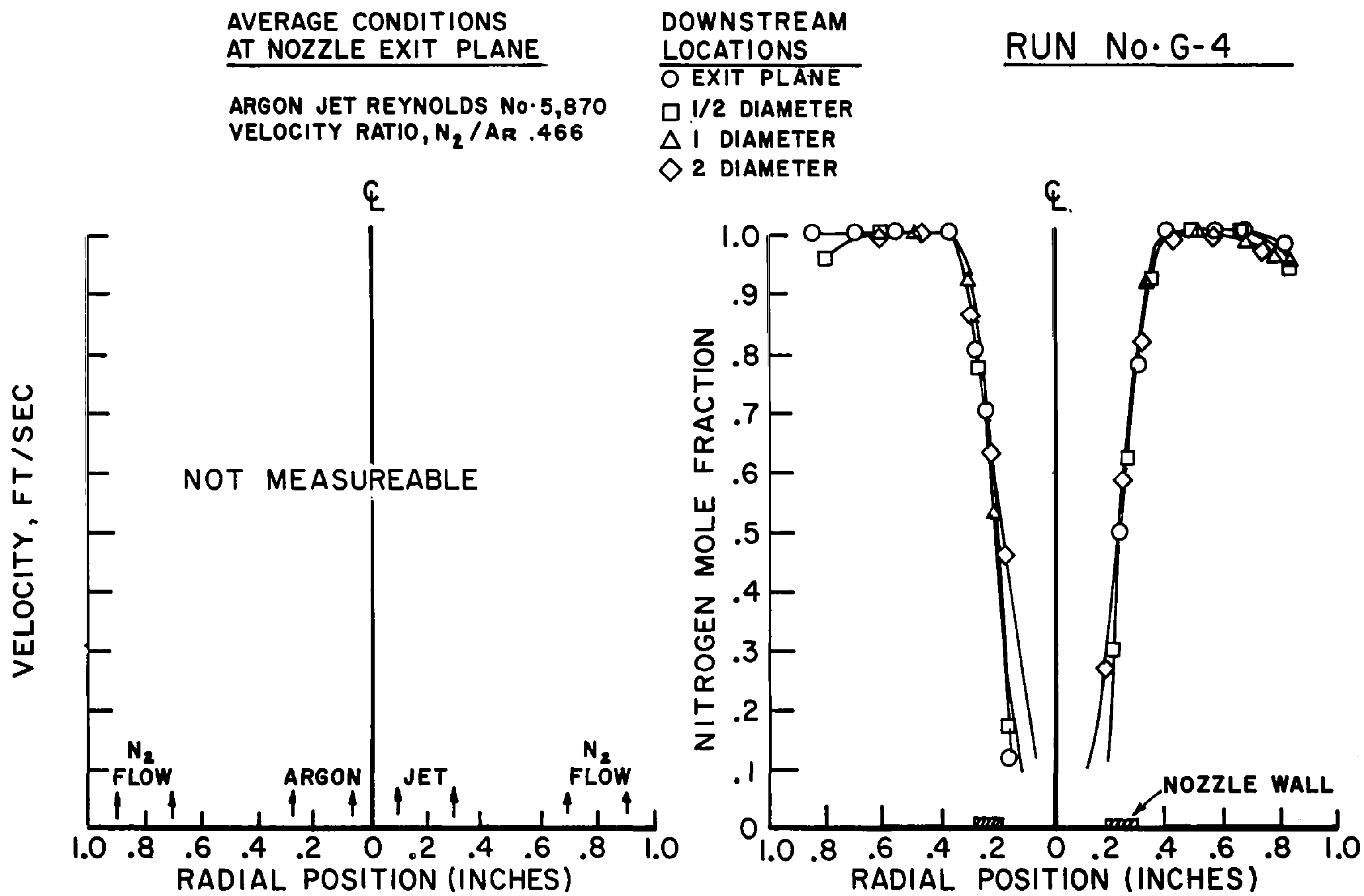

PROFILES OF ARGON JET MIXING ISOTHERMALLY WITH COAXIAL NITROGEN FLOW

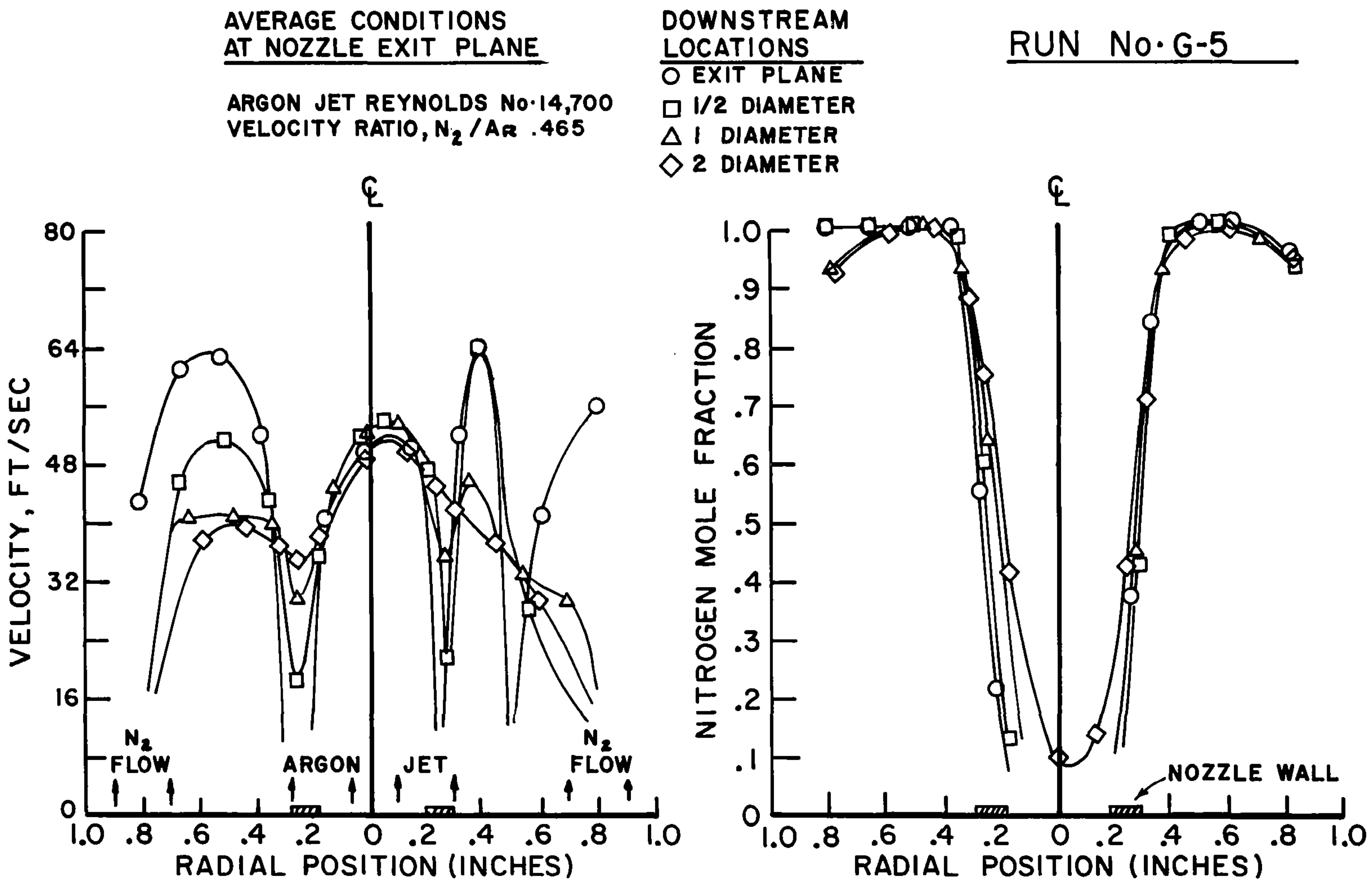

PROFILES OF ARGON JET MIXING ISOTHERMALLY WITH COAXIAL NITROGEN FLOW

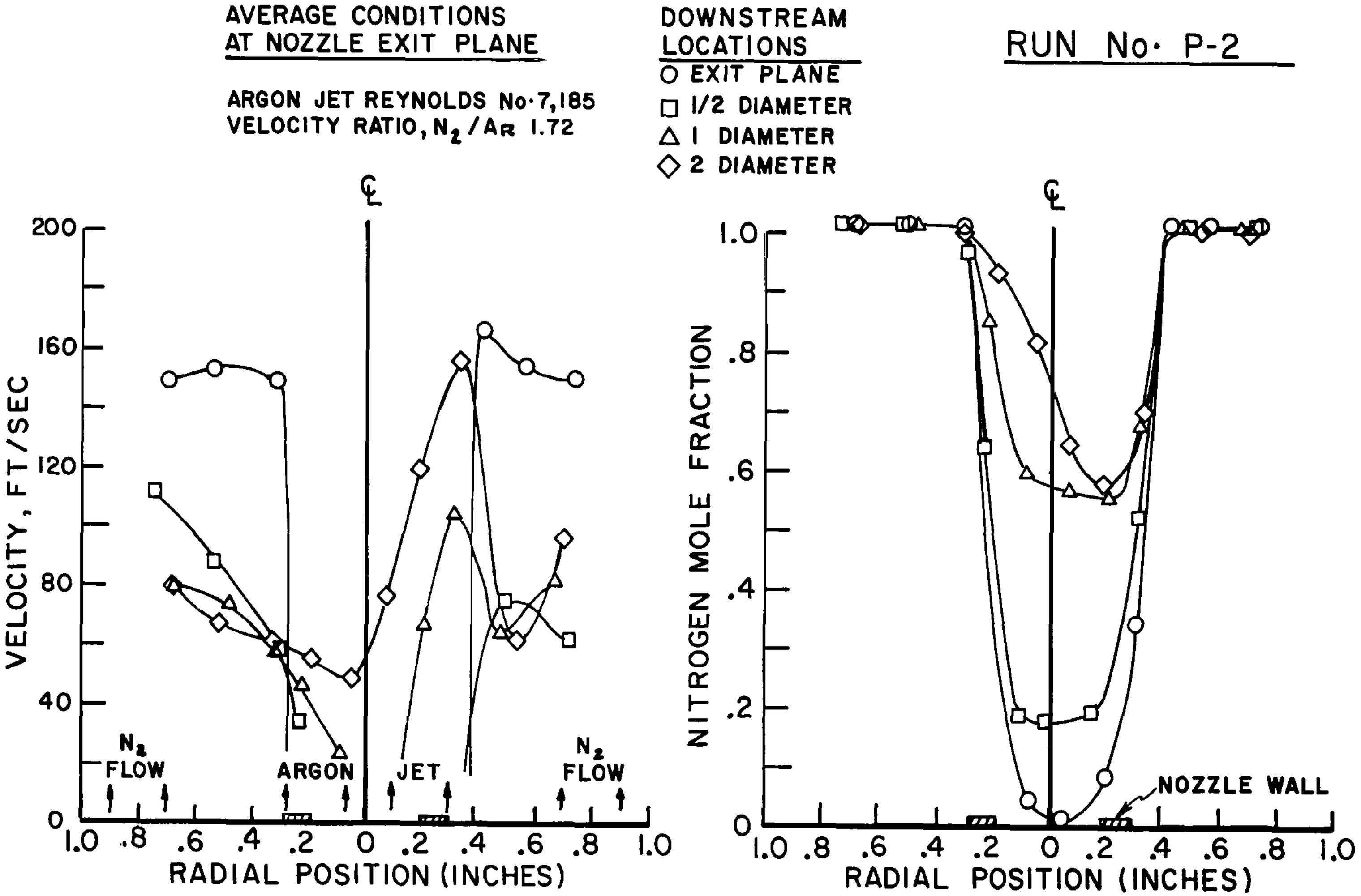

PROFILES OF ARGON JET MIXING ISOTHERMALLY WITH COAXIAL NITROGEN FLOW

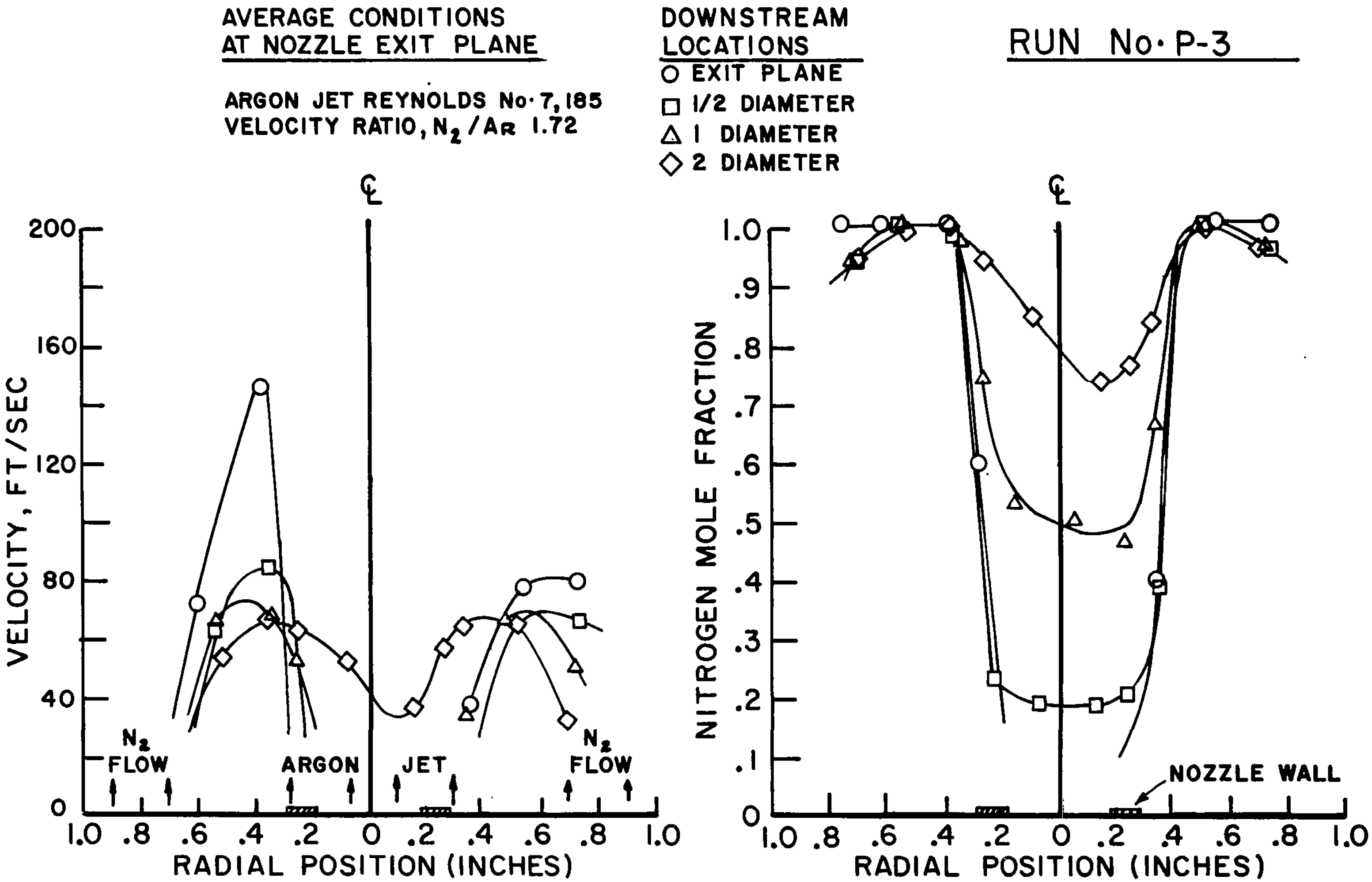

PROFILES OF ARGON JET MIXING ISOTHERMALLY WITH COAXIAL NITROGEN FLOW

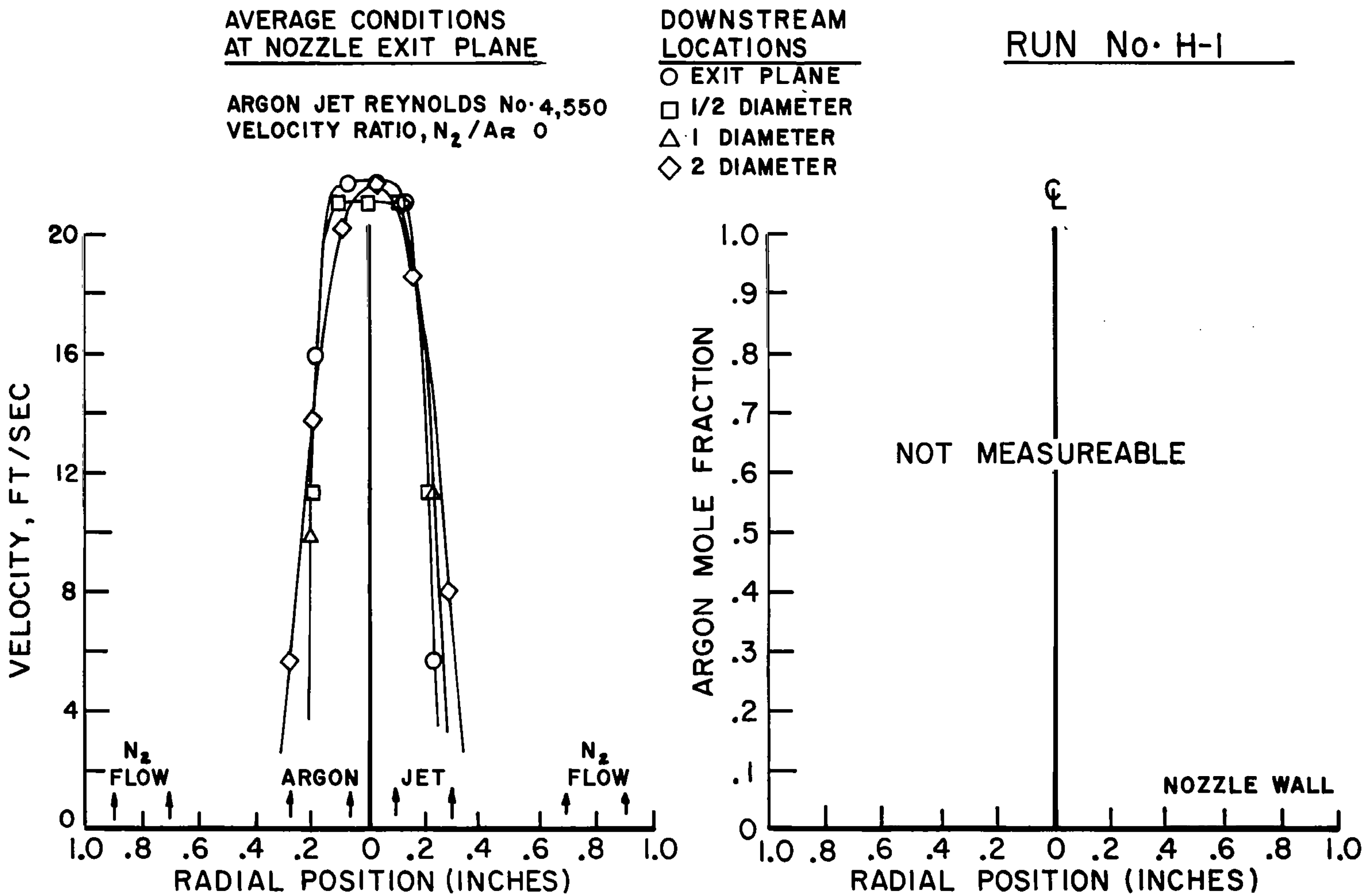

PROFILES OF ARGON JET MIXING ISOTHERMALLY WITH COAXIAL ARGON FLOW

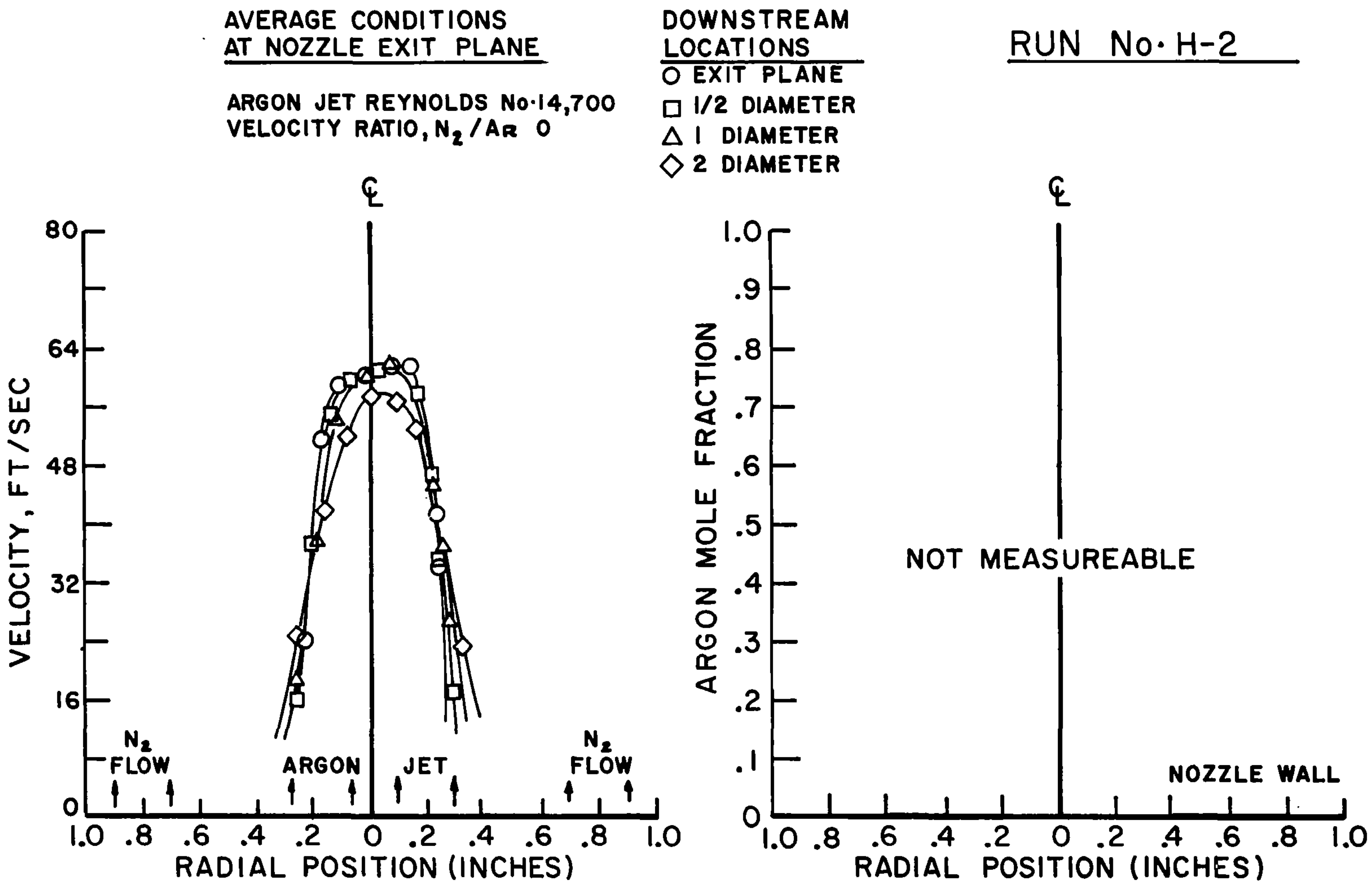

PROFILES OF ARGON JET MIXING ISOTHERMALLY WITH COAXIAL ARGON FLOW

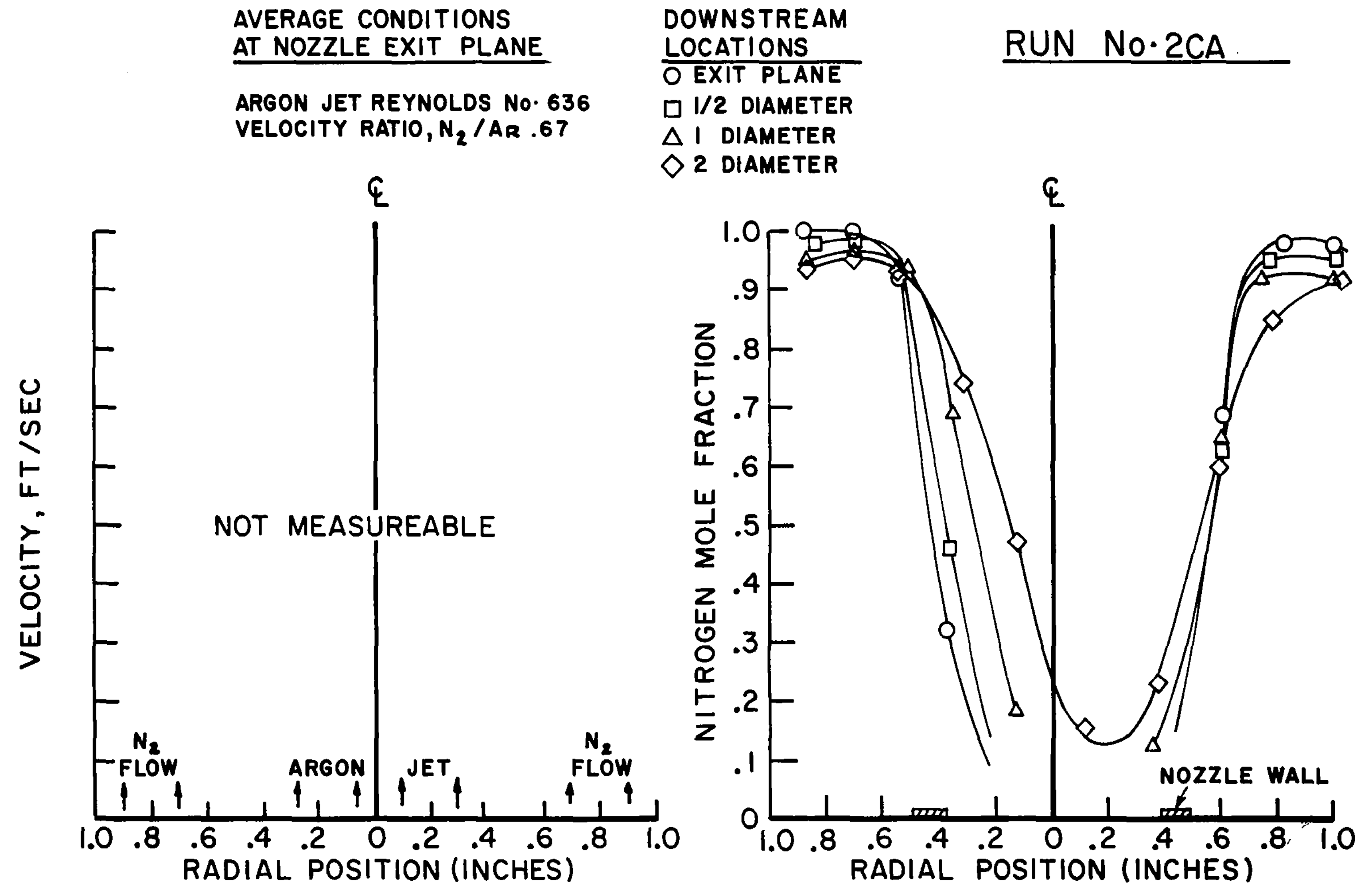

PROFILES OF ARGON JET MIXING ISOTHERMALLY WITH COAXIAL NITROGEN FLOW

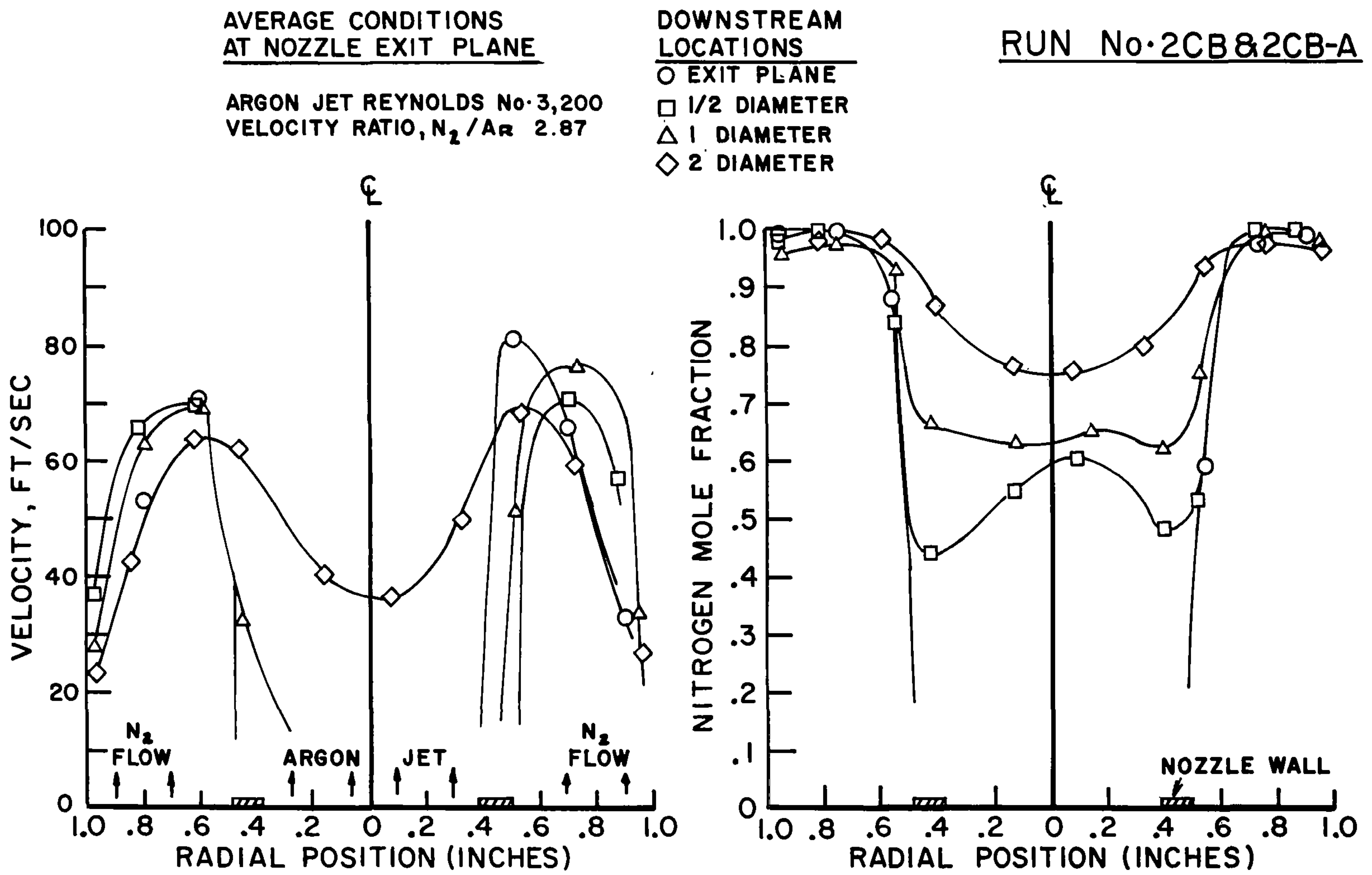

PROFILES OF ARGON JET MIXING ISOTHERMALLY WITH COAXIAL NITROGEN FLOW

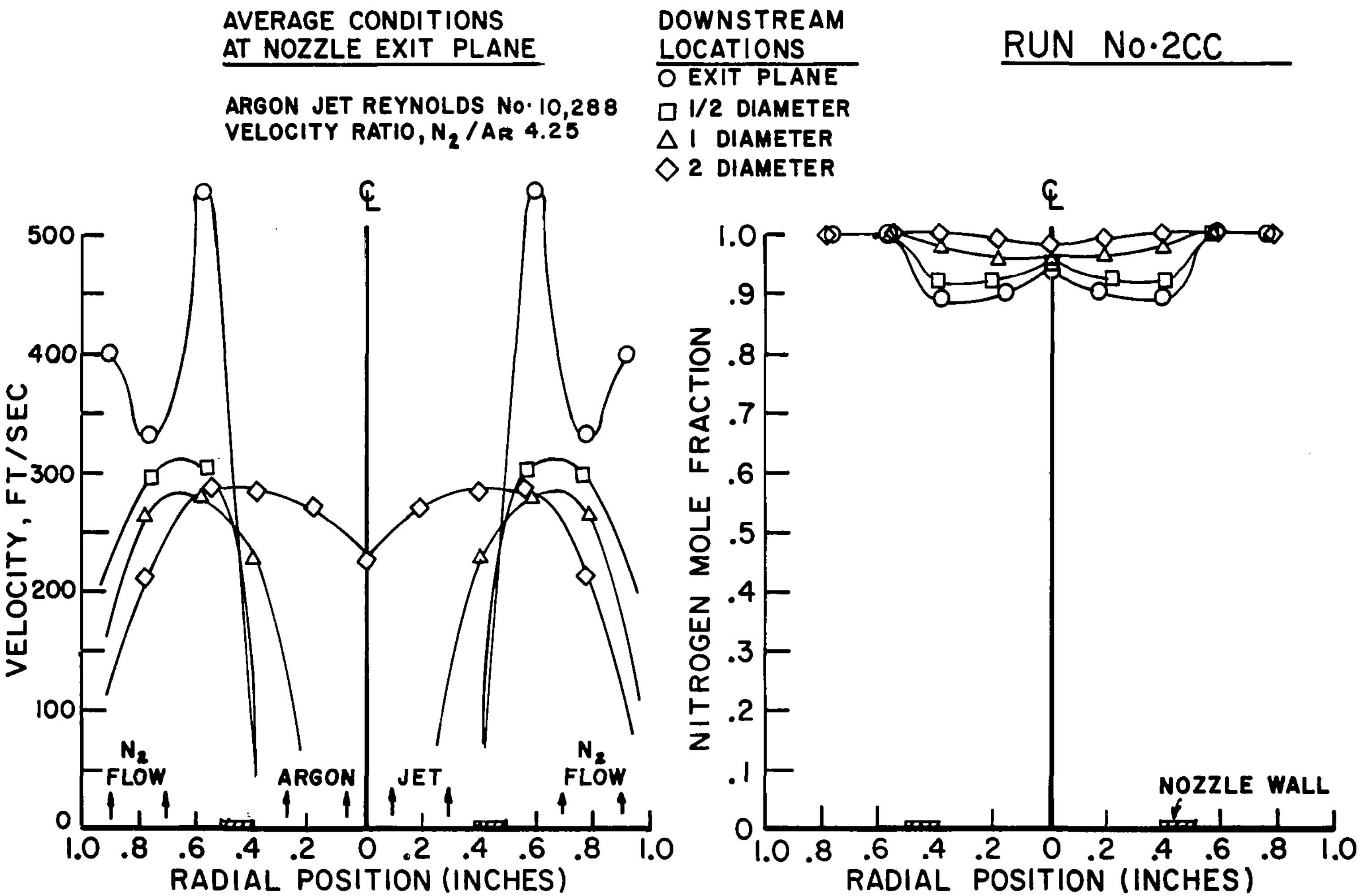

PROFILES OF ARGON JET MIXING ISOTHERMALLY WITH COAXIAL NITROGEN FLOW
(LEFT HAND PROFILE MEASURED, RIGHT HAND PROFILE DRAWN SYMETRICALLY)

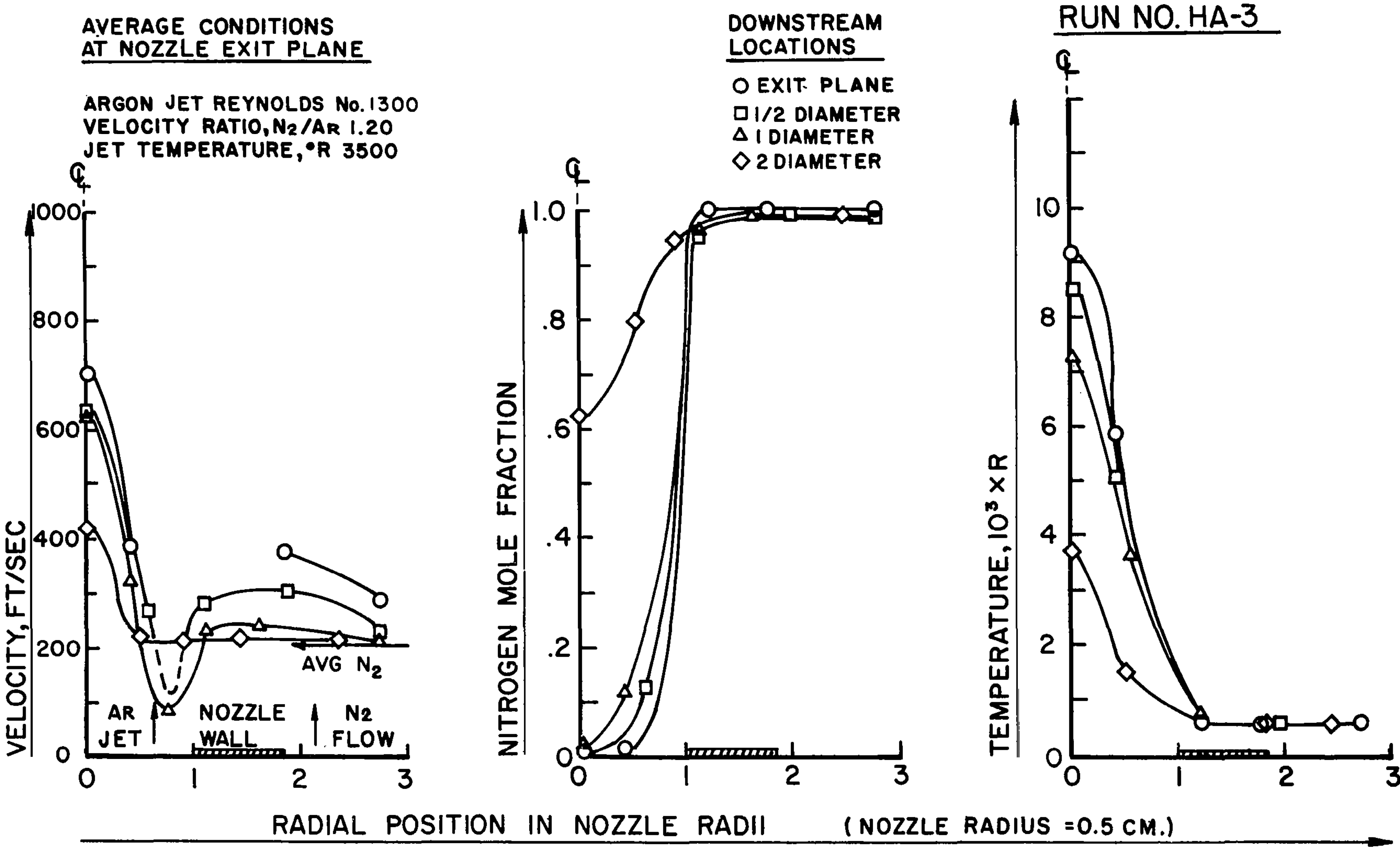

HALF-PROFILES OF ARGON ARCJET JET MIXING WITH COAXIAL NITROGEN FLOW

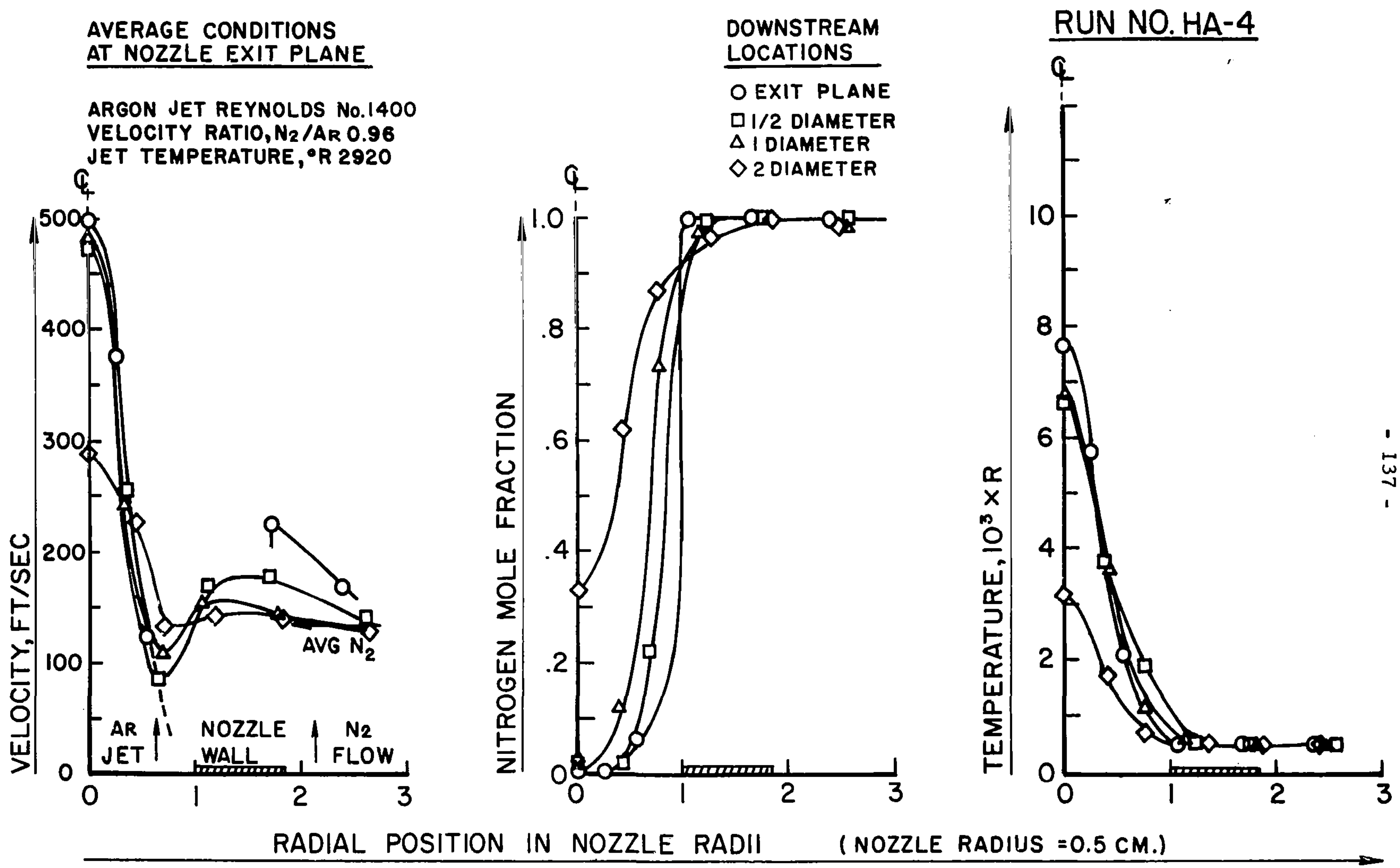

HALF-PROFILES OF ARGON ARCJET JET MIXING WITH COAXIAL NITROGEN FLOW

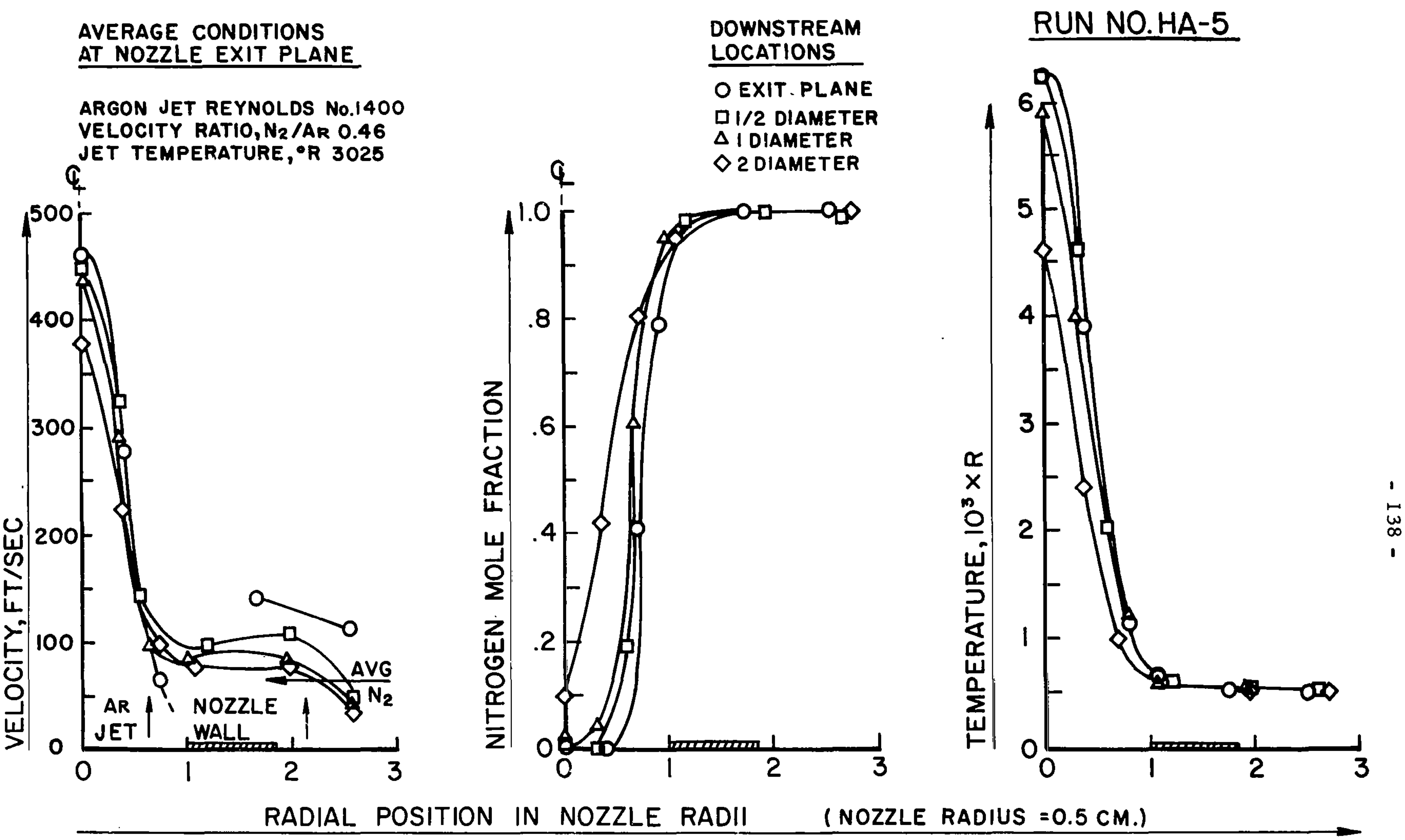

HALF-PROFILES OF ARGON ARCJET JET MIXING WITH COAXIAL NITROGEN FLOW

- 138 -

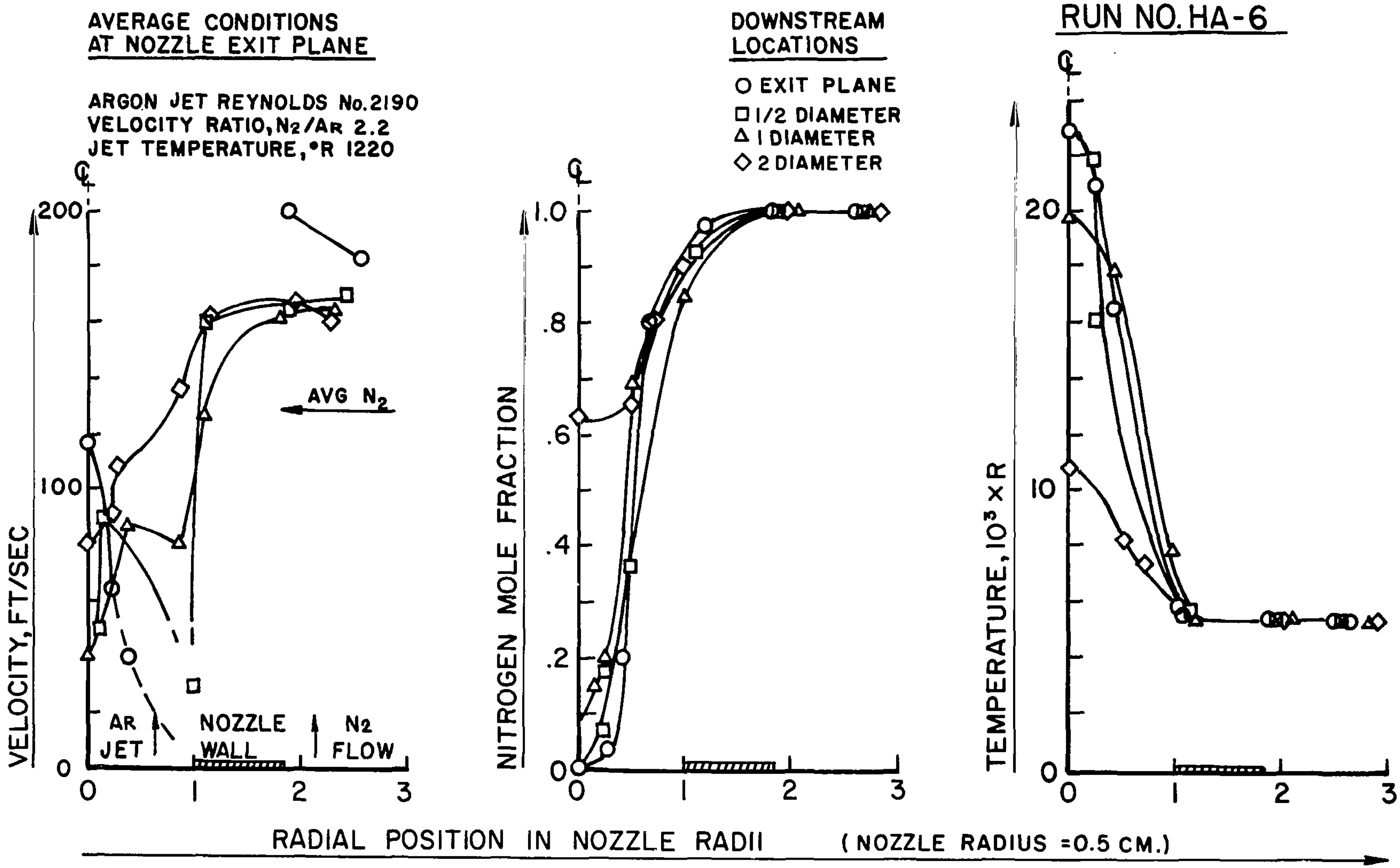

HALF-PROFILES OF ARGON ARCJET JET MIXING WITH COAXIAL NITROGEN FLOW

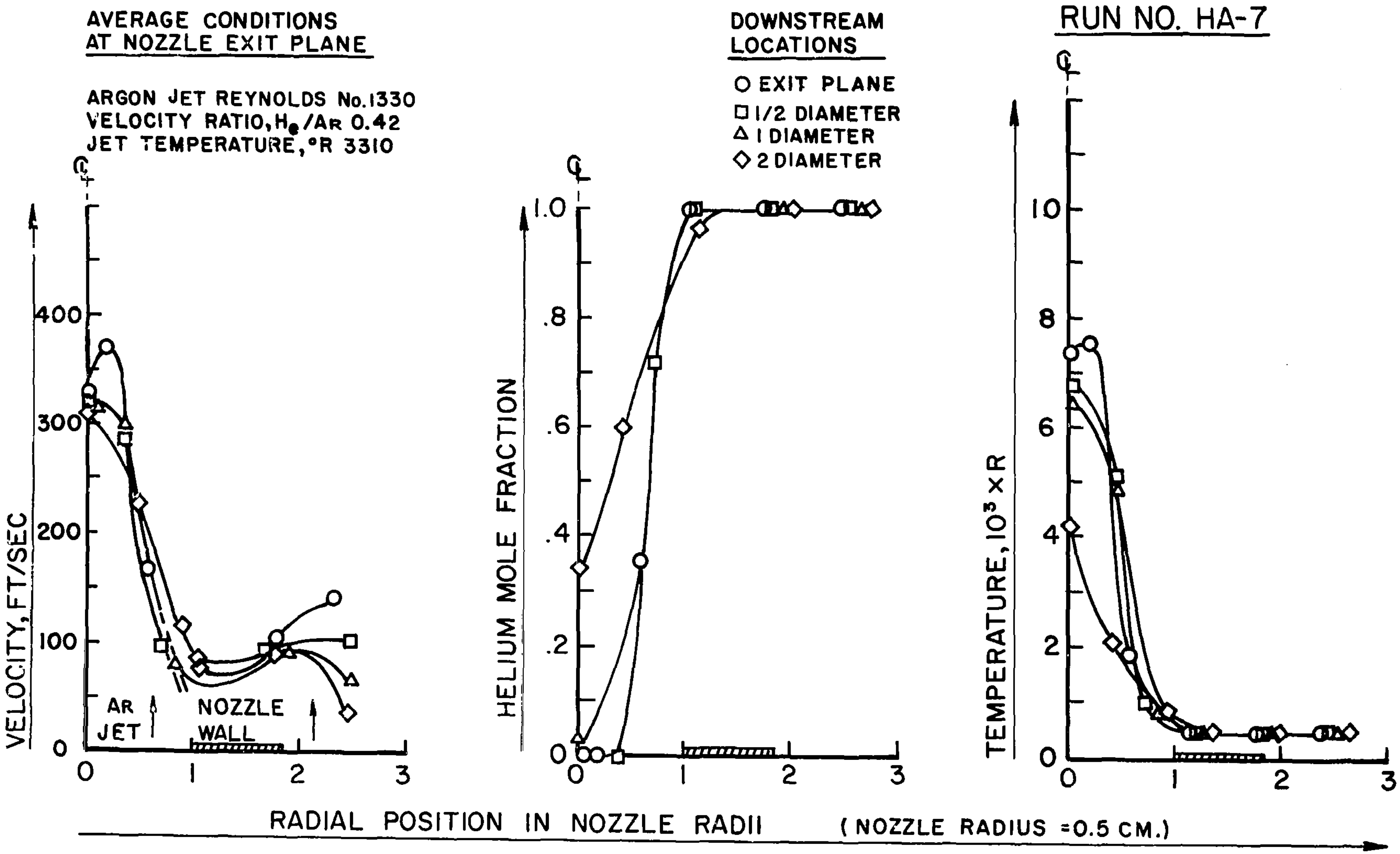

HALF-PROFILES OF ARGON ARCJET JET MIXING WITH COAXIAL HELIUM FLOW

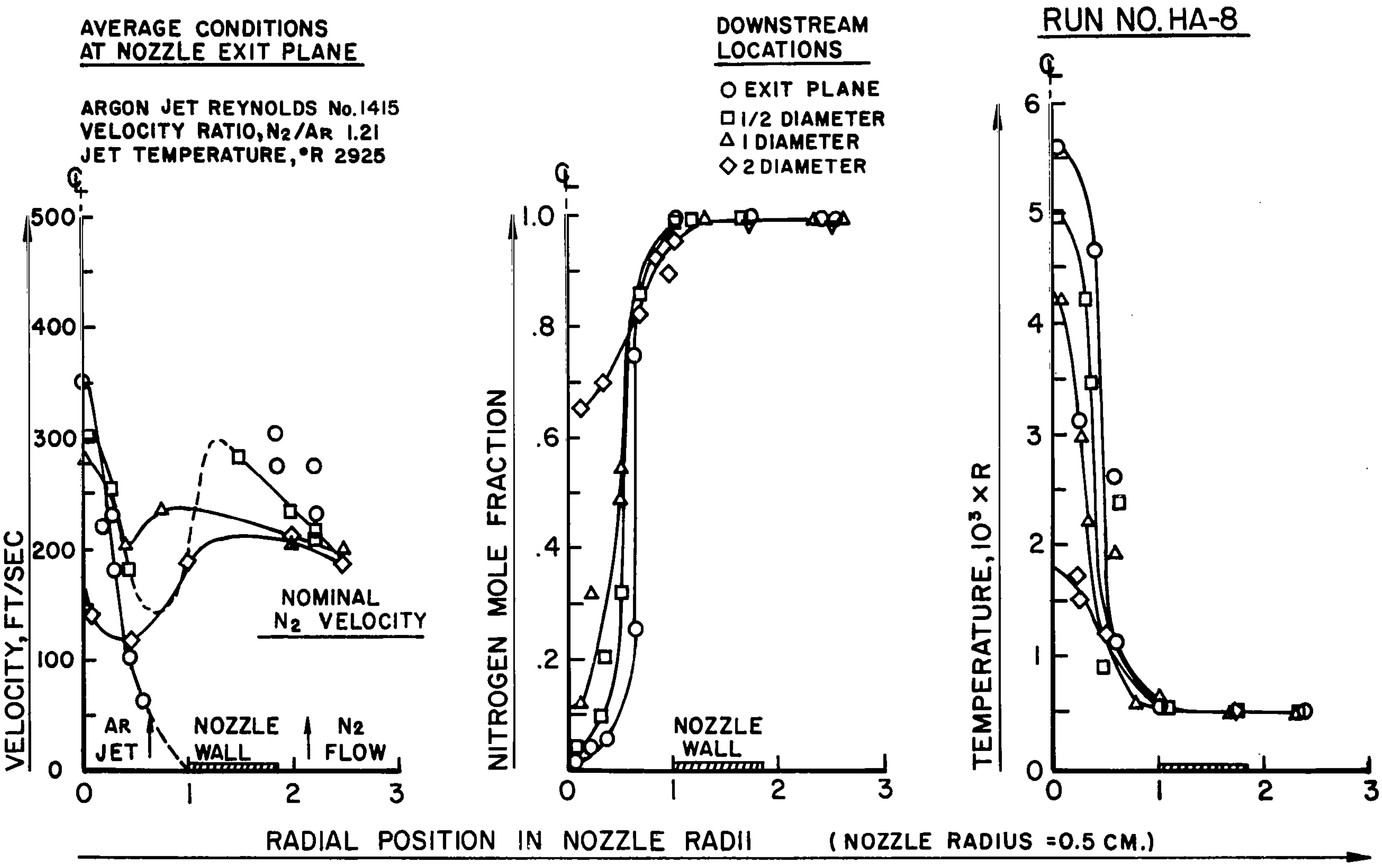

HALF-PROFILES OF ARGON ARCJET JET MIXING WITH COAXIAL NITROGEN FLOW

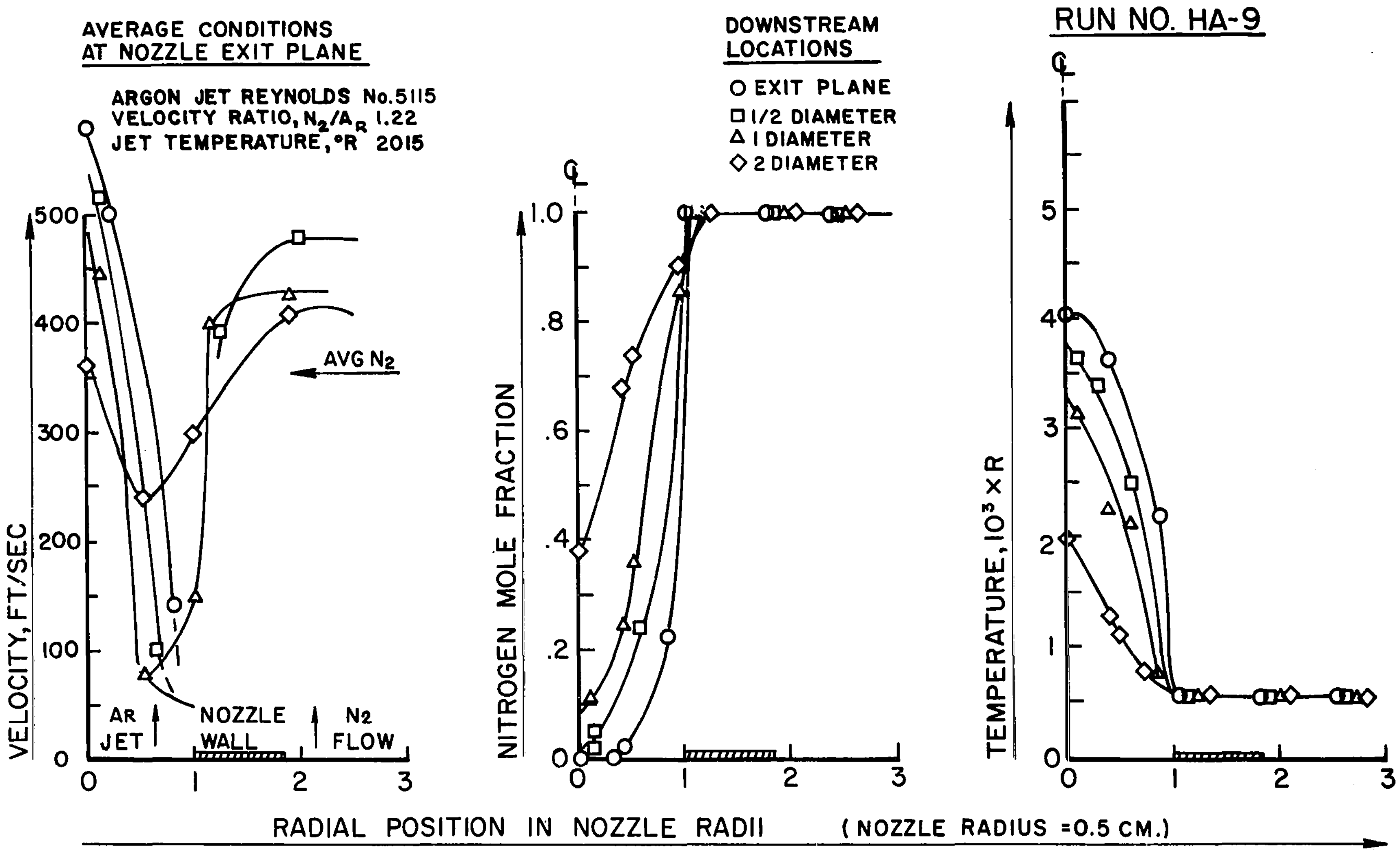

HALF-PROFILES OF ARGON ARCJET JET MIXING WITH COAXIAL NITROGEN FLOW

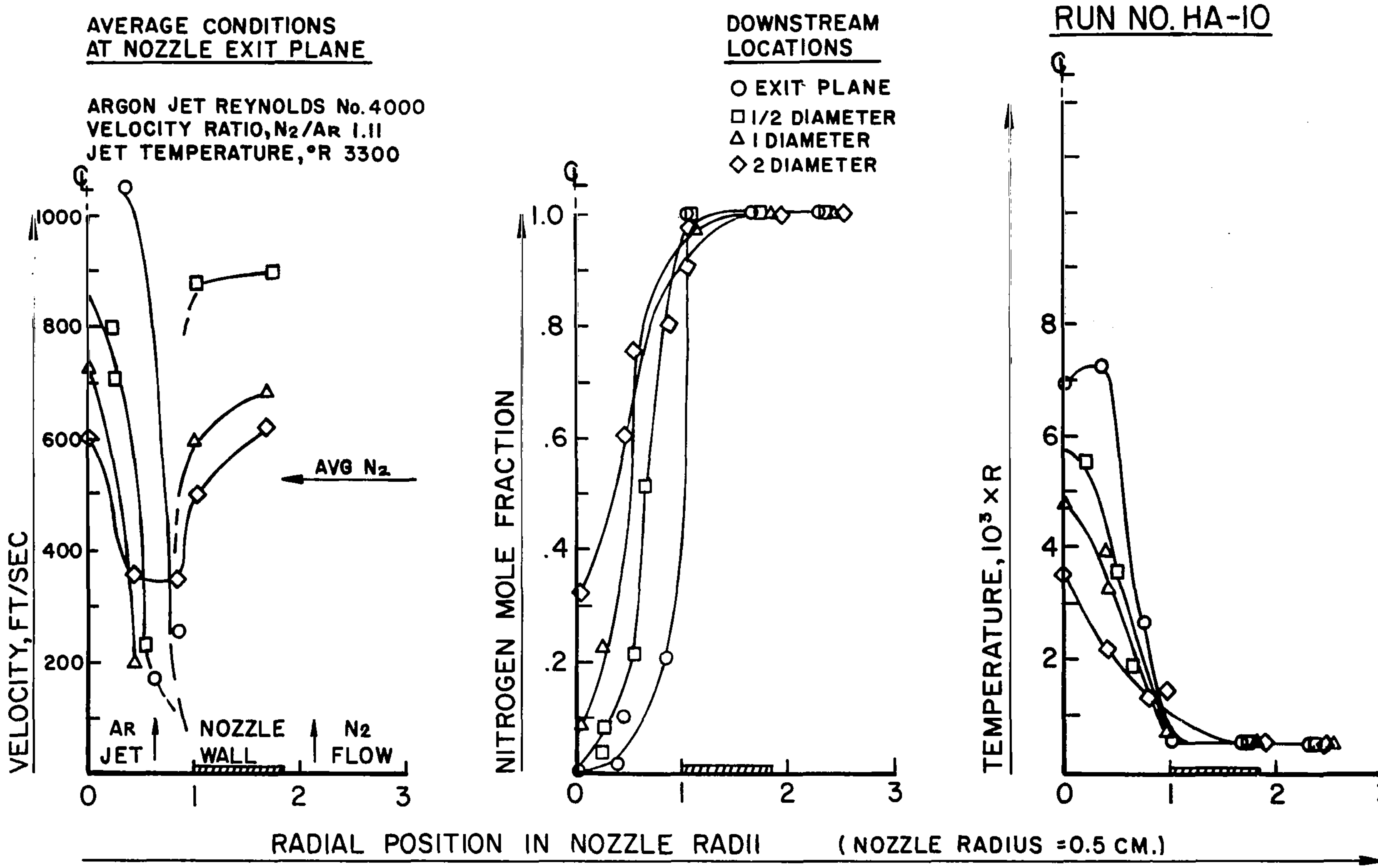

HALF-PROFILES OF ARGON ARCJET JET MIXING WITH COAXIAL NITROGEN FLOW

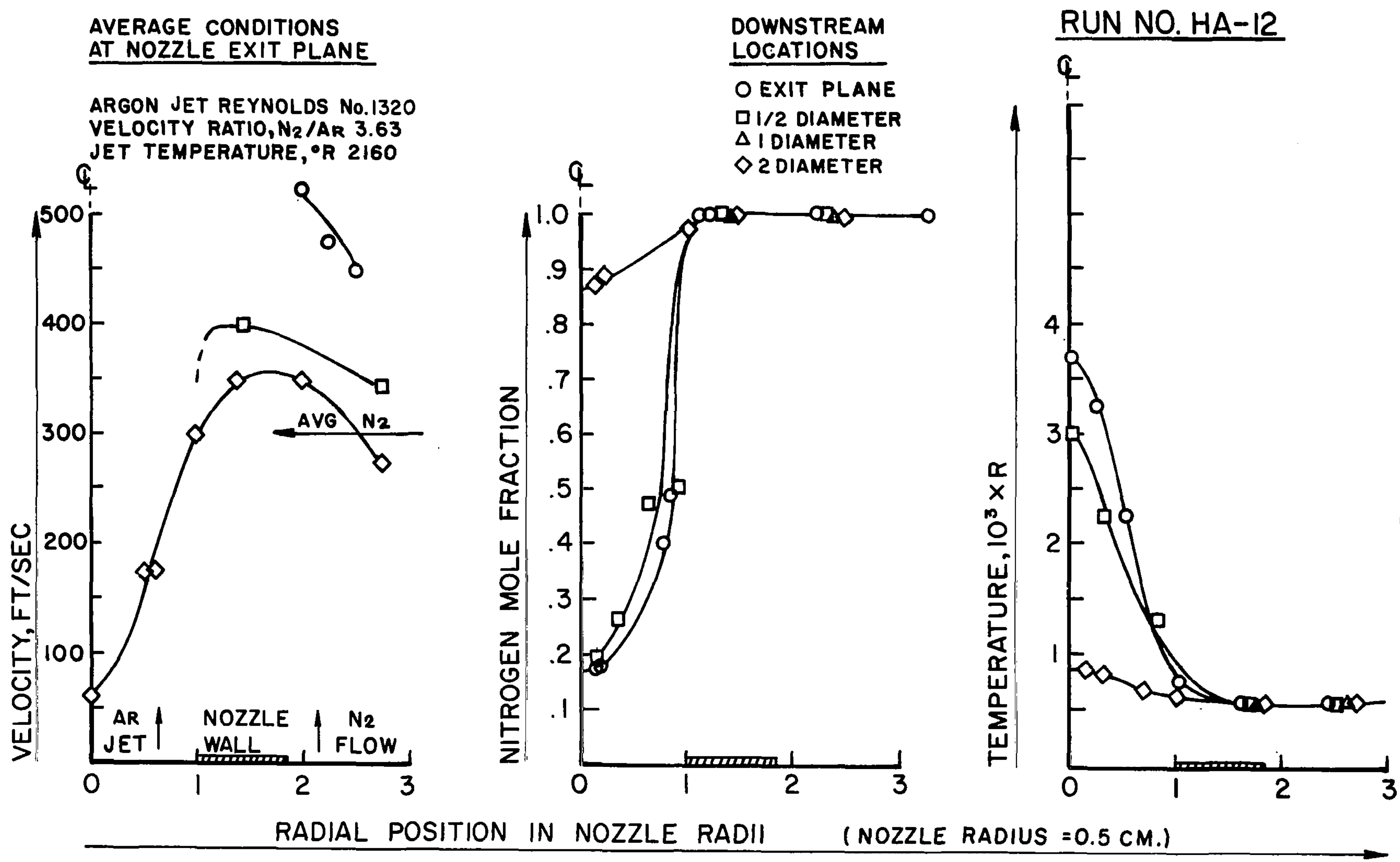

HALF-PROFILES OF ARGON ARCJET JET MIXING WITH COAXIAL NITROGEN FLOW

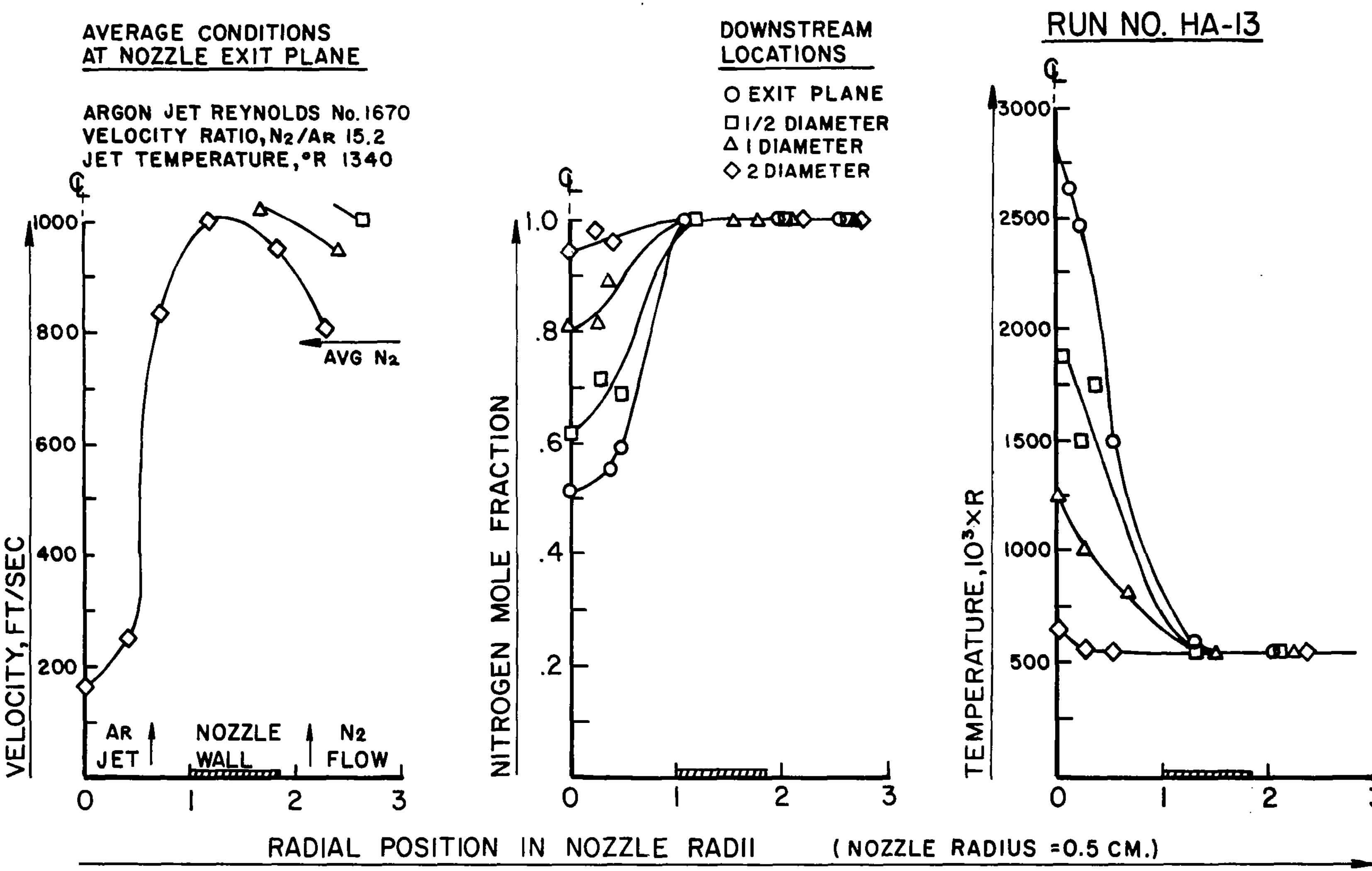

HALF-PROFILES OF ARGON ARCJET JET MIXING WITH COAXIAL NITROGEN FLOW

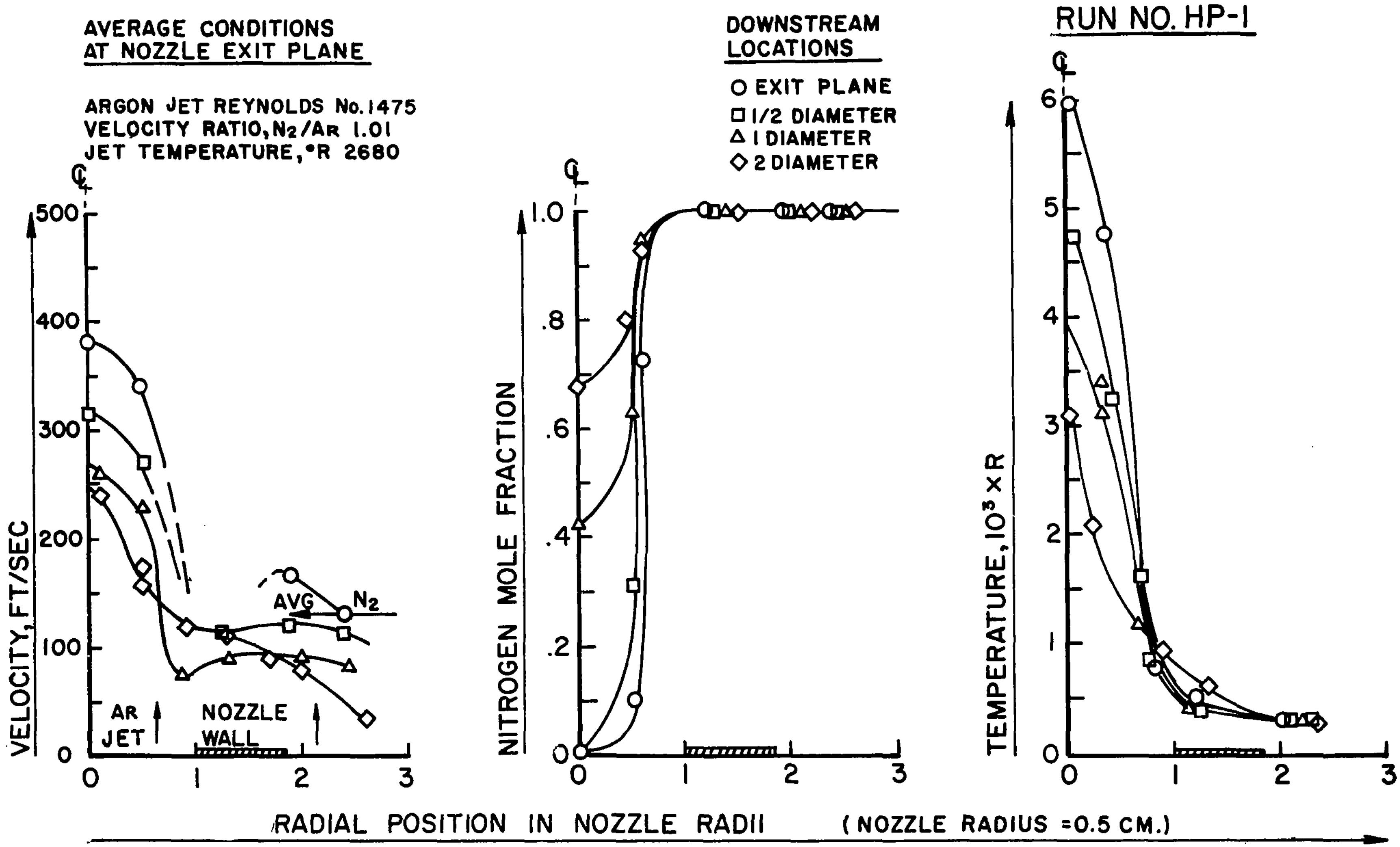

HALF-PROFILES OF ARGON ARCJET JET MIXING WITH COAXIAL NITROGEN FLOW

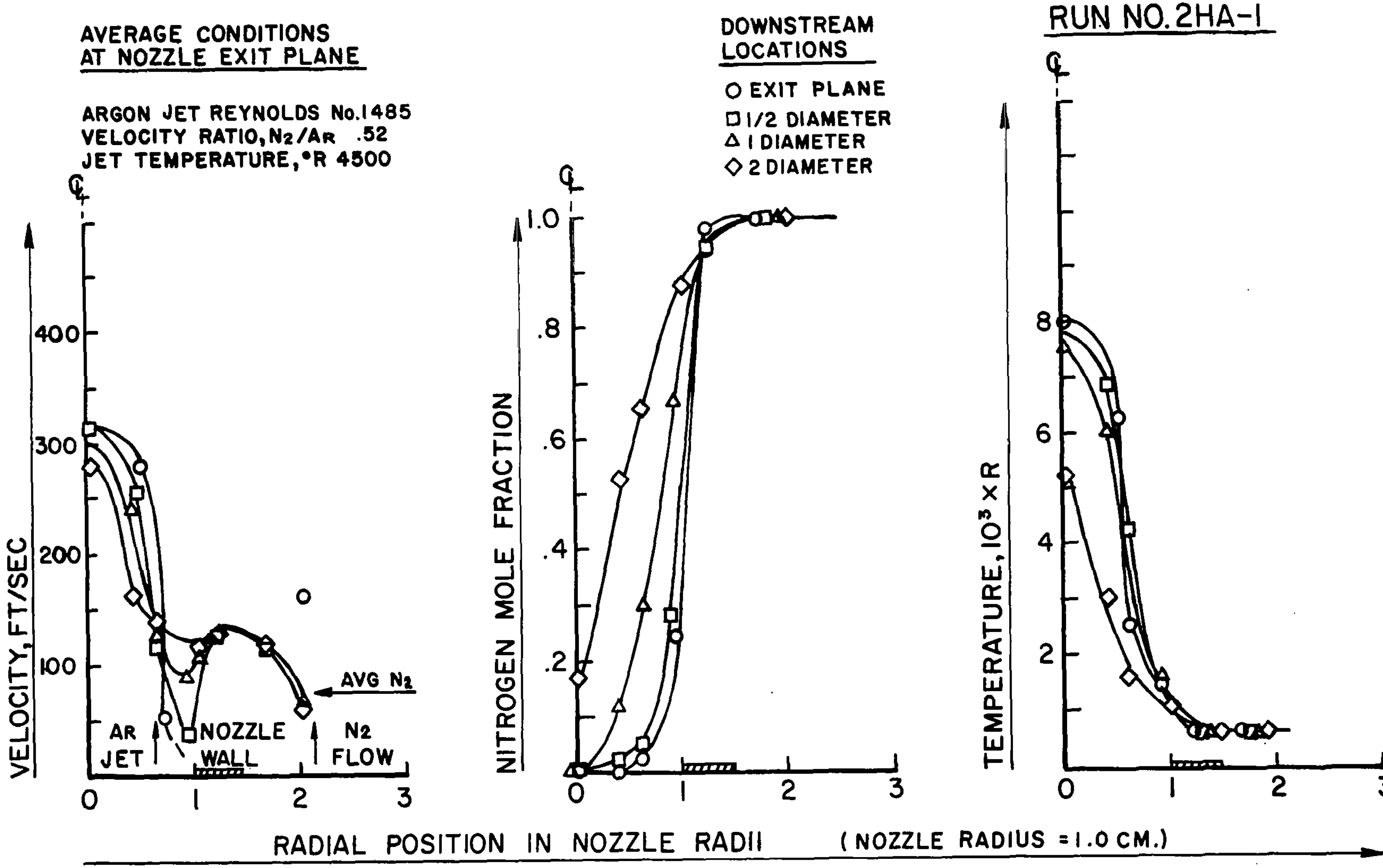

HALF-PROFILES OF ARGON ARCJET JET MIXING WITH COAXIAL NITROGEN FLOW

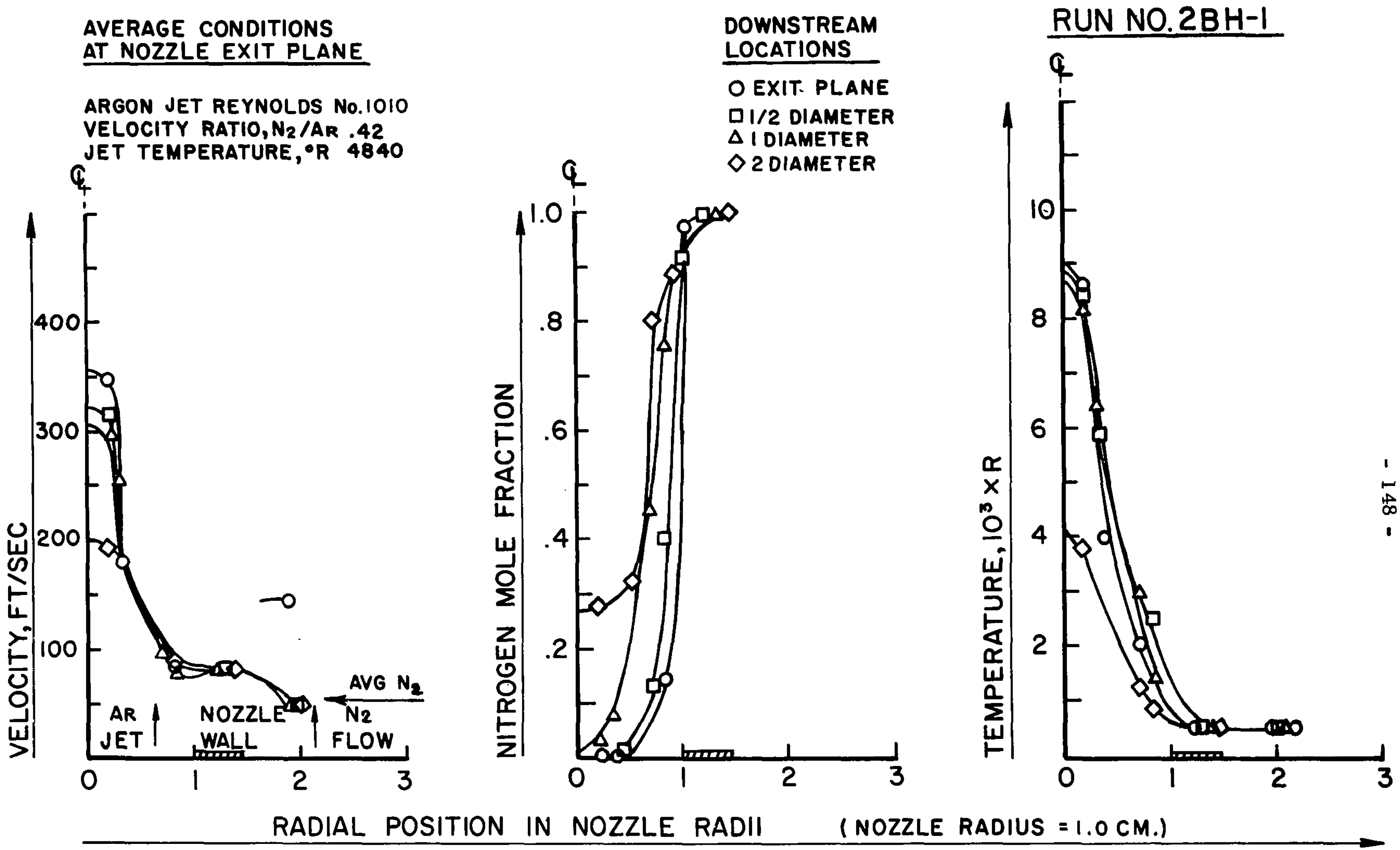

HALF-PROFILES OF ARGON ARCJET JET MIXING WITH COAXIAL NITROGEN FLOW

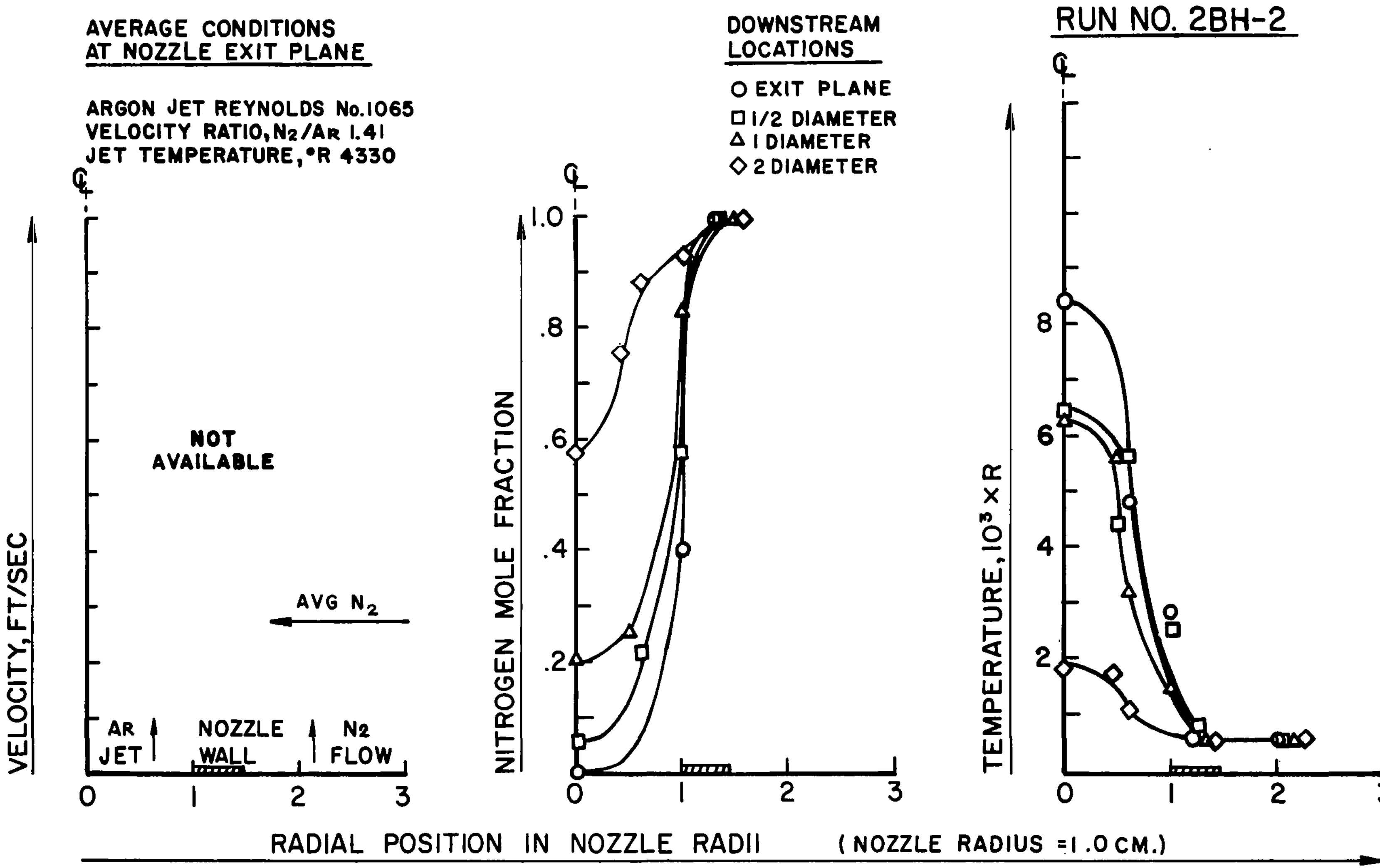

HALF-PROFILES OF ARGON ARCJET JET MIXING WITH COAXIAL NITROGEN FLOW

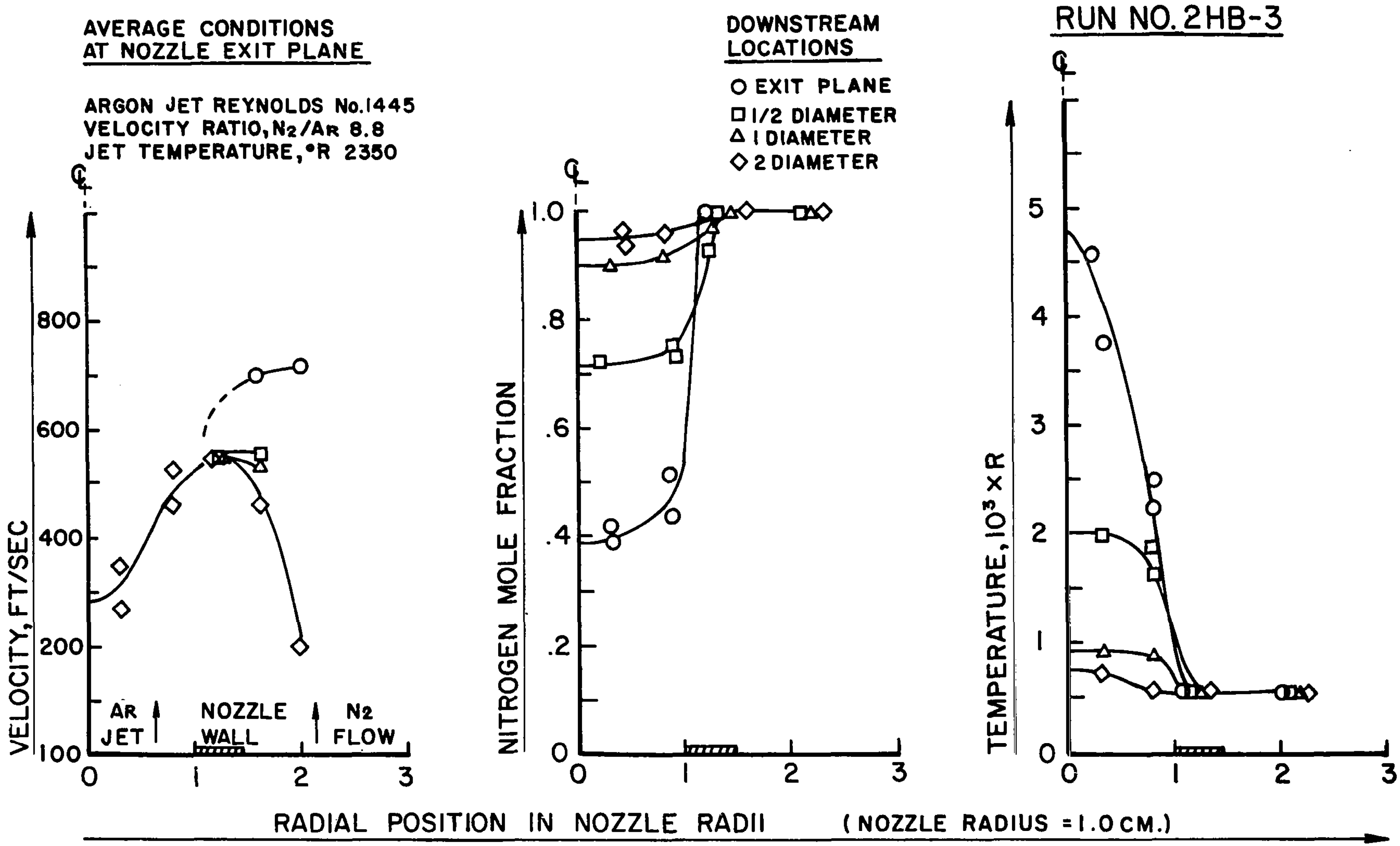

HALF-PROFILES OF ARGON ARCJET JET MIXING WITH COAXIAL NITROGEN FLOW

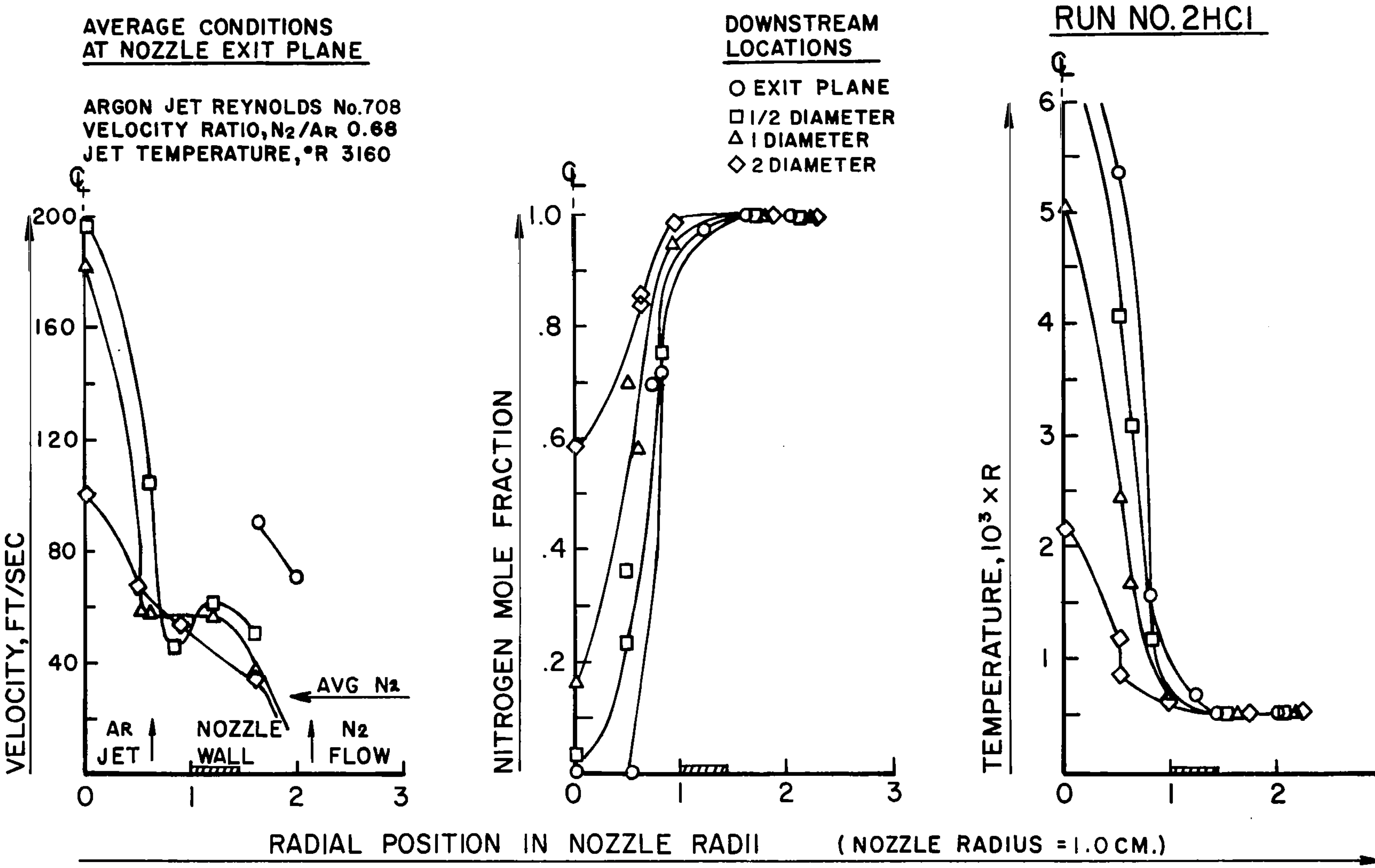

HALF-PROFILES OF ARGON ARCJET JET MIXING WITH COAXIAL NITROGEN FLOW

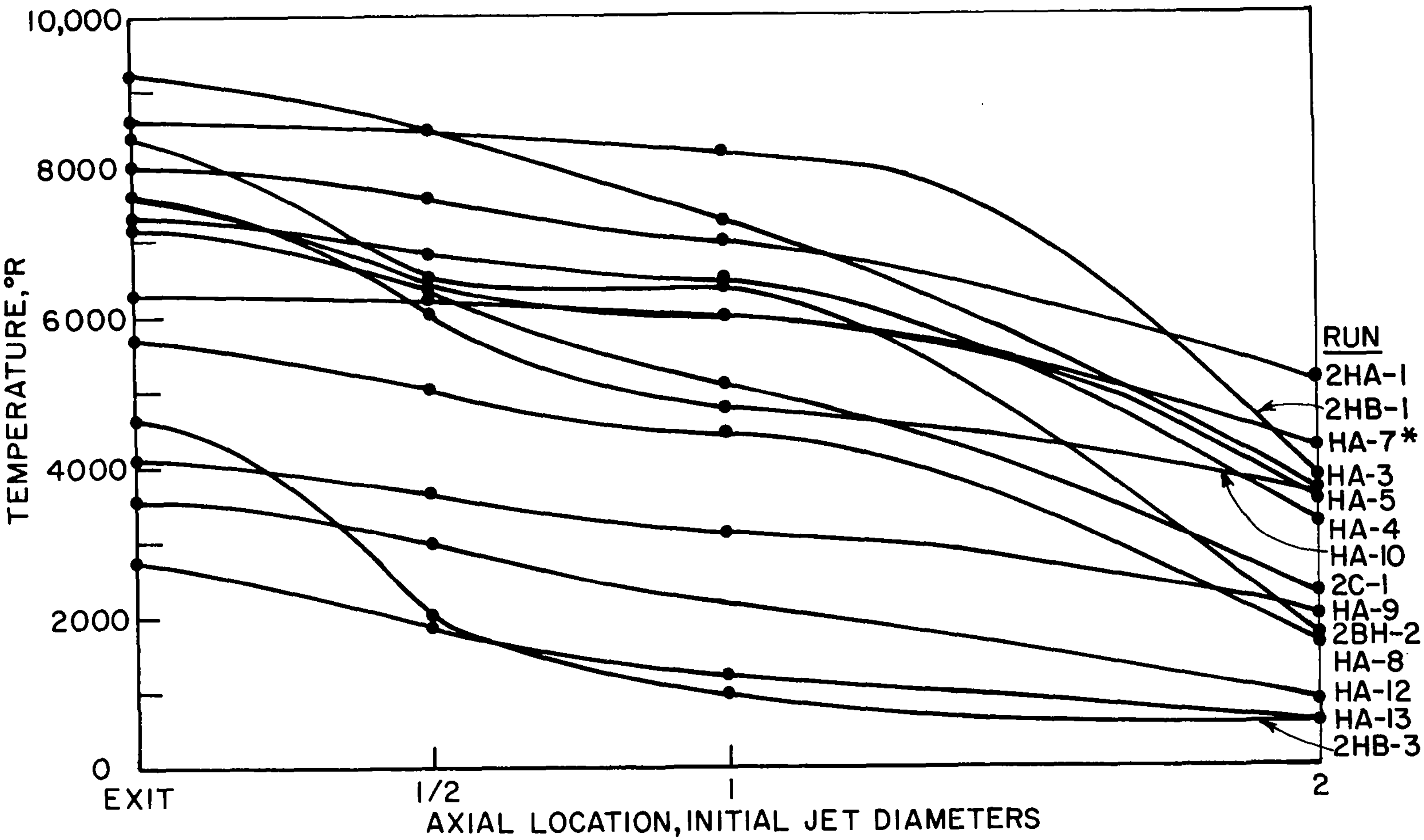

CENTERLINE TEMPERATURE
HEATED ARGON JETS IN COAXIALLY FLOWING NITROGEN

* COAXIAL HELIUM

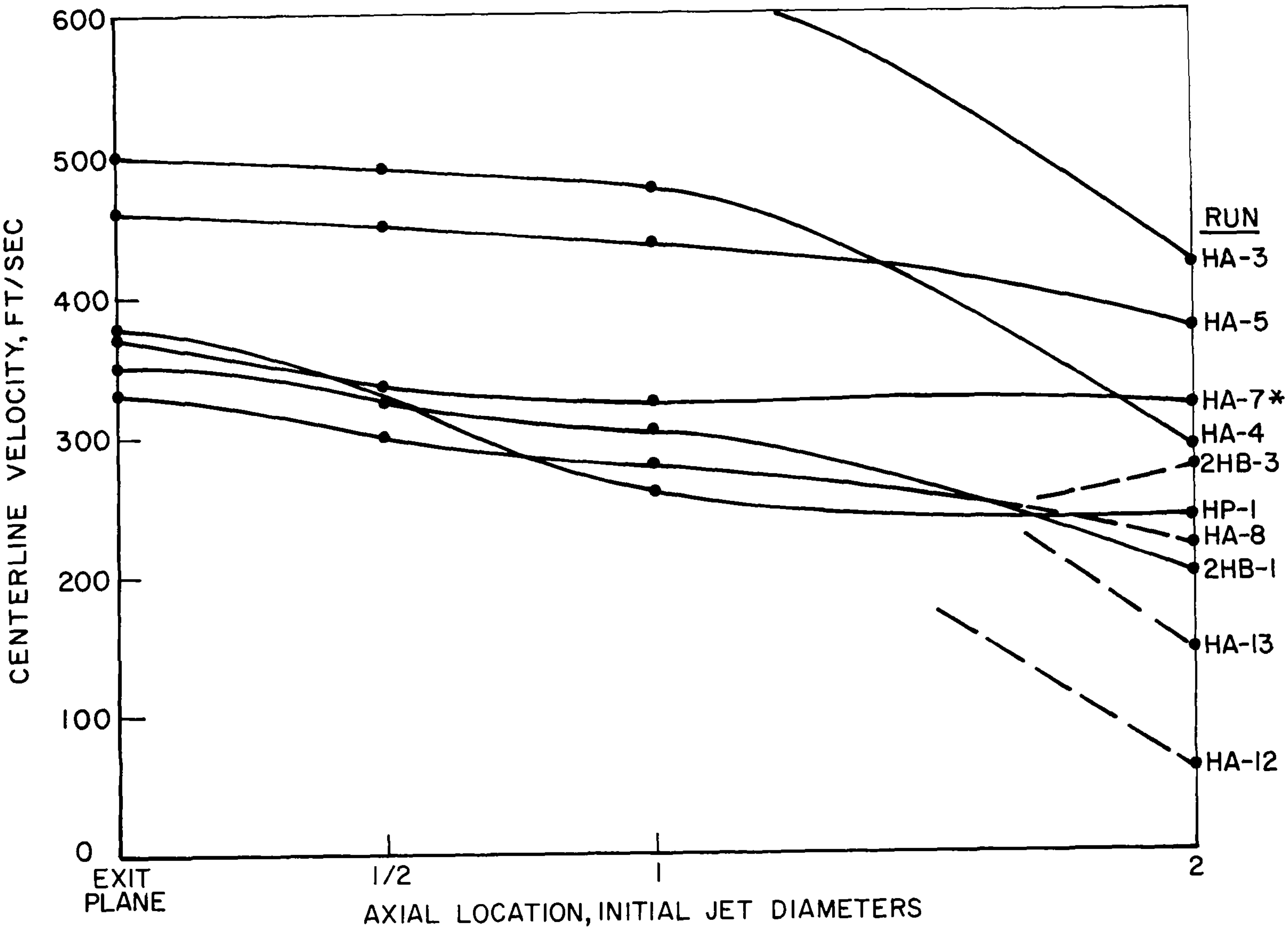

CENTERLINE COMPOSITION
HEATED ARGON JETS IN COAXIALLY FLOWING NITROGEN

* COAXIAL HELIUM

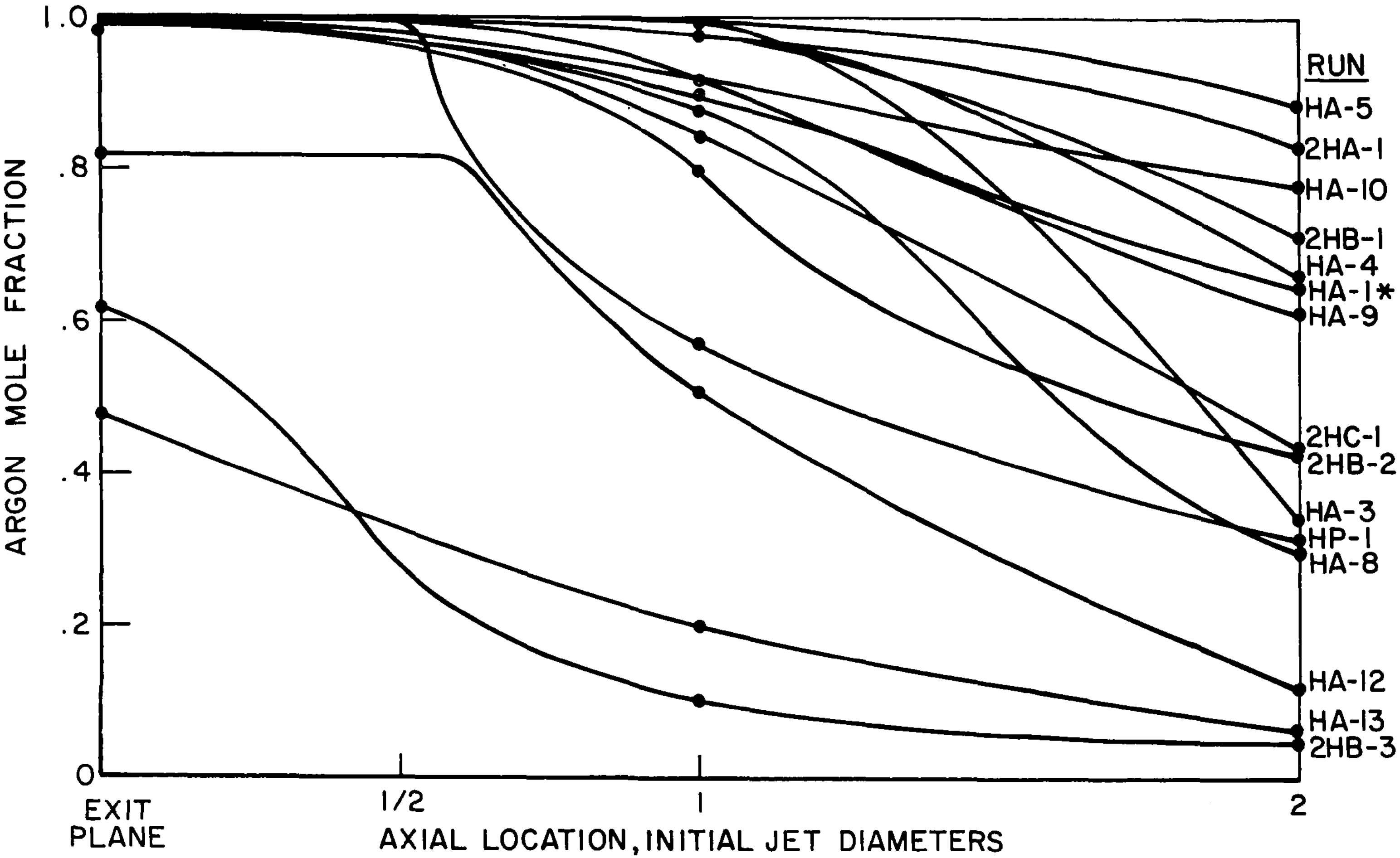

CENTERLINE COMPOSITION
HEATED ARGON JETS IN COAXIALLY FLOWING NITROGEN

* COAXIAL HELIUM

NASA-Langley, 1967 — 12 E-3707